Welchy Leite Cavalcanti · Kai Brune ·
Michael Noeske · Konstantinos Tserpes ·
Wiesław M. Ostachowicz ·
Mareike Schlag *Editors*

Adhesive Bonding of Aircraft Composite Structures

Non-destructive Testing and Quality Assurance Concepts

OPEN ACCESS

Springer

Adhesive Bonding of Aircraft Composite Structures

Welchy Leite Cavalcanti · Kai Brune ·
Michael Noeske · Konstantinos Tserpes ·
Wiesław M. Ostachowicz · Mareike Schlag
Editors

Adhesive Bonding of Aircraft Composite Structures

Non-destructive Testing and Quality Assurance Concepts

Springer

Editors
Welchy Leite Cavalcanti
Adhesive Bonding Technology and Surfaces
Fraunhofer IFAM
Bremen, Germany

Kai Brune
Adhesive Bonding Technology and Surfaces
Fraunhofer IFAM
Bremen, Germany

Michael Noeske
Adhesive Bonding Technology and Surfaces
Fraunhofer IFAM
Bremen, Germany

Konstantinos Tserpes
Department of Mechanical Engineering and Aeronautics
University of Patras
Patras, Greece

Wiesław M. Ostachowicz
Institut of Fluid Flow Machinery
Polish Academy of Sciences
Gdańsk, Poland

Mareike Schlag
Adhesive Bonding Technology and Surfaces
Fraunhofer IFAM
Bremen, Germany

ISBN 978-3-319-92809-8 ISBN 978-3-319-92810-4 (eBook)
https://doi.org/10.1007/978-3-319-92810-4

© The Editor(s) (if applicable) and The Author(s) 2021. This book is an open access publication.
Open Access This book is licensed under the terms of the Creative Commons Attribution 4.0 International License (http://creativecommons.org/licenses/by/4.0/), which permits use, sharing, adaptation, distribution and reproduction in any medium or format, as long as you give appropriate credit to the original author(s) and the source, provide a link to the Creative Commons license and indicate if changes were made.
The images or other third party material in this book are included in the book's Creative Commons license, unless indicated otherwise in a credit line to the material. If material is not included in the book's Creative Commons license and your intended use is not permitted by statutory regulation or exceeds the permitted use, you will need to obtain permission directly from the copyright holder.
The use of general descriptive names, registered names, trademarks, service marks, etc. in this publication does not imply, even in the absence of a specific statement, that such names are exempt from the relevant protective laws and regulations and therefore free for general use.
The publisher, the authors and the editors are safe to assume that the advice and information in this book are believed to be true and accurate at the date of publication. Neither the publisher nor the authors or the editors give a warranty, expressed or implied, with respect to the material contained herein or for any errors or omissions that may have been made. The publisher remains neutral with regard to jurisdictional claims in published maps and institutional affiliations.

This Springer imprint is published by the registered company Springer Nature Switzerland AG
The registered company address is: Gewerbestrasse 11, 6330 Cham, Switzerland

Foreword

Whether high in the sky, on the ground or deep below, on the surface of the water or below, whether in industrial, craft or private environments, in the manufacture and processing of tangible products, adhesive bonding technology is almost always used. Modern products in the way in which we know and use them today are barely conceivable without their use.

The reason for this is that in the context of joining techniques, it is only adhesive bonding that has the potential to join the same, but also different, materials with long-term stability while fully preserving their properties. This adhesive bonding-specific property, namely the preservation of the material properties during joining, enables products to be manufactured to meet increasing requirements, such as weight reduction, miniaturization, functional expansion or design optimization, and thus to enable new, innovative designs for a product. This is precisely where the potential of adhesive bonding technology lies as the No. 1 joining technology in the twenty-first century; a century that requires the new and further development of a wide variety of materials with their specific properties in order to meet increasing requirements. Nevertheless, it is true that these materials only become—economically and technically—usable materials with a material-appropriate joining technology, in this case, a material property-maintaining joining technology. Materials development and joining technology are therefore inseparable.

Like all joining techniques, such as welding, riveting, screwing or soldering, adhesive bonding according to ISO 9001 is a so-called "special process". This term covers all processes that cannot be verified non-destructively with one hundred percent certainty and is therefore not expressly limited to adhesive bonding. All joining techniques—and actually almost all manufacturing and processing processes in industry and trade—cannot be verified one hundred percent non-destructively, and that makes them all "special processes".

In order to be able to deal effectively with this still unalterable fact, it is now necessary to pursue two directions of development, on an equal footing and complementary to each other. One is more technical and methodical, and the other more organizational.

The more technical–methodical development direction consists of the further development of non-destructive testing techniques and methods. The latest possibilities are presented here in this book. They are essential because only with non-destructive testing technology can the tested joint and the adhesively bonded product continue to be used without loss of quality. The more experience we gain and the more scientific knowledge we acquire, the more non-destructive testing techniques can one day be combined into a possibly comprehensive non-destructive testing methodology, and the closer we come to the (future) goal of converting the "special process" of adhesive bonding into a "non-special process". This will mean, i.e. verifying the adhesively bonded product one hundred percent non-destructively in a scientifically proven manner and with the ability to continue using it after testing without any loss of quality.

Until this goal is achieved, however, the above-mentioned second, more organizationally oriented path must be taken at the same time. This is where the ingenious core idea of ISO 9001 comes into its own. It simply states that in "special processes", all possible errors must be avoided from the outset. This (and only this!) is, according to ISO 9001, the required goal in setting up a quality management system. With its help, the respective (adhesive bonding) processes are to be "controlled-mastered", i.e. designed in such a way that defects that cannot as yet be proven one hundred percent non-destructively cannot demonstrably occur in the first place.

In this context, too, adhesive bonding technology is on the right track, as accompanying regulations for ISO 9001 (DIN 2304, DIN 6701, prEN 17460, ISO/DIS 21368) have been or are being published. Their exclusive function is to concretize the ingenious ISO 9001 core idea of error prevention outlined above in such a way that it helps user companies to (even) more securely implement adhesive bonding with confidence.

Both the more technical–methodical and the more organizational development paths not only complement each other, but they also pursue exactly the same goal: To create even more confidence in the adhesive bonding application! Ultimately, confidence is the basis for realizing innovations, which is crucial to the continuing success of any organization.

These innovations are, in turn, undoubtedly necessary for the future. Numerous application examples have shown over the years that adhesive bonding already works today: Nobody would sit in an airplane, a car, a train or a bus if its adhesive bondings were not safe.

We will come to increasingly need adhesive bonding technology with its material-preserving properties, and so adhesively bonded applications will become even safer and better known in the future. There is no way around this in our progress towards a circular economy, and adhesives and sealants have long been enabling sustainable solutions by improving the recyclability of products.

The implementation of the methodologies in this book will enable organizations to adopt adhesive technology with confidence and to achieve a competitive advantage through successful innovation.

Andreas Groß and Gareth McGrath, the authors of the foreword, have been active for many years as chairmen, convenors and project managers in DIN and DVS as well as EWF, CEN and ISO within the framework of adhesive bonding quality assurance.

Andreas Groß
Adhesive Bonding Technology and Surfaces
Fraunhofer IFAM
Bremen, Germany

Gareth McGrath
Flexible Manufacturing Solutions Ltd.
Cambridge, UK

Preface

This book presents some of the recent progress in research, development and application in the quality assessment of the adhesive bonding of composite structures using extended non-destructive testing (ENDT). Its aim is to be useful as a compendium for quality or process engineers during their professional lives as well as for students as an application-oriented introduction to an array of interdisciplinary topics comprising physicochemical, material and process engineering aspects.

Over the past decade, the concepts and technological approaches substantiating the ENDT approach have been developing fast. They have attracted intense interest in ascertaining selected properties that are critical to the performance of adhesive bonds. Referring to the European Horizon 2020 research project "Quality assurance concepts for adhesive bonding of aircraft composite structures by advanced NDT", or ComBoNDT, the six interrelated and coordinated chapters of this comprehensive book were composed to further establish quality assessment procedures for the processes of manufacture and repair on an industrial scale.

In Chap. 1, the recent advances in quality assessment for adhesive bonding technology are introduced. Following the presentation of ten heuristic principles for quality assessment, concepts are demonstrated for establishing material and process-specific correlations between joint features and quality data measured using ENDT during the steps contributing to the applied bonding process. The implementation of quality assurance concepts is exemplified in the subsequent chapters. In Chap. 2, an expert approach is detailed for characterising intentionally applied pre-bond contamination and the ageing effects of CFRP bonded joints using reference laboratory methods, mechanical tests and numerical simulation. In Chaps. 3 and 4, ENDT procedures for surface and bondline quality assessment of composite structures are presented. The demonstration of ENDT techniques in a realistic environment and a technology assessment are presented in Chap. 5. In the concluding Chap. 6, some perspectives are outlined for integrating ENDT in the life cycle management of bonded products.

Our expectation for the decade to come is that topics like the factory of the future, Industry 4.0, and integrating new and established technologies based on gathering and exchanging digital datasets will become a powerful trend, one that will promote and will be promoted by quality-related data obtained through ENDT.

We hope to intrigue our readers and enliven what is a comprehensive concept for ENDT and quality assessment in adhesive bonding.

Bremen, Germany — Welchy Leite Cavalcanti
Bremen, Germany — Kai Brune
Bremen, Germany — Michael Noeske
Patras, Greece — Konstantinos Tserpes
Gdańsk, Poland — Wiesław M. Ostachowicz
Bremen, Germany — Mareike Schlag

Acknowledgements

The editors and authors are very thankful for the project Quality assurance concepts for adhesive bonding of aircraft composite structures by advanced NDT (ComBoNDT) and the funding received from the European Union's Horizon 2020 research and innovation programme under grant agreement number 636494.

The authors would like to thank Sören Lunkwitz (IFAM) and Maria Lahmann (IFAM) for conducting LIBS measurements, Stephani Stamboroski (IFAM) for performing OSEE investigations and Amit and Mantosh Chawla (Photoemission Tech, Inc.) for fruitful discussions when evaluating the OSEE findings. We also like to thank Mauricio Zadra Pacheco (IFAM) for programming LIBS mapping software. Furthermore, the authors acknowledge Marcela Martins Melo (IFAM), Marcel Sieben (IFAM) and Tim Strohbach (IFAM) for programming the robots for LIBS and OSEE measurements. The authors are very grateful to Thorsten Fladung (IFAM), Jonas Aniol (IFAM) and Andreas Volkmann (IFAM) for acquiring and evaluating XPS data and for the fruitful discussions related to the analysis of the data sets. Michael Hoffmann (IFAM) is gratefully acknowledged for supporting, advising and performing investigations with the centrifuge testing technology. Thanks to Stefan Dieckhoff (IFAM) for helpful discussions related to the outline of the manuscript.

Authors and editors are very thankful to Albulena Berbatovci who professionally took care of the design and preparation of several images. In particular, many thanks to Laura Davies for accurate proofreading and competent feedback. The authors would like as well to thank for the support from Bruna Johann Barbiero, Selina Gabric, João Pedro Costa Rheinheimer and Susanne Karamanc to adapt contributions into templates.

Contents

Abbreviations

0 method	A method used with ENEA e-nose ver.1
AbiTAS	Joint research project "Advanced Bonding Technologies for Aircraft Structures" that received funding from the European Union's Sixth Framework Programme under the grant agreement number 30996
AdaptHEAT	A heating blanket tailored to A350 structural components
ADH failure	Adhesive failure
AERNNOVA	Aernnova Composites Illescas S.A.
ATL	Automated tape laying
AUC	Area under curve
AWR	Automation W+R GmbH
AWT	Aerosol wetting test
BFO	Basic formal ontology
BoL	Beginning of life, a life cycle phase
BOPACS	Joint research project "Boltless assembling of Primary Aerospace Composite Structures" that received funding from the European Union's Seventh Framework Programme under the grant agreement number 314180
CAB	Computer-aided bonding
CCD	Charge-coupled device
CEA	Commissariat à l'énergie atomique et aux énergies alternatives
CFRP	Carbon fibre reinforced polymer
CHADA	Characterisation data, a documentation structure for materials characterisation
CleanSky	Clean Sky Joint Undertaking, one of Europe's Joint Undertakings
CNN	Convolutional neural network, an artificial neural network
CNRS	Centre National De La Recherche Scientifique
CO failure	Cohesive failure

ComBoNDT	Joint research project "Quality assurance concepts for adhesive bonding of aircraft composite structures by advanced NDT" that received funding from the European Union's Horizon 2020 research and innovation programme under grant agreement number 636494
CPS	Cyber-physical systems
CZM	Cohesive zone model
DCB	Double cantilever beam
Dechema	DECHEMA Gesellschaft für Chemische Technik und Biotechnologie e.V. (Society for Chemical Engineering and Biotechnology)
DI	De-icing fluid scenario, as used in ComBoNDT research project
DTI	Department for Trade and Industry
DVS	Deutscher Verband für Schweißen und verwandte Verfahren e. V., German Welding Society
EASA	European Aviation Safety Agency
EASN	EASN Technology Innovation Services BVBA
EMI	Electromechanical impedance
EMMO	European Materials Modelling Ontology
ENCOMB	Joint research project "Extended Non-Destructive Testing of Composite Bonds" that received funding from the European Union's Seventh Framework Programme (FP7/2007-2013) under the grant agreement number 266226
ENDT	Extended non-destructive testing
ENEA	Agenzia nazionale per le nuove tecnologie, l'energia e lo sviluppo economico sostenibile
ENF	End-notched flexure
E-nose	Electronic nose
EoL	End of life, a life cycle phase
EUREKA	EUREKA Project EU 716 QUASIAT related to Quality Assurance in Adhesive Technology
FC	Faulty curing scenario, as used in ComBoNDT research project
FEW, Bond, BWE	Back wall echo, as observed during ultrasonic inspection
FFNN	Feedforward neural network, an artificial neural network
FOS	Fibre optic sensor
FOSTA	Forschungsvereinigung Stahlanwendung e.V. (Research Association for Steel Applications)
FP	Fingerprint scenario, as used in ComBoNDT research project
FP7	Seventh Framework Programme of the EU
FRP	Fiber-reinforced polymer
FT failure	Fibre tear failure
FTIR	Fourier transform Infrared (Spectroscopy)
FWE	Front wall echo, as observed during ultrasonic inspection

GAK	Gemeinschaftsausschuss Klebtechnik, Joint Committee on Adhesive Bonding
G_{IC}	Mode I Fracture toughness (also G_{1c})
G_{IIC}	Mode II Fracture toughness (also G_{2c})
GMI	GMI Aero SAS
GUI	Graphical user interface
HALT	Highly accelerated life tests
HANOB	Joint research project "Entwicklung Referenzsystem zur handgeführten Oberflächen-Benetzungsprüfung"
HCI	Human–computer interaction
HF	Immersion in hydraulic oil scenario, as used in ComBoNDT research project
HMI	Human–machine interaction
IFAM	Fraunhofer Institute for Manufacturing Technology and Advanced Materials IFAM
IMP-PAN	Instytut Maszyn Przepływowych im. Roberta Szewalskiego Polskiej Akademii Nauk
IMS	Ion mobility spectrometer
Industry 4.0	The fourth industrial revolution, referring to the digitalisation of manufacturing processes
IPA	Isopropanol
iVTH	Internationaler Verein für Technische Holzfragen e.V., International Association for Technical Issues related to Wood
KPI	Key performance indicator
LASAT	Laser shock adhesion testing
LCA	Life cycle assessment
LCC	Life cycle costing
LCM	Life cycle management
LFT failure	Light fibre tear failure
LIBS	Laser-induced breakdown spectroscopy
LIF	Laser-induced fluorescence (spectroscopy)
LS	Linear scanning, as used during ultrasonic inspection
LSCM	Laser scanning confocal microscopy
LS-DYNA	An explicit simulation program (Ansys, Inc.)
LTSM-UPAT	Laboratory of Technology and Strength of Materials, University of Patras
LV	Latent variables
MAE	Mean absolute error
MEK	Methyl ethyl ketone
MGSS	Magnetostrictive sensors
MO	Moisture uptake scenario, as used in ComBoNDT research project
MODA	Materials Modelling data
MoL	Middle of life, a life cycle phase
MOX sensor	Metal-oxide (gas) sensor

MSQC	Multivariate statistical quality control
NDE	Non-destructive evaluation
NDT	Non-destructive testing
NUS	Nonlinear ultrasound scanning
OSEE	Optically stimulated electron emission
P-	Prefix of sample names for specimens from production-related scenarios, as used in ComBoNDT research project
PC method	A method used with ENEA e-nose ver.1
PCA	Principal component analysis
PEN	Portable electronic nose (AIRSENSE Analytics GmbH)
PID	Photoionization detector
PLS-DA	Partial least squares discriminant analysis
POD	Probability of detection
QA	Quality assessment
R-	Prefix of sample names for specimens from repair-related scenarios, as used in ComBoNDT research project
RA	Release agent scenario, as used in ComBoNDT research project
R-Combi	Prefix of sample names from repair-related combined contamination scenarios, as used in ComBoNDT research project
REF	Reference scenario, as used in ComBoNDT research project
RH	Relative humidity scenario, as used in ComBoNDT research project
RMSEP	Root mean square error of prediction
SAUL	Surface adaptative ultrasonic laws, as used for ultrasonic inspection
SCADA	Supervisory control and data acquisition
SHM	Structural health monitoring
SLCA	Social lifecycle assessment
SLDV	Scanning laser Doppler vibrometry
SMART	Stanford Multiactuator–Receiver Transduction
SNIFFI	First version of the ENEA e-nose (ENEA e-nose ver.1), a compact, stand-alone, light-weight and rugged laboratory gas sensor system
SPF	Single point focusing, as used during ultrasonic inspection
SPM	Statistical process monitoring
SVM	Support vector machine
SWAT	Shock wave adhesion test
TD	Thermal degradation scenario, as used in ComBoNDT research project
TLC failure	Thin-layer cohesive failure
ToF	Time of flight
TRL	Technology readiness level
TWI	The Welding Institute
VOC	Volatile organic compound
XPS	X-ray photoelectron spectroscopy

Chapter 1
Introduction to Recent Advances in Quality Assessment for Adhesive Bonding Technology

Michael Noeske, Welchy Leite Cavalcanti, Hauke Brüning, Bernd Mayer, Antonios Stamopoulos, Apostolos Chamos, Thomas Krousarlis, Paweł H. Malinowski, Wiesław M. Ostachowicz, Konstantinos Tserpes, Kai Brune, and Romain Ecault

Abstract The first chapter highlights the relevance of both adhesive bonding technology and in-process quality assessment for mastering twenty-first-century challenges in joining functional and lightweight materials like carbon fibre reinforced polymers. The ongoing developments of the relevant technological and regulatory procedures and frameworks are hereby outlined, following trends for data-driven innovation and standardisation. Advances from monitoring process variables towards the in-depth and objective Extended Non-destructive Testing (ENDT) of material-related features are presented, based on methodological and technological innovation and insights from recent European joint research projects like Horizon 2020s ComBoNDT—"Quality assurance concepts for adhesive bonding of aircraft composite structures by advanced NDT". Introducing ten heuristic principles for quality assessment in bonding processes, a concept is demonstrated for establishing empirically consolidated sets of quantitative material and process-specific correlations between design-relevant joint features and quality data measured during the manufacture or repair of adhesive joints using ENDT. Each correlation is obtained by systematically introducing disturbances of relevant process features identified by experts and is levelled once by linking findings from standardised mechanical tests

M. Noeske (✉) · W. Leite Cavalcanti · H. Brüning · B. Mayer · K. Brune
Fraunhofer Institute for Manufacturing Technology and Advanced Materials IFAM, Wiener Str. 12, 28359 Bremen, Germany
e-mail: michael.noeske@ifam.fraunhofer.de

A. Stamopoulos · A. Chamos · T. Krousarlis
EASN Technology Innovation Services, Terweidenstraat 28, 3440 Budingen, Belgium

P. H. Malinowski · W. M. Ostachowicz
Institute of Fluid–Flow Machinery, Polish Academy of Sciences, Fiszera 14, Gdańsk 80231, Poland

K. Tserpes
Laboratory of Technology & Strength of Materials, Department of Mechanical Engineering & Aeronautics, University of Patras, 26500 Patras, Greece

R. Ecault
Airbus Operations S.A.S., 316, Route de Bayonne, B.P. D4101, 31060 Cedex 9 Toulouse, France

© The Author(s) 2021

W. Leite Cavalcanti et al. (eds.), *Adhesive Bonding of Aircraft Composite Structures*,
https://doi.org/10.1007/978-3-319-92810-4_1

with ENDT results obtained for joints that have intentionally been manufactured or repaired in an off-specification way. Subsequent chapters will demonstrate the suitability of the broadly applicable process.

Keywords Adhesive bonding technology · Quality assessment · In-process data · Extended non-destructive testing (ENDT) · Heuristic principles · Concepts from ComBoNDT project

1.1 Introduction

Adhesive bonding was already being applied more than 35,000 years ago in the Upper Palaeolithic in the Near East using naturally occurring bitumen [1] as well as in Europe during the contemporaneous last Ice Age [2] and starting from the Middle Palaeolithic to the Iron Age using wood or birch-bark tar [3, 4]. Adhesive joints based on biomaterials are also known from the Swabian Aurignacian [5] in the Upper Palaeolithic. For example, hollowed-out adherends consisting of flint and split animal bones or mammoth teeth were re-joined and re-sealed using an airtight resin glue (an organic mastic that was possibly birch tar obtained using fire [6]) to manufacture a single piece of work that contributed to the social cohesion inside fire-heated caves inhibited by modern humans or even Neanderthals. These joints created musical instruments, highlights of humanity's cultural repertoire, and their product quality was tested by the musicians and their audience. As early as the Neolithic, inorganic sandwich composite adhesives consisting of fillers and binders were used to manufacture poly-layered joints as ornamental artefacts [7]. In the Taklamakan Desert in north-western China, early evidence of adhesives and their development around 3500 years ago was recently collected in the form of a bone sculpture-inlaid wooden artefact [8]. The development of adhesives and bonding applications was further advanced in ancient Greece and the Roman Empire [9]. In fact, throughout human history, adhesives have been among the most widely applied materials [8] and their use was one of the earliest known transformative technologies [10], yet many of these historical advances have only recently been revealed through archaeological excavations and investigations.

In Europe, the modern era was initiated by the re-discovery of Greek and Roman cultural and knowledge heritage, triggering the three Industrial Revolutions, which facilitated machine-driven mass customisation and computer-driven digital data processing. The fourth Industrial Revolution is currently ongoing, encompassing exchangeable decentralised datasets and individualised information available anytime and anywhere and joining the biological, physical, and digital fields to form cyber-physical systems. The advent of Industry 4.0 is updated music to the audience's ears—be it students or professionals, engineers or natural scientists, and it will connect more than seven billion humans worldwide. Such extensive communication will be based on documenting and preserving, sharing and high-speed exchanging trackable digital data or even knowledge, a development that is

entering site-comprehensive production chains step by step. This advancement also challenges modern adhesive bonding for the series production of multifunctional materials for the simple reason that quality assessment and quality management in production technologies are not based on archaeological methods or tools. Nonetheless, we suggest that making relevant material-based aspects accessible is a crucial endeavour, both in archaeology and in forward-looking production technologies, and that this perspective will spawn the analysis of augmentable domain-specific data sources that are virtually unbounded in both cases.

We consider modern tools for quality assessment in adhesive bonding technology worth the readers' attention, and we present recent progress in the research, development and application of process-integrated monitoring technologies for joining composite structures. We systematically introduce our readers to extended nondestructive testing (ENDT) and provide a compendium for quality or process engineers throughout their professional lives as well as for students as an application-oriented introduction to the interdisciplinary topics at hand, comprising physicochemical, material and process engineering aspects.

In this section, we give a short introduction to ENDT and quality assessment in adhesive bonding processes relevant to the manufacture or repair of composite structures.

Why are these topics so highly relevant at present? Fundamentally, we share expectations that in the twenty-first century, progress in joining functional or lightweight materials and components will essentially be driven by innovations based on adhesive bonding technology and by developments that will enable manufacturers to safeguard the quality and optimise production [11–13], integrating these three drivers into a factory-of-the-future approach for composite manufacture, e.g. in the aerospace or automotive industries [14–16]. With the aim of achieving cost efficiency and increased flexibility with many degrees of freedom [17, 18], computer-integrated manufacturing will be established for all process steps, including those related to adhesive bonding. In this way, the increasing market demand for new and highly customised products with high quality [19] will be met and a small time-to-market delay will be achieved. In view of challenges like shorter response opportunities and flexibility in a turbulent and unpredictable market environment while preserving product quality [19], knowledge capturing and processing profiting from formal methods, e.g. taxonomies and ontologies [20], are gaining importance and may greatly contribute to rule-driven manufacturing control [21]. In addition to the software and information technology infrastructure presently being developed, hardware that facilitates the gathering of precise in-process data from all process steps will be needed as a third pillar [18, 22, 23] within less than a decade. These intelligent hardware elements of machines and devices such as sensors and actuators contribute to the "field-level" base of the industrial automation pyramid [19, 24], which highlights the numerous components and pathways of industrial communications, as sketched in Fig. 1.1. Within an automation pyramid, the upper levels are characterised by a deeper understanding and a higher responsibility for the performance of the complete overall system. The deeper levels within the hierarchy are distinguished by increasingly detailed knowledge about individual processes and process steps or

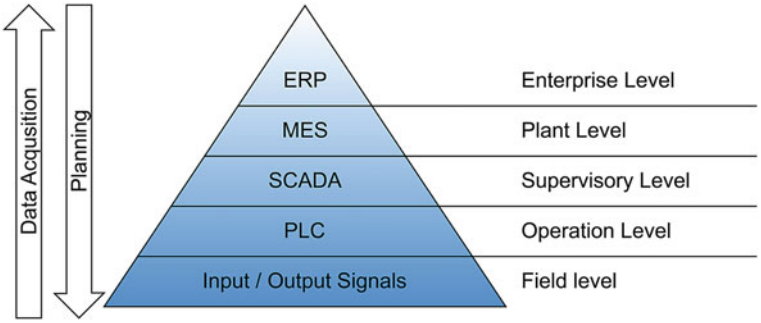

Fig. 1.1 Hierarchical model of an industrial automation pyramid based on field-level sensing. The first level or "field level" comprises the physical devices such as actuators and sensors. The second level or "operation level" includes logical devices such as Programmable Logic Controllers (PLC) or PCs usually found in complex machinery. The "supervisory level" (third level) corresponds to the supervisory control and data acquisition systems (SCADA) used to monitor and operate individual processes. The manufacturing execution systems (MES) are responsible at a higher "plant level". The top of the pyramid ("enterprise level") comprises the company's integrated management system (ERP) controlling the company's global operations. Providing, implementing and evaluating hardware that enables precise in-process data to be gathered within a comprehensive concept for quality assurance is a key target of the present book

technologies. In matters of smart manufacturing knowledge management, the basic data form the foundation for the higher levels, which are targeted towards manufacturing information, scientific understanding (e.g. providing predictive models), and knowledge [25]. In the future, for some systems, e.g. for monitoring bonded repair of composite aircraft structures, highest level standalone and autonomous opportunities appear accomplishable from a scientific point of view [26].

Bearing these expectations and challenges, but also the self-limiting frame of this book, in mind, we will introduce one comprehensive concept, ten pathbreaking heuristic principles, and more than a dozen tools which are accessible for interoperability and facilitate implementing and operating a quality assessment (QA) system. These form a profound base for quality assurance within a superordinate and nevertheless interlinked quality management system. We expect that sensing systems comprising ENDT tools and concepts [27, 28] as well as sensors and sensor concepts [18] will thus provide a solid foundation both for this approach following Industry 4.0 and for quality assessment as a technical pre-requisite for quality assurance.

1.2 Technological and Regulatory Framework

In this section, we will introduce a succinct description of adhesive bonding processes and render some aspects of quality assurance and monitoring before describing the ongoing advancement of quality assessment with a focus on adhesive bonding processes. After detailing ten heuristic principles for quality assessment, we will

integrate methods and tools for ENDT. Finally, we will present a concept for ENDT and quality assessment in adhesive bonding, which will then be further elaborated in the subsequent chapters of this book.

1.2.1 Adhesive Bonding Processes

The track record and success story of adhesive bonding technology are based on establishing and safeguarding reliable joining processes. The early one and a half decades of the twenty-first century highlighted that quality assurance "for correct adhesive application and documented via certification" contributes to minimising faults, saving money, generating trust, promoting the wider use of adhesives, and sustainably improving the image of adhesive bonding, which may be clouded by observations that "bonding errors are often still encountered" [11]. So, let us first and foremost grasp a clearly arranged and predominantly technical image of this promising joining technology.

According to DIN EN 923, adhesives are non-metallic substances capable of joining materials through surface bonding (adhesion), with the bond possessing adequate internal strength (cohesion) [9]. The result of applying bonding as a material joining technique, i.e. the product of the bonding process, is an adhesive joint. Concerning the feasible lifecycle of an adhesive joint, such a bonding process may occur during manufacture [12] or during repair [29].

Characteristically, an adhesive bonding process may be divided into consecutive phases of the preparation of the constituent materials (such as adherends, [optionally] prepregs and the adhesive system comprising [optionally] primers and the adhesive), the application of the adhesive system, the assembly/lay-up, the curing and the final finishing. Each of these phases may be subdivided into further steps and finally strung together to form the process chain [30].

In the framework of these technical processes (or process chains), the adherend and adhesive materials may be described as operands, i.e. objects with initial relevant properties that are changed by the effect of one or more factors [31]. Following a procedure presented by Mattmann [31] for describing a product lifecycle, these factors are provided by technical systems denoted as operators. Correspondingly, at the end of a bonding process, the final state of the operands is different from the initial state, with the difference being described by the new, process-induced properties. In most cases, the bonding process is a successive multi-step process which may be described as a process chain with a chronologically defined sequence of process steps grouped in process phases [30]. Other operands in addition to the adherends and the adhesive will often need to be considered, e.g. in the case of a multi-layer adhesive system.

Therefore, in a short formal description consistent with Mattmann's approach [31], we suggest the diction for the adhesive bonding process as comprising the time-dependent (state and property) transformation T(t) of several operands starting from an (overall) initial state $S_i(t_0)$ prevailing at the onset of the process at the point

in time t_0. When the process is completed at time t_f, a final state $S_f(t_f)$ is achieved. As expressed by Eq. (1.1), the states $S_i(t_0)$ and $S_f(t_f)$ are described by property vectors at the defined points in time t_0 and t_f, and the achieved change and difference resulting from the process. Within a process chain, the operand is unequivocally described by the entity of its properties (in three spatial dimensions) at any time (as the fourth dimension) for all consequentially feasible intermediate process states.

$$S_f(t_f) = T(t_f) \bullet S_i(t_0) \tag{1.1}$$

In a technical engineering approximation highlighted by Eq. (1.2), among the operand properties, process-relevant time-dependent features, such as $s_A(t_1)$ and $s_B(t_1)$, may be identified based on the requirements to be met. Thus, the related feature vector $S(t_1)$ is a quantitative descriptor for the prevailing state of the operands as governed by the effect of the, respectively, performed set of operations, represented by the transformation $T(t_1)$, having been executed for (i.e. until) the point in time t_1.

$$S(t_1) = (s_A(t_1), s_B(t_1), \ldots) \tag{1.2}$$

Subsequently, the initial and final states of the operands will be technically described by the feature vectors $S(t_0)$ and $S(t_f)$, respectively. Clearly, the complete description of these states using the respective property vectors may comprise additional properties which are not significantly modified during the course of the adhesive bonding process. In this way, the pursued concept for systemically approaching the features will determine the accuracy of this approximation, which in practice will crucially depend on the iteratively achieved process and material know-how.

In a nutshell, following this diction the adhesive bonding process is described by the time-dependent procedure and changes of both the operator and operand states, as highlighted in Fig. 1.2. In more detail, when implementing such process representation as described by Eq. (1.1), the estimated operator-operand interactions may either be neglected, i.e. considered small as compared to the main effects of the operations affecting the operators or the operands, or they may be included in the concept of the operator or operand.

Visualising the first approach, a process in a controlled environment—with small and controlled deviations from a known and understood procedure described by $(T + \Delta T)(t) \bullet (S_i + \Delta S_i)$—may be assessed based on the knowledge of the main effects in the "reference" process, e.g. a qualified process. As a first example, in a wet cleaning step, the accumulation of known auxiliary materials of preceding process steps within the cleaning bath is maintained within evaluated parameter intervals $[(T - \Delta T)(t), (T + \Delta T)(t)]$ through the tailored measures of the process control. As a second example, identifying a deviation of the adherend surface cleanliness exceeding the evaluated parameter interval $[(S_i - \Delta S_i), (S_i + \Delta S_i)]$ may result in deciding to perform a further, e.g. repeated, cleaning step rather than deciding to, e.g. change the adhesive system of the following bonding steps.

Visualising the second approach, the material-dependent effects of processes may be attributed to respective material features in a material-specific process described

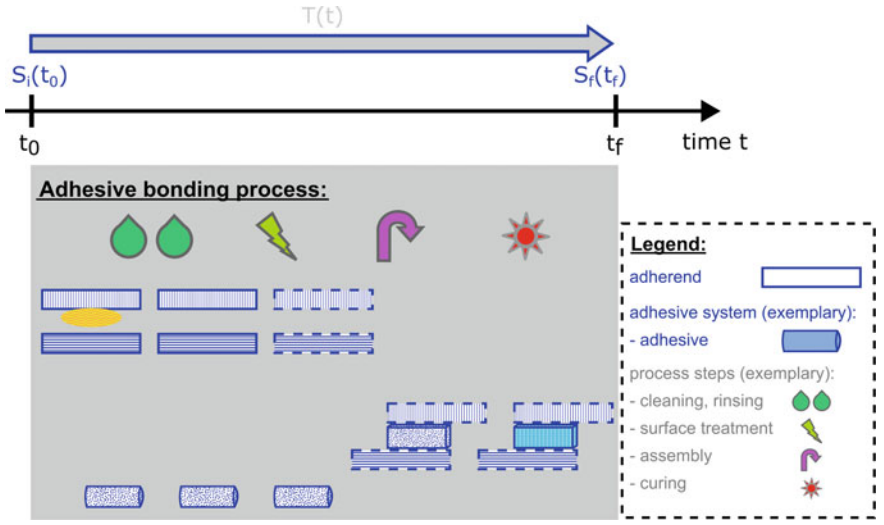

Fig. 1.2 An example of a process chain in adhesive bonding, with operands (with a blue outline) being successively changed through a time-dependent transformation $T(t)$ from an initial state $S_i(t_0)$ to a final state $S_f(t_f)$ due to the effects of the operators (with a grey outline). In this example, the top adherend is partially covered by contamination (shown in yellow) at the beginning of the bonding process

by $T(t, S_i)$, i.e. promptly adapting the operator action following the detection of deviations from an "expected" initial operand state. For instance, in the curing oven of an adhesive bonding process, the temperature reached by the pre-connected adhesive system and adherends within a given time may be consciously adjusted following the heat capacity and heat conductivity of the involved materials and devices. Therefore, using different operands will mean applying a different, "new" process tailored to the materials and the geometry of the joint to be manufactured.

From our point of view and following the perception highlighted in Fig. 1.1, technically facilitating the first approach is currently feasible and in the near future will increasingly be substantiated based on access to manufacturing information. We expect that the second approach will require a more profound understanding, which will prospectively be provided by longer term information-related data evaluation.

When geometrically extended specimens or even devices are to be adhesively bonded, the comprehensive prevailing feature vector $S(t_1)$ may be complex and comprise regions of the devices which are insignificantly affected by the considered bonding process. In such cases, a reduction of the topological complexity of the respective process description may be necessary and can be achieved by predominantly embracing the relevant conformational elements, e.g. those characterising the design regions comprising the bonding areas of the adherends. As adhesive bonding is based on adhesion, the feature vector describing the operands "adherend1" and "adherend2" shall necessarily comprise the surface properties of these solids in

the bonding region. Meanwhile, the time-dependent feature vector describing the adhesive system shall comprise the interaction with the adherend surfaces.

In the following sections, we will demonstrate the application of these aspects for a described bonding process.

1.2.2 Quality Assurance and Monitoring

According to a strict definition, quality is first and foremost the compliance of services with the requirements. These requirements can be created by customers, manufacturers or users, but also by the services themselves. Briefly, with respect to competitiveness, an essential aspect of quality is "the elimination of waste" [32].

However, there is also a far-reaching aspect behind the term quality, one which is often associated with product safety and by extension, for example, the financial success of a company. The reliability of a product can often only be achieved through good quality. Moreover, high-quality products provide the basis for manufacturing in the high-wage countries of the EU, as these reach higher market prices. Nevertheless, quality control is a challenge for many manufacturing companies. House-made standards and testing standards usually help to achieve internal quality goals, but in order to demonstrate quality to external customers, it is often necessary to refer to norms and known standards or even be certified according to a recognised standard. Therefore, proof of compliance with a standard is provided by a certification process, followed by the issuance of a temporary certificate by independent certification bodies. One of the best-known quality standards is ISO 9001, which specifies a quality management system that an organisation (e.g. in the frame of a manufacturing process) must meet in order to comply with the quality requirements. Among other aspects, it introduces the concept of the so-called "special process", which is a process "in which the result cannot be fully verified (checked) by subsequent monitoring and measurement or non-destructive testing of the product" [33]. This includes processes such as welding or bonding. With these "special processes", a strategy for avoiding errors must be developed through a complete planning of the process, whereby all error-influencing factors must be identified and defined. In the production phase, all parameters must be checked and finally documented for the feasibility of the considered process. Even if this standard only defines the minimum requirements for a quality management system, the basic idea is ingenious. Secured processes prevent errors at specific points in the process, and over the entirety of the individual secured process steps, the quality of a product is controlled [34]. An example detailed by Espie et al. [32] highlights that "adhesive bonding can be a more complex procedure to control than other joining methods", demonstrated by the fact that "on a car assembly line spot welding is the responsibility of one station, but up to five points of the line can contribute to success or failure of a bonded joint". This indicates of course that the basic idea of ISO 9001 must be put into practice in a technology-specific way, since it is very general and the quality management system only conducts specific checks. It does not contain any further information on specific

application techniques such as joining technology, e.g. bonding. Based on the core idea of ISO 9001, standards such as DIN 2304 [35] apply and specify the requirements in a technology-specific manner. DIN 2304-1 specifies requirements for the quality-assured execution of structural, i.e. load-carrying, adhesive bonds along the process chain of bonding—from development to manufacture and repair—and thus provides a basic framework for achieving high-quality bonded products.

Quality management thus comprises the product which the customer is buying, the process to manufacture or deliver this product, and the organisational system behind it [32]. Aiming at effectively implementing the continuous improvement of the product, the process and the system, the monitoring of events is desirable in addition to establishing a controlled environment [32]. Perceived as a tool, "the essence of monitoring is to look at trends and changes (or the lack of them) *over time* to reveal actions necessary to be taken with processes and the system, or to confirm that all is well" [32].

One immediate effect of monitoring in the age of digitalisation is that data are not only measured but also stored in great quantities, making them accessible for extensive evaluation and analysis [23]. Formally, the acquired data contribute to a complex materials characterisation data space. The precise format and architecture of such data are subject to ongoing research and industrial initiatives, e.g. considering concerted taxonomies and ontologies for contextual data. For example, Allotrope Foundation, founded in 2012, "is developing advanced data architecture to transform the acquisition, exchange, and management of laboratory data throughout its complete lifecycle" [36]. Within the Allotrope Taxonomies Domain Model, an entity of data is composed of the five domains of material (e.g. sample), equipment (e.g. spectrometer), process (e.g. method), result (e.g. spectrum) and property (of the data type or object). A similar approach for laboratory data appears feasible for structuring in-process monitoring data. Indeed, for the evaluation of monitoring data as a tool of quality control, mathematical, e.g. statistical, approaches are currently being discussed in the literature, which deals in-depth with structuring, e.g. clustering, the data and identifying their relevance to the quality of a manufactured product. Some key aspects are the following:

- Monitored data, i.e. the data vector or matrix obtained, may include on the one hand measurements of process variables related to the manufacturing process (and formally $\mathbf{T}(t_1)$), and on the other hand measurements of quality variables related to the manufactured product (and formally $S(t_1)$) [37, 38]. For example, statistical process monitoring (SPM) is based on both process variables and quality variables, while the focus of multivariate statistical quality control (MSQC) literature is on the monitoring of quality variables [37]. As highlighted above, the measurement process itself also consistently requires process monitoring and documentation.
- Process variables are often measured frequently and come in large quantities, while quality variables are measured at much lower rates and often come with a significant time delay [37].
- Root causes of potential quality problems may sometimes be related to a set of certain process variables [37], which is why two [39] or more [40] sub-blocks

for process data have been suggested, depending on their correlation with quality variables which are characterised by, e.g. mutual information (MI) values [39].

- Smart manufacturing which links physical and cyber capabilities will profit from managing large amounts of information and will facilitate improved diagnostics and prognostics, e.g. for fault detection or predictive maintenance [41]. Manufacturing operations and product quality may be improved by implementing process analytics delivering high-quality data and by "incorporating subject matter expertise in solution design" [41]. Combining such domain knowledge like subject matter expertise in analytics with the process and material expertise appears especially relevant to approaching the relationship and possibly the correlation between the measured data vector and the material feature vector $S(t_1)$.
- Additional information for quality control purposes may be generated by a combination of multiple information sources (that provide data) using information (data) fusion, e.g. by combining non-destructive testing and simulation [42]. Berger et al. laid out that "concurrent", "complementary" and "cooperative" integration types may be considered, depending on the amount and types of sensors that are being applied in combination. Following these authors, the method of combining data from a sensor network depends on the spatial and temporal relationship between the sensors.

The authors of this chapter forecast that in addition to regulatory requirements the availability of appropriate non-destructive testing devices for monitoring will in the medium term at the latest boost the frequency of their application, for instance, in adhesive bonding technology and especially in view of quality variables. We recommend identifying, monitoring and collecting high-quality data relevant to product quality. In the subsequent chapters, and especially in Chaps. 3 and 4, we will draw on subject matter expertise to characterise and categorise monitoring techniques and devices.

As depicted in Fig. 1.3, our quality monitoring approach will follow a description of a material analytical process considering an impacting probe P_i, a detected probe P_d and their interactions with the investigated sample material. The P_i-sample

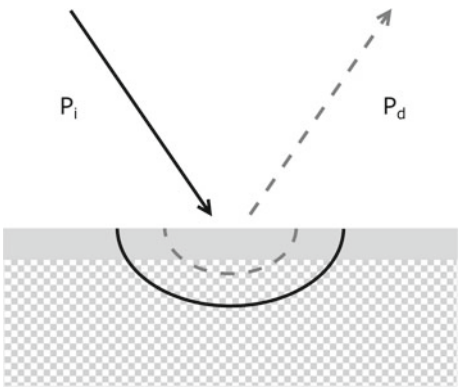

Fig. 1.3 The material analytical process considering an impacting probe P_i (solid line) and a detected probe P_d (dashed line) as well as their respective interaction volumes with the investigated sample material comprising the sample surface

interaction volume may be larger than the information volume produced by the P_d-sample interaction, but due to causality not vice versa. Finally, the focus will be on knowledge-based monitoring, which needs to answer the key question of this book: "How significantly does the state of the detected (set of) probe(s) P_d depend on the state of the monitored operands?" Evidently, monitoring the state of the operators is equally essential.

We observe that advanced information in combination with cyber-physical systems is currently establishing the fourth generation of manufacturing [41]. Indeed, in the past two decades the assessment that "monitoring adds cost but no value and may save cost at a later stage" [32] may have even hampered the speed of innovation in quality monitoring techniques, since "it is very hard to get companies to invest in something of which the added value is vague" [43]. Based on interviews with representatives from the NDT sector, C. Wassink spotted that companies looking for NDT solutions appeared to do so at a rather low aggregation level (plant-by-plant basis), on a rather small time scale of weeks or a few months, and by predominantly addressing technical issues. Subsequently, he suggested that a new and alternative innovation mindset should be applied at the industry level and on a time scale of several years, advancing innovation by multiple iterations and improvements and by widening the focus from mere defect detection to safety and risk reduction considering the economic value and social acceptance. Such an approach was to be followed by "mixed teams of practitioners and scientists" that were formed "to launch and improve new innovative solutions" and to establish a shared vision and innovation model comprising the active role of NDT service providers.

Following this perception, we intend the present book and the presented work to contribute our subject matter expertise in analytics and in adhesive bonding technology to a vision implementing extended non-destructive testing, thereby embracing the far-reaching aspects underlying the concept of quality.

1.2.3 Quality Assessment for Adhesive Bonding

We dedicate this section to the advancement of selected aspects in quality assessment for adhesive bonding technology over the past quarter of a century. We decided to tackle this agenda by first inviting the reader to engage in some time travel to the past decade of the past millennium, to about 1990. The idea is that we intersperse numerous citations from the comprehensive report of the EUREKA research project EU716 "Quality Assurance in Adhesive Technology" authored by Espie et al. [32], which was already touched upon in Sect. 1.2.2 Quality Assurance and Monitoring, thereby highlighting the awareness and vision of 20 years ago. The reader will thus be given the opportunity to compare their experience and perception of the challenges and perspectives with ours, which will be detailed subsequently and can be summarised as follows: Basic requests for in-process QA in adhesive bonding technology have been persistent for the past three decades, and these have been expedited

with increasing intensity from several aspects. It is expected that, with the achieved progress described in the following chapters of this book, they will advance quickly.

As outlined in the previous section, Espie et al. highlighted that quality management in adhesive bonding relies on two major concepts [32]:

(1) "The control of joint design and specification of materials and processes".
(2) "The process monitoring and/or inspection".

In line with this, over one decade later a typical QA program was said to be composed of three parts, including the aim of applying the QA concepts and reference to criteria for the acceptance of operands [44]:

(1) "Establishing limits on bonding process factors that will ensure acceptable joints and product".
(2) "Monitoring the production processes and quality of bond in joints and product".
(3) "Detecting unacceptable joints and product, determining the cause, and correcting the problem".

Nowadays, QA is assigned an even wider mission, embracing the service life of the product resulting from the bonding process. For example, sustainability is a central environmental, economic and social concern on the "adhesive bonding roadmap", which was recently published by Dechema (Society for Chemical Engineering and Biotechnology) and the Joint Committee on Adhesive Bonding (GAK), supported by the German Welding Society (DVS), the Research Association on Welding and Allied Processes, FOSTA (the Research Association for Steel Applications) and iVTH (International Association for Technical Issues related to Wood) [13]. This wider sense, based on the future-oriented public and technological perceptions, makes further "increasing the trust in adhesives" the essential caption on the frame of this roadmap. The three pillars for the roadmap are based on "managing production processes", "understanding ageing" and "computer-aided bonding (CAB)". Within the first pillar, aspired targets are "quality assurance using non-destructive testing methods" using standardisation, guidelines and training and with—on the horizon in the year 2025—the "introduction of health and monitoring systems".

Thus, concerning quality assurance, we nowadays perceive that widening the focus to include economic value and social acceptance (as highlighted by Wassink [43]) is indeed a common sense in adhesive bonding technology. Moreover, it appears that after mastering static aspects, the upcoming decade will focus on assessing time-dependent changes within the operand materials during bonding and the application of adhesive joints. Following the up-to-date "adhesive bonding roadmap", managing a production process will embrace non-destructive testing, 100% monitoring in production, networked systems and sensors, quality assurance and practical NDT [13].

What foundation has been laid in this regard over the past three decades? What contributions have promoted the progress beyond that which this book and its authors intend to highlight? In 1989, Light and Kwun described in a state-of-the-art report "the bonding process, the destructive methods used to measure bond strength, and the

various NDE methods that have been evaluated for determining the quality of a bond. These NDE methods include sonics, ultrasonics, acoustic emission, nuclear magnetic resonance, X-ray and neutron radiography, optical holography, and thermography". They concluded that with respect to non-destructive evaluation (NDE), "each of these methods has shown some limited success in detecting debond conditions", and that "at the present time" partially a "potential capability to differentiate *qualitatively* the gradations between a good bond and a debond" is ascertainable, which may "provide a correlation to bond strength" [30]. Approximately ten years later, in the EUREKA EU716 project [32] it was claimed that in adhesive bonding processes "continuous monitoring and compliance with documented procedures are required to provide assurance of quality" because adhesive bonding is a special process. The "application of general quality management systems already in place in manufacturing industry" was one of the aims of this 3-year collaborative project between the Centre for Adhesives Technology at The Welding Institute (TWI), Cranfield University and the Department for Trade and Industry (DTI). The project "identified that highlighting design and production issue during very early stages of design" and "well before a component reaches the production stage … enabled potential problem areas to be recognised and avoided". We will return to this latter (design) aspect and begin by reporting the details observed by researchers two decades ago.

In contact with eleven enterprises and institutions, exemplary manufacturing process checklists were completed in the EUREKA EU716 project by following the subsequent aspects/factors for describing and documenting the (two) adherends of adhesive joints:

- Description of the part,
- Manufacturer,
- Grade,
- Incoming specification,
- Supplier QA status, e.g. ISO 9001,
- Acceptance test(s),
- Sampling basis,
- Key attributes (critical factors), e.g. physical form, chemical composition, mechanical properties,
- Shape (critical factors), e.g. dimensions, tolerance,
- Surface condition (critical factors), e.g. as received, known contamination (like oil, grease, moisture, mould release agents, dust, dirt), existing coating,
- Required surface condition prior to bonding,
- Pre-treatment(s), listing process, materials, monitoring methods.

Among the required surface conditions prior to bonding, several of the following aspects were typically indicated by the contributing manufacturers:

- Not specified,
- No damage, e.g. intact peel-ply,
- Clean (we comment that from our viewpoint this could be "cleaned", i.e. with a cleaning process having been performed), grease-free, dirt-free,

- Free of loose cement, gravel or dirt,
- Dry,
- No contamination from preceding processes (steps), e.g. free from abrasion debris,
- Untreated, or with pre-treatment (e.g. passivation, abrasion, as-processed, primer application) and optionally with calibration within 1 h of bonding,
- Surface tension >56 mN/m,
- Less than a maximum number of pin-holes per length (or area),
- Sterile.

Among the monitoring methods for pre-treatments, typically one aspect among the following optional methods was specified by the manufacturers:

- None,
- Operator control (for a solvent cleaning process),
- Visual examination, e.g. colour, side to be bonded, no evidence of contamination, clean and dull appearance of (abraded) surfaces, reflectivity, thickness control, optionally with specified illumination (e.g. strobe light),
- Surface temperature,
- Surface tension, e.g. ink,
- Non-oiled, handling kept to a minimum.

Further aspects recommended in the EUREKA EU 716 report to be considered for adherend materials checklists were appearance, surface energy, exposure, handling, storage, and despatch. We would like to highlight in this context that with a technological background the (informative) Annex A within "Adhesive bonding of railway vehicles and parts—Part 2: Qualification of manufacturer of adhesive bonded materials, English translation of DIN 6701-2:2015-12" [45] comprises an overview of relevant aspects ranging from assessing the main function of the bond, surface preparation, type of adhesive used, testing and degree of mechanisation.

The numerous and often rather qualitative selected aspects concerning the state of the adherend surface(s) before the application of the adhesive system reflect concerns that are common in adhesive bonding technology and which address the area that will contribute to the bond line of the resulting joint. The integrity of this region often is considered "a significant 'Achilles heel' in the outright acceptance of adhesive bonding in structural engineering" [46]. Following M. Michaloudaki, who refers to the situation prevailing in 2005, "the predominant strategy to quality assurance is based on destructive testing of the bonded joint with subsequent statistical evaluation". She points out that "this procedure is combined with high costs and does not allow 100% controlling of the components or a repair of defects occurring during manufacturing" and, moreover, that such "testing itself or process mistakes during manufacturing (e.g. false applicator nozzle positioning) inevitably lead to product waste". Essentially at the same time, M. Davis, a Principal Research Scientist at the Directorate General Technical Airworthiness of the Royal Australian Air Force attending a workshop of the Federal Aviation Administration in 2004 [47], reported some observations considered characteristic for applying adhesive bonding technology for the construction and repair of (military) aircraft structures. The author

considered surface preparation to be the "most significant factor in long term bond durability", and claimed that failures are often "caused by ineffective processes not just contamination". He concluded that "a clean surface alone is not sufficient" and that "process specifications are useless unless properly validated". Among the "causes of service bond failures", the author listed "inappropriate quality assurance tests". With this respect, he reported that "NDT only tells of bond-line gaps", which may be a reason why "you never hear reports about good bonds". The situation that "some OEMs claim good bonds, blame failures on operators" might be overcome by a quality management that including as best practice "to manage quality through the process, not just to measure it after bonding". The author highlighted that with respect to repair bonding, "requirements are the same as construction" but "the processes are different", e.g. with regards to surface preparation or the heating and pressurisation because heater blankets and vacuum bags are often used instead of autoclaves during production. We would like to highlight the essential aspect of quantifying the process quality implied in these observations—an approach that has typically been based on mechanical characteristics in the past decade. Glancing at adhesive bonding as a substantial and complex technology, Niermann et al. [48–50], when reviewing and discussing quality assurance aspects, outlined the distinct phases and respective process steps, finally flowing into the manufacture of a well-designed adhesive joint, i.e. the planning, concept, design and final development as well as the production and the usage phases, which require cross-process quality assurance measures. A guiding mechanical principle was highlighted for proving usage safety: the load capacity throughout the service life must be greater than the expected loads. The authors stressed that in production, processing parameters are to be defined by manufacturers for cleaning and pre-treatment products, primers and adhesives, and—above all—that these must be observed. Any change in the parameters should occur (after being authorised) only after testing. Certified training courses in quality assurance measures for bonding technology were identified to help recognise and prevent errors from the beginning, and these were highlighted as an essential tool for quality assurance in adhesive bonding [50].

In this context of a complex technology based on numerous process steps, from a current viewpoint we would like to highlight again the relevance of the process chain characteristics when manufacturing adhesively bonded joints. Interfaces for handing over the operands from one process step to the next need to be as carefully addressed as the interphases between each adherend and the adhesive system. Global sourcing from multiple sources may result in process steps being performed at different locations and with a certain time delay, accompanied by storage, conditioning or transport operations [51]. For example, a cleaning step preceding the bonding steps is contained in most adhesive bonding processes. The process management in parts cleaning aims at ensuring "sufficient parts cleanliness as required for the respective follow-up process" with a minimal consumption of resources [52]. Consequently, within the bonding process chain an interface-comprehensive quality assurance concept is required, e.g. involving expertise from cleaning specialists and bonding specialists. Moreover, the exchange of quality-related information on the state of the operands is expected to be especially intensive at such interfaces, and

in practice an all-over monitoring is aspired to, reliably linking the process steps to literally form a chain.

One accepted approach for assessing quality-related information about the state of the operands is to introduce a process-control specimen which (i) accompanies the production (or repair) parts throughout the phases of cleaning, assembly and cure [45, 53], and (ii) remains accessible in the cured state for destructive testing, thus documenting the effects of the performed bonding process. A second approach is highlighted in this book and is based on extended NDT, comprising (i) in-process monitoring of the actual operands by performing time-dependent control within the very regions of technological relevance and (ii) post-process characterisation of the resulting adhesive joints.

Generally speaking, we consider the objective in applying techniques to monitor materials in the frame of manufacturing processes the same as two decades ago: contributing to collecting and documenting facts [32] which support safeguarding the compliance of the state of the material with the requirements, which are typically set during the process qualification. This objective indispensably holds true for the material state, which corresponds to the product of the manufacturing process. Concerning quality assurance in adhesive bonding technology and visualised in a pyramid model in Fig. 1.4 (which is based on Fig. 1.1), considering additional elements of upstream quality assurance is highly recommended. Technical provisions for pre-process

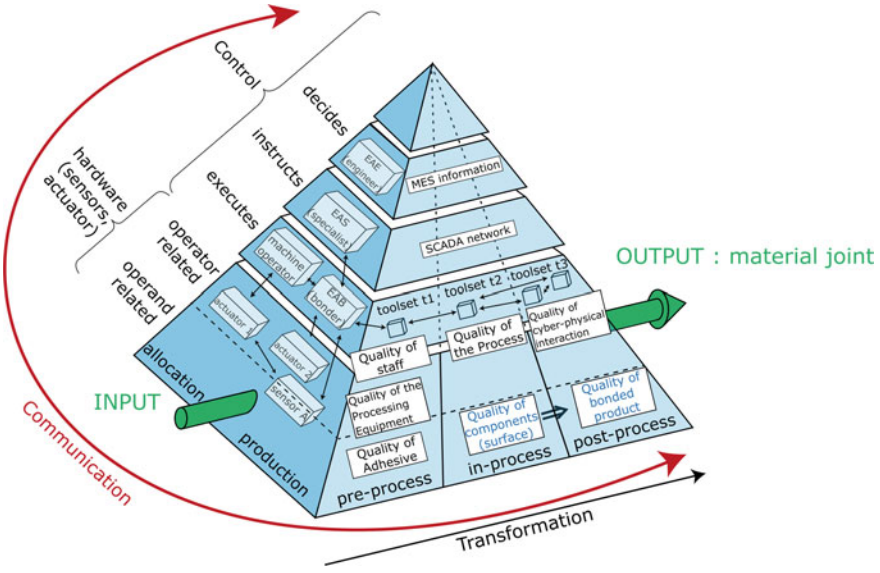

Fig. 1.4 Illustrative triangular pyramid showing actors—e.g. holding a European Adhesive Engineer (EAE) qualification—as well as material and process-related aspects contributing to quality assurance in adhesive bonding technology during manufacture or repair. The hidden and yet meaningful rearward face of the tetrahedron is related to ecological aspects. Quality topics in blue characters are the focus of the following chapters

quality assurance, e.g. incoming inspection [54], and in-process quality assurance, e.g. after each production step [9], are requested. This is because the closer to the error source within the production chain the technologically relevant amendments for clearing material state deviations from the requirements are performed, the easier, more precise, faster, more sustainable and altogether cheaper they can be. In addition for the "continuous monitoring and control of process parameters", qualified operational staff and compliance with documented procedures, as claimed by Espie et al. [32], strongly contribute to the quality of adhesively bonded products. As highlighted in Fig. 1.4, great emphasis must be placed on employee qualifications, processes, reliable testing equipment and first-class communication [51]. We recommend considering interface-comprehensive communication among humans, between humans and machines (HMI or also human-computer interaction—HCI), and exchange within cyber-physical systems (CPS) in this context.

From the analytical point of view, the implications for the monitoring techniques and processes are manifold. A suitable monitoring should facilitate a comparison between the actual states and the target states of the process and the material, i.e. the states of the operators and the operands, and relevant deviations from the qualified target state should be significantly and reliably be indicated. With the target state typically being defined by a data interval, the monitoring process shall facilitate a differentiation between, on the one hand, states corresponding to the boundaries of that interval and, on the other hand, states corresponding to the centre of that interval.

In regard to monitoring in adhesive bonding technology, the analytical requirement for an in-process monitoring process is, therefore, much less complex than predicting the extent of property deviations for the ultimately manufactured adhesive joint or predicting properties which are not accessible without destructive testing, like the initial (or even the final) joint strength (respectively fracture toughness), which is often a fundamental design specification. In other words and in view of the formalism represented by Eq. (1.1), the monitoring is clearly not intended to contribute to assessing $S'_f = \mathbf{T}'(t_f)S'_i$ in the case that the initial feature vector $S'(t_0) = S_i(t_0) + \Delta S_i$ deviates from the qualified feature vector S_i or in the case that the process characteristics $\mathbf{T}'(t_1) = \mathbf{T}(t_1) + \Delta\mathbf{T}$ deviate from the qualified ones ($\mathbf{T}(t_1)$) Rather, monitoring is intended to contribute to revealing whether $\Delta S(t_0)$, $\Delta S(t_1)$ or $\Delta\mathbf{T}(t_1)$ are acceptable based on the qualified corridors, i.e. the parameter ranges which conform with the qualification. Therefore, the analytical requirement for a monitoring process is "to look at trends and changes (or the lack of them) *over time* to reveal actions necessary to be taken with processes and the system, or to confirm that all is well" [32]. Concerning the surface properties of adherends before the application of the adhesive system in a bonding process, the lack of changes or differences as compared to the qualified process may reveal that the adherends are "ready to bond" based on the requirements of this particular process, the material combination and the application by customers. Clearly, among the required surface conditions listed above an attribute like "bondable" was not indicated, possibly due to the fact that it can hardly be considered a metric, numerical or steadily continuous material feature. In contrast, "ready to bond" is considered to refer to the feedback given to a technical operator or worker within the bonding process and is accounted for by the bonding

supervisor in charge [11]. Such feedback is based on comparative monitoring and evidence of compliance with the quality/requirement-relevant data obtained for a qualified benchmark system. Finally, from the user's point of view the monitoring should be plausibly applicable in-line, in a non-destructive way, and executed at all positions relevant to the technical properties of the product.

Further aspects intended to spur the approach between monitoring system providers and users in adhesive bonding technology will be developed in the subsequent sections.

1.2.4 Ten Heuristic Quality Assessment Principles for Adhesive Bonding Processes

In this section, we present some qualitative aspects for discussion which we consider relevant for assessing quality assurance in adhesive bonding processes [55]. We call them heuristic principles and understand them here as a kind of set of pragmatic rules of thumb which will need to be refined by ongoing research; nevertheless, we have formulated and recorded them to support the reader in directing quality assessment in the direction of understanding and interpreting quality-related data rather than merely gathering them. Inherently, these principles may become a starting point for developing a guide for recommended practice. These heuristics are also intended to be principles in the sense of a starting point for iteratively improving the steps of the QA system. This improvement will contribute to further developing a superordinate quality management system that contains targeted actions in cases where the QA indicates quality-related issues. Based on experience (e.g. from the ENCOMB project [27], detailed in the subsequent section), discussions (e.g. within the ComBoNDT team [28] or with colleagues at Fraunhofer IFAM), ongoing literature studies (e.g. aspects from Nielsen's contributions concerning the usability design of user interfaces [56], or the methodology for discovery described by Kleining and Witt [57]), we propose a consideration of the following ten heuristic QA principles when targeting user-friendly quality assurance for the discovery of possible errors in adhesive bonding processes.

Heuristic Principle 1: "QA during an adhesive bonding process shall comprise the initial state of the operands, i.e. the adherends and the adhesive system, as well as their final state, i.e. the adhesive joint".

- An incoming component inspection is to be performed.
- At the start of the bonding process, i.e. at the initial time t_0, the initial state of the operands shall be characterised and documented. At best, this may include properties beyond the quality-relevant features.
- During the bonding process, the complexity of the operands' property vector may be reduced by following a feature vector, which considers surface and bulk

features. The data resulting from monitoring these features are documented within the data vector.
- At the end of the bonding process, i.e. at the final time t_f, the final state of the operands shall be characterised and documented. At best, this may include properties beyond the quality-relevant features.

Heuristic Principle 2: "QA shall comprise the time-dependent features describing the state of the operands and the acting operators".

- The process-relevant features shall be identified and then monitored during the bonding process.
- Interactions between operands and operators are only accessible if the features of all operands and operators are measured, especially close to the bonding region.
- Time intervals between measurements shall be chosen reasonably; they ultimately govern the dimensions of the data matrix which comprises the data vectors obtained at distinct points in time.
- Referring to adhesive bonding technology, the period during which QA is performed may definitely go beyond the manufacture of the joints. This means that it may encompass the manufacture of the operands themselves in addition to the application of the joint (or non-destructive testing of the obtained joint when applying application-specific operational demands).

Heuristic Principle 3: "QA shall be part of each step of an adhesive bonding process".

- The bonding process is considered a process chain of subsequent process steps, with the chronological sequence being relevant ("non-commutative steps" that follow causality).
- The time resolution of an assessment embracing the initial and final states of the operands shall be improved by pursuing QA for each step within each phase of the bonding process.
- The monitoring shall comprise process parameters (characterising the operators) and quality-relevant features (characterising the operands), and the acquired data shall be evaluated and rated following the QA approach.

Heuristic Principle 4: "The status of the QA monitoring system shall be made perceivable".

- The monitoring system shall be regularly calibrated using reference calibration standards and reference materials, and the determined status of the instrumentation shall be displayed.
- The monitoring system and the subsequent data evaluation procedure shall indicate to the adhesive bonding supervisor and to the respective worker the level of quality of the performed measurement. Measurements of low quality shall be rerun.

Heuristic Principle 5: "As a result of a QA inspection, the QA system shall give digital documentation/reports to the adhesive bonding supervisor and indications shall be passed to workers".

- The inspection system indicates information about the state of the bonding process; decisions are taken and imparted by (interacting) persons who are part of the adhesive bonding staff.
- An in-process and real-time availability of such information is often desirable during the manufacture and repair of adhesive joints.

Heuristic Principle 6: "The position inspected by the monitoring systems shall be promptly linked with the progressive position within the operand".

- User-friendly representations of spatially resolved monitoring data should be referenced to visual documentation (e.g. by scaled photographs) considering the magnifications.
- For user-friendly representations of several discrete spatially resolved quality-related data, the monitored regions of operands should be located considering their relative orientation.
- The time of the monitoring should be indicated and it should be referenced to the moment of the process start.
- Besides the spatial relationship between several monitoring devices and monitored regions, the temporal relationship between the acquired data also needs to be considered.

Heuristic Principle 7: "Consistency with the DIN 2304 standard and the qualified bonding process shall be assured".

- These are the benchmarks to be achieved during a manufacturing or repair process. Specifically, not only must non-bonding situations, such as a (local) lack of adherend pre-treatment or adhesive application as well as kissing bonds, be avoided, but also good bonds must be safeguarded and documented.
- Consider all process-relevant and application-relevant factors (in a controlled system), involving the adhesive bonding supervisor in the QA process.

Heuristic Principle 8: "QA inspection shall help to optimize the bonding and the QA processes".

- The monitoring of quality data and process data for the operands and operators as well as their evaluation and rating shall be documented.
- Workers shall be continuously educated and trained to contribute process-relevant perceptions. Subjective observations and information given by workers shall be stimulated and taken seriously and shall be documented and evaluated, aiming to make them objective.

Heuristic Principle 9: "QA data shall be collected under the paradigm of the maximum structural variation of perspectives"

- During the qualification of the manufacturing or QA processes, the expected variability of well-defined initial sample states shall be considered by scheduling intervals of acceptable feature values.
- When performing monitoring, different (modes of) ENDT techniques shall be considered. In detail, several mono-modal ENDT techniques may be applied or multi-modal techniques shall be used.
- Time-dependent or stimulus-responsive interactions between ENDT probes and the materials to be investigated shall be considered, both when documenting the parameters of the ENDT data acquisition and when elaborating ENDT procedures.

Heuristic Principle 10: "Analysis of QA data shall embrace the discovery and quantification of similarities".

- A first question to be quantitatively answered by the data analysis shall be "How big is the similarity to the qualified operand state?"
- When an error is detected, a second question to be quantitatively answered shall be: "Is the error pattern similar to known operand states which were deemed necessary to reject during qualification?"
- Check the observed changes in process parameters and quality parameters for common time-dependent trends, patterns or correlations.
- Basically, this aspect assesses part of the Industry 4.0 cyber-physical connection and smart manufacturing because it aims to gain information by understanding patterns and rooting causes to their situation and use cases [24, 37].

We anticipate that the thus assessed quality-related data sets will be amply accessed for documentation, reporting and evaluation purposes. In particular, capturing the features describing the actions of relevant operators contributes to preserving often proprietary manufacturing domain knowledge, which presently may only reside in the heads of engineering staff [21]. Evaluating the monitored operand-related features in the framework of manufacturing control will form the basis of rule-driven decisions [21], for example, determining if a certain time-dependent operand state is to be classified "in order" (or "not in order"), if actions are to be taken, or which actions are expedient. On the one hand, we expect that such rules and the recipes to be followed will be based on human reasoning in the decades to come, but the availability of binary data will help to enhance and refine the criteria upon which these rules work. On the other hand, documenting such rules themselves, the human reasoning and strategies behind them as well as the decisions taken and the formalised recipe to be followed is a task for the steady optimisation of the interacting QA and quality management systems. We assert that this task will be supported by ontologies. Therefore, we recommend applying a clear-cut taxonomy for the elements of a production or repair process, and the things or concepts which are subset to "operator" or "operand" will be specified with greater clarity, more concretely, and customised for each manufacturing site.

Assessing sets of binary data which represent quality-relevant operand features will be detailed in the following chapter. We will highlight, on the one hand, CFRP adherends and adhesive joints thereof as exemplary and descriptive materials and, on

the other hand, NDT tools to monitor the quality-relevant features of CFRP adherends and/or adhesive joints thereof in the frame of quality assessment. Afterwards, we will introduce a concept for quality assessment in adhesive bonding which is based on these environments, our experience and human reasoning.

1.2.5 Extended Non-destructive Testing for Bonding CFRP

In this section, we do not comprehensively survey all ENDT approaches, but instead focus on the characterisation of composites based on fibre-reinforced polymers (FRP), especially carbon FRP (CFRP), distinguished by layers made from electrically conductive long fibres. We may highlight that the performance of adhesively bonded joints manufactured from such composite materials depends on the intensity of the operational loads to which the adhesive bond is exposed during in-service operation (e.g. of an aircraft), on the density and size of defects such as debonds, pores and delamination, and on the physico-chemical properties of the adhesive bond. While the operational, environmental and mechanical loads are considered in the structural design, the question remains as to how issues regarding the quality assessment of the joints contemplated here were considered and tackled at the end of the first decade of the third millennium.

In a nutshell, we may state that the defects in the joint area could (and still can) be detected by means of conventional NDT. However, there were no methods available to test the physico-chemical properties of adhesive bonds. In more detail, we present the complex line-up starting with the requirements for the said joints and the main parameters affecting the product quality, which comprise the surface treatment, joint configuration, geometric and material parameters, and failure mode [34, 58]. In their recent review, Budhe et al. stress that the durability of adhesive joints is governed by environmental factors such as temperature and moisture (including pre-bond moisture). Especially in the manufacture of automotive parts made from CFRP, variations in material quality (e.g. the thickness of the fibre-covering polymer matrix) or a variety of different contaminations, to some extent with considerably varying surface concentrations [16, 59, 60], call for the implementation of in-process surface quality monitoring, e.g. using scattered light technology. Concerning the repair of FRP structures, as for any substrate "skilled repair technicians, good surface preparation, well-designed repair procedures and the use of first-rate materials" are required [61]. The National Composites Network Best Practice Guide further highlights "stringent quality control encompassing reliable damage detection, surface cleanliness and texturing examination, drying to known limits, undertaking work within permitted temperature and humidity envelopes, and controlling resin cure to manufacturers' recommendations", "followed by NDT inspection of the finished repair or destructive testing of sample coupons or bars". During a typical repair procedure, thorough cleaning and degreasing may be succeeded by a water-break test and thorough drying [61]. After finishing the repair, inspection and certification of the resulting outcome are recommended [61].

Considering the quality assessment in more detail, the available NDT tools which can be applied during the production of FRP composites comprise facilities for monitoring the flow front, curing degree, void content, and possible delaminations (between matrix and fibres), for which established and various techniques are available, e.g. based on the electromagnetic, optical, mechanical or thermo-dynamical properties [17]. We may summarise that quality assurance processes for adhesively bonded CFRP primary structures that are not load-critical existed and were applied. Adhesively bonded structures were (and are) inspected by means of such conventional NDT in order to detect defects like pores, debonds or delaminations in the joint area. The materials (e.g. adhesives, prepreg materials) and process parameters (e.g. surface treatment, curing) were also controlled and monitored. In addition, specimens that had run through the complete manufacturing cycle were tested by both non-destructive and destructive methods to identify systematic process failures. However, in order to ensure the performance of adhesively joined load-critical CFRP structures, technologies suitable for the detection of the adhesion properties of bonded components were required [27]. Driven by central challenges within the aeronautics industry and with the above-mentioned requirements set, the ensuing development and adaptation of ENDT methods for the pre- and post-bond inspection of CFRP aircraft structural components is ongoing [62], and it is being expedited as a basis for establishing a reliable quality assurance concept for adhesive bonding. Briefly, as introduced in the ENCOMB project [27], the principle of such ENDT methods is based on the detection of selected physico-chemical properties which are important for the performance of an adhesive bond. Within the ENCOMB consortium, leading experts in aeronautics research and development from ten European countries cooperated to provide advanced non-destructive testing methods for reliable quality assurance of adhesive bonds in CFRP structural components, respecting the fundamental aspects most relevant from a manufacturer's and ENDT user's point of view. The constellation is schematically depicted in Fig. 1.5.

Two essential questions to be answered during the ENCOMB project were the following:

- From the point of view of the manufacturing process: "Which changes in which physico-chemical properties of the adherend surfaces and adhesives (i.e. the discrete operands) result in which changes to the properties of the adhesive bonds (between the joined operands), such as mechanical strength?"
- From the point of view of a feasible monitoring process: "Does a deviation in the state of the monitored operands influence the state and distribution of the detected (set of) probe(s) P_d?"

Concerning the physico-chemical properties of adherend surfaces, the degree of contamination or the type and level of surface pre-treatment, for example, needs to be considered. The physico-chemical properties of adhesives depend on a range of conditions, from the curing parameters and age of the adhesive, to the application parameters and ambient conditions. The adhesion, the morphology of the interphase and the cohesion of the cured adhesive are a direct product of these properties and

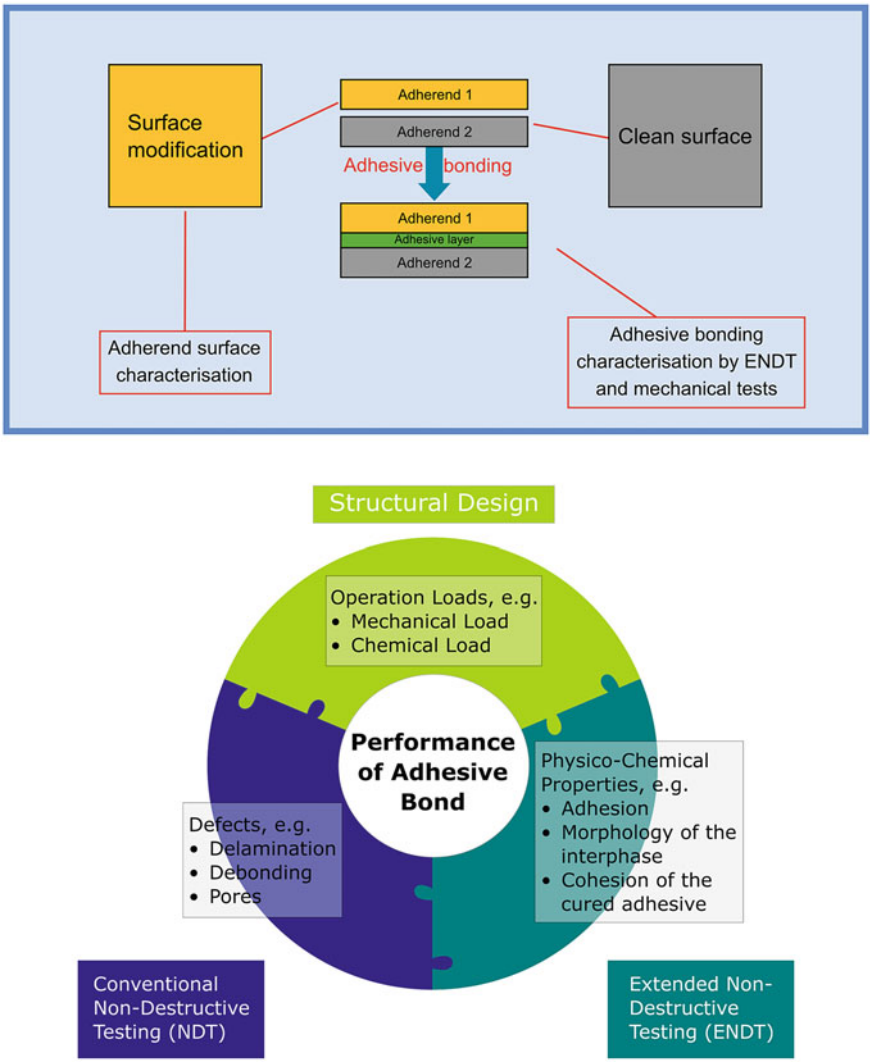

Fig. 1.5 The target and procedure of the ENCOMB project [27]. The focus of this project was to identify, develop and then adapt methods that are suitable for the assessment of adhesive bond quality, comprising investigations of CFRP adherend surfaces and adhesives. Not only the detection capabilities but also the sensitivity of measuring techniques were tested, evaluated and improved in order to achieve analytical results that could be quantified

are fundamental to the strength and durability of the adhesive joint. If the physico-chemical properties of adhesive bonds are not sufficient, then adhesion failure, weak bonds or bonds that weaken in-service can occur. Based on this rationale, ENCOMB identified and provided promising and developable non-destructive testing (NDT) methods for the pre- and post-bond inspection of CFRP aircraft structural components. State-of-the-art NDT techniques were screened, with the most suitable being adapted to important application scenarios with regard to aircraft manufacturing and in-service repair; finally, the performance was validated.

From the point of view of joint manufacture, the physico-chemical properties of CFRP adherend surfaces and the quality of the adhesive bonds were affected by intentionally applying different contamination levels down to the threshold levels of an insignificant impact on bond strength. From the point of view of identifying capable ENDT technologies, a screening was performed from among 31 technologies. Technologies facilitating a differentiation between treated specimens and a clean reference specimen were then adapted and validated in five different application scenarios that had been identified as being of primary importance for aircraft manufacturers. For each of the application scenarios, several techniques were developed that were able to detect different contamination levels and that had passed the validation step. Furthermore, several techniques with good potential were also developed further to comply with the requirements.

With these advancements in mind, we may state that research and development in extended non-destructive testing have been ongoing for over a decade, and the advances are increasingly providing tools and procedures for approaching the technical aspects of quality assessment in adhesive bonding technology. The trends we perceive in terms of progress in monitoring and the growing impact facilitated by ENDT are highlighted in Fig. 1.6.

Details of several promising ENDT techniques as well as their present performance and future potential in adhesive bonding technology are presented in the subsequent chapters. The contributions in this book highlight the development status which, as compared to ten years ago, clearly exceeds the prototyping stage, as will be substantiated by the assessment of the respectively accomplished technology readiness level (TRL). That being said, we are aware that the development of ENDT techniques is at present very dynamic, and we are confident that further progress will be achieved over the decade to come, motivated by the increasing interactions and exchange of views between specialists in the fields of monitoring, quality assurance and the manufacture and application of adhesive joints, accompanied by increasing standardisation.

To exemplify the technological perspectives of ENDT for the decade to come, we will focus on two of the surface-sensitive ENDT techniques, namely the aerosol wetting test (AWT) and optically stimulated electron emission (OSEE), and deduce advancements that may be achieved based on evaluating the dynamics of the respective measuring processes. Presently, key information is gained from the signals measured after a certain fixed period of time, starting with the deposition of primary liquid droplets or with the ultraviolet light illumination of the solid adherend surface, respectively. This observation implies on the one hand that these time periods need

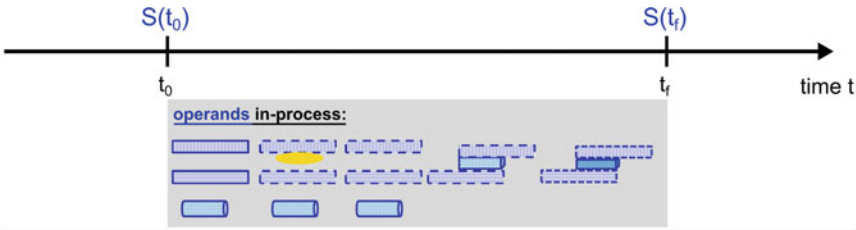

Inspection					
pre-process		in-process		post-process	
frequency	non-destructive	**frequency**	**non-destructive**	frequency	non-destructive
in 2010 (before ENCOMB project):					
random	**0** (laboratory: +)	random	- (visual: +)	up to 100 %	**0** (strength: -)
in 2018 (after ComBoNDT project):					
100 %	+	**100 %**	**+ (extended NDT)**	100 %	+

Fig. 1.6 The fields of application for the inspection of operand-related and process-relevant material features, considering the schedule of an adhesive bonding process and thus, comprising incoming inspection, manufacturing (or repair) inspection, and final inspection. The domain for ENDT inspection is shaded blue, and the basic contributions achieved in the ENCOMB [27] and ComBoNDT [28] projects are highlighted. We evaluated the availability and distribution of the respective inspection tools and procedures qualitatively and indicate our rating by "+" (widespread), "0" (temporary), or "–" (rather rare)

to be carefully documented among the ENDT measuring conditions in the respective metadata set. We expect that this will call attention towards standardising formats for documenting these metadata, e.g. for achieving interoperability, for instance, following the approach developed by Allotrope Foundation [36]. On the other hand, any observed time-dependent effects on the data may provide additional information about the adherend surface state and may even be purposefully triggered or stimulated. For the examples of AWT or OSEE based surface inspection, additionally accessible adherend surface properties might be the rate of liquid (droplet) evaporation or the electrical charging upon electron emission. Prospectively, the optically stimulated electron emission of an adherend surface may be purposefully modified by the stimulus, which is temporarily effective during an AWT measurement, i.e. by the deposition of aerosol droplets. A stimulus-responsive ENDT (SR-ENDT) approach may be realised in this way [63].

As anticipated in Fig. 1.6 and as a first-hand example of advancing ENDT towards a new and hopefully brilliant horizon, the following scope of this book is attributed to the progress and outcomes of the three-year Horizon 2020 European research project ComBoNDT [28].

1.2.6 Concepts for ENDT and Quality Assessment in Adhesive Bonding

In this section, as a consequence of the above-mentioned considerations for ENDT and quality assessment in adhesive bonding, we exemplarily describe for the reader a feasible concept which complies with the ten heuristics and the systematics upon which the approaches described above are based, while also providing a comprehensive and customisable toolbox and schedule for implementing monitoring-based decisions in a quality assurance system.

Following this concept, sets of several empirically obtained correlations will have to be compiled between, on the one hand, destructively tested quantitative and design-relevant joint features and, on the other hand, operand-based quality data measured during the manufacture or repair of adhesive joints using ENDT. Each correlation is obtained by systematically introducing disturbances of one operator-related process feature (as performed within the ENCOMB project [27]), or even by introducing disturbances of several process features together in a set (as performed within the ComBoNDT project [28]). For example, a disturbance of one operator-related process feature might be due to contacting the adherend surface, such as when the finger of a worker touches freshly cleaned CFRP material. As a consequence, a deviation of the material state from the requirements may result because during the contact time some material may have been transferred from the finger to the CFRP surface. Strictly speaking, the process characterised by accidentally touching the surface may be referred to as a contamination (or a contamination operation), while the material transferred as an effect of this process is a contaminant (or contamination agent) affecting the CFRP surface quality. While bearing in mind the differences in meaning behind the words, the contemplated phenomenon might simply be referred to as a contamination. However, the exemplified approach based on semantics highlights that consciously recognising the cause-and-effect chain during a process chain is a basic element of the quality assurance process, which may be built on monitoring causes or effects (or even both) in the course of the quality assessment.

The working hypothesis behind the concept that we introduce to the reader is the following. If all feasible (or pragmatically all imaginable) disturbances of process features are identified, implemented and their effects tested, then such a set of all feasible (or imaginable) empirically obtained correlations (based on the respectively measured ENDT data sets and the data sets resulting from testing quantitative and design-relevant joint features) will reveal

- Whether applying selected ENDT investigations will to a full extent provide quality data that allow an identification (during the manufacture or repair process) of all feasible (or imaginable) joints that will not fulfil the design-relevant joint requirements as given by the qualification procedure;
- Whether one or several ENDT methods (or the measurement modes of multi-modal ENDT tools) will be necessary to obtain a set of quality-related data which covers and provides significant quality-relevant information for all feasible (or imaginable) disturbances of process features;

- Which measures of quality assurance are required in order to clear the detected distinctive quality-related operand features of the particular joint;
- What the consequences are when potentially clearing quality-assurance actions are taken in response to detecting a "not in order" state of the operands (already during manufacture or repair);
- Which operator-based measures of quality assurance are required in order to avoid a recurrence of the observed variation in quality.

The concept thus relies on evaluating experimentally acquired data sets, and we intend to devise a way towards an elaborate data acquisition process on the basis of the following steps:

- The identification and quantification of feasible (or pragmatically all imaginable) disturbances of process features;
- The separate or combined implementation of the identified and quantified disturbances in the fabrication of specimens, e.g. adhesive joints; testing and quantifying the effects of an implemented quantified disturbance applying;
  - An in-process quality assessment of operand-related features (e.g. using ENDT approaches and methods), specifying both the limit and the probability of detection (POD);
  - A post-process assessment of quantitative and design-relevant operand features (e.g. performing destructive testing to determine the strength or fracture toughness, including an inspection of the fracture pattern);
- Plotting the data set obtained by post-process assessment against the data set resulting from in-process assessment, highlighting the significance of the considered operand feature for the quality of the product, with the obtained relationship being specific for each implemented disturbance.

We are aware that applying (at least) the integral parts of such a concept is presently becoming increasingly widespread and is entering the phase of research, development and technology [15, 16, 63, 64]. In this book, we highlight the usefulness of our application-oriented approach in a descriptive and concrete way.

The subsequently discussed set of sketches shown in Fig. 1.7 displays how an application-relevant "not in order" statement which is based on destructively testing quantitative and design-relevant operand features (denoted as Y), may be translated to a threshold criterion related to an ENDT data set that comprises information on quality-relevant operand features (denoted as y). In Fig. 1.7 we imply that instead of the directly measured quality-relevant operand feature itself, its deviation from the value obtained during the process qualification is considered. In an example of use based on non-destructive quality assessment in adhesive bonding manufacturing, we note on the one hand that following a common qualification procedure the design-relevant operands feature Y may be joint strength, as obtained in a defined test bench for as-manufactured or aged adhesive joints. On the other hand, following an expedient ENDT monitoring procedure, a quality-relevant operand feature y may be the surface wetting behaviour of one adherend, as obtained with a process-integrated

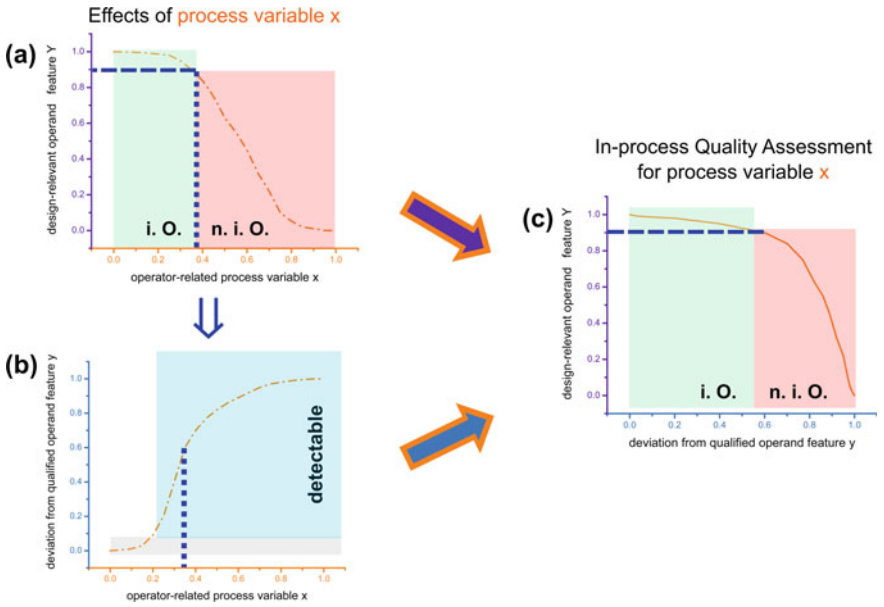

Fig. 1.7 Schematic introduction to the concept of ENDT and quality assessment in manufacturing processes, e.g. in adhesive bonding. For exemplification, the two functions y(x), and Y(x) were selected as one-to-one functions in a way that for each value of operator-related process variables, i.e. x, one value results in each one of the operand features y or Y. Y represents a design-relevant operand feature, and y represents a quality-relevant operand feature. On the left column of the plots, the functions Y(x) and y(x) are displayed, and on the right column the correlation $Y(y)|_x$ is shown, tied with the boundary condition that the regarded process variable is x. More details can be found in the text

setup prior to the bonding step. Basically, the correlation $Y(y)|_x$ links two observable responses of testing procedures, with a Y and y pair being obtained for the same disturbance x of the qualified bonding process.

We would like to accentuate that this set of sketches in Fig. 1.7 illustrates the following:

- Figure 1.7a shows that the accuracy of the experimental approach may iteratively be optimised aiming at finally introducing any disturbance in a way that its grading (e.g. represented by levels of intentionally applied contamination) is particularly fine around the crucial value of the regarded process variable (denoted here as x), which corresponds to the "in order"/"not in order" transition point of the design-relevant operand feature Y; we would like to highlight here that such an optimisation was one of the advancements achieved in the ComBoNDT project as compared to the ENCOMB project;
- Figure 1.7b shows that variations around the crucial value of the regarded process feature x should manifest in significant signal alterations upon an in-process assessment of quality-relevant data y (e.g. concerning the signal obtained when

applying ENDT; a minimum requirement is thus that the respective feature is detectable by the ENDT investigation);

- Figure 1.7c shows that the result of an in-process quality assessment might anticipate the "in order"/"not in order" categorisation which will be revealed by the post-process inspection $Y(y)|_x$ of the manufactured specimen only if precisely that investigated process feature x is the only uncontrolled feature of the inspected process;

We would like to accentuate that the set of sketches in Fig. 1.8 aims at a more elaborate contemplation and illustrates the following:

- Figure 1.8a corresponds to Fig. 1.7c and is related to effects resulting from the impact of process variable x.
- Figure 1.8c, d, which are similar to Fig. 1.7a, b but address a different process variable (namely $X \neq x$), show that the progression of the characteristic line y(X) is sketched differently from y(x), which is done to indicate that it is usually specific, e.g. for the respective intentionally applied contaminations;

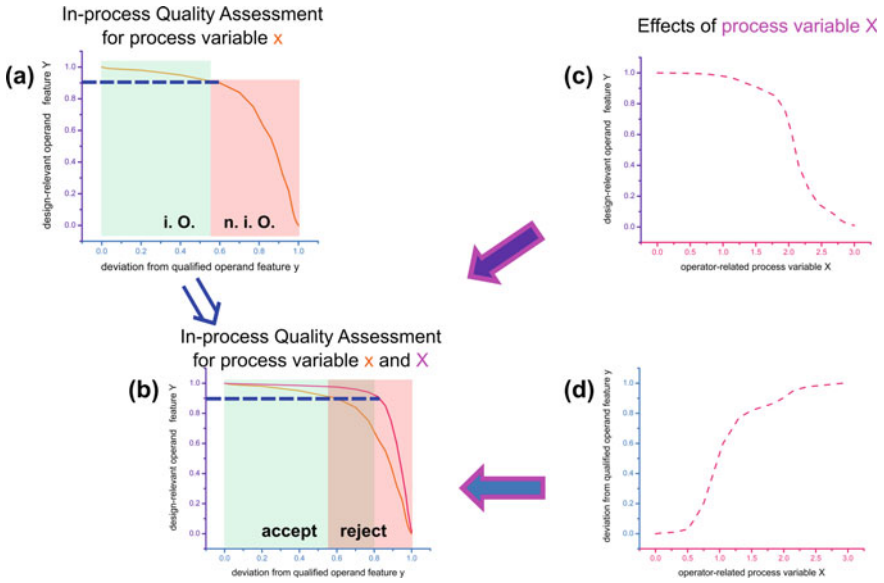

Fig. 1.8 The elaborated concept of ENDT and quality assessment in manufacturing processes, e.g. adhesive bonding, which is central to this book. For exemplification, the four functions y(x), Y(x) as well as y(X) and Y(X) were finally selected as one-to-one functions in a way that for each value of operator-related process variables, i.e. either x or X, one value results in each one of the operand features y or Y. Y represents a design-relevant operand feature, and y represents a quality-relevant operand feature. In the left column of the plots, the functions $Y(y)|_x$ and finally both the functions $Y(y)|_x$ and $Y(y)|_X$ are displayed (in plots a and b, respectively). More details can be found in the text

- Figure 1.8b, which is the aggregation of the sketches in Fig. 1.8a, c, d, shows that to avoid false positives, the decision to set a threshold value in a binary in-process categorisation is governed by the most sensitively detected process disturbance whenever more than one process variable may not be controlled in-process.

We prominently applied the presented concept in the ComBoNDT project [28], which is introduced in the next section.

1.3 Recent Joint Research for Advancing QA in Adhesive Bonding

In the following subsections of the present chapter, we will introduce the reader to the framework of the joint research project "Quality assurance concepts for adhesive bonding of aircraft composite structures by advanced NDT" (ComBoNDT) [28] and address its characteristics as well as the beating heart of this project, namely our consortium. This project received funding from the European Union's Horizon 2020 research and innovation programme under grant agreement No. 636494 and our consortium was active from 01-05-2015 to 30-04-2018 to achieve substantial progress beyond the starting position described in the previous chapter. The present book is based on the advances for quality assessment in adhesive bonding technology which were achieved over the course of the EU Framework Programme for Research and Innovation aspiring for smart, green and integrated transport. Briefly, the input and the output provided by the ComBoNDT project is essential but not confining for this book, and all authors of this book contributed to this project.

Subsequently, we will detail the overall concept, the goals pursued in this book, the step-by-step planning towards the achievement of the goals, the strategies followed as well as the intended impact according to the project workflow.

1.3.1 Objectives and Rationale

The context in which we were working had previously been defined by the key performance indicators (KPI) of the European aeronautics industry as defined by Flight Path 2050 "Maintaining and extending industrial leadership" [65]. Among these KPI, "process time reduction 80%, cost reduction 70%, and competitiveness of products produced in Europe compared with those produced in low labor cost countries" were the key factors inspiring the activities performed early in the second decade of the third millennium. To this end, we aimed at the development of ENDT tools for CFRP, adherend surfaces and bonded CFRP joints that could potentially cope with the technological problem in two ways:

- Safety improvement and cost reduction for building this kind of structure due to more reliable and longer lasting adhesively bonded joints
- Augmentation of the competitiveness of the European aeronautics industry by adopting such lightweight structures and joints, which may lead to a further cost reduction and greener air transport

More precisely, even though there is a strong need to exploit the potentials of lightweight CFRP structures in the aeronautic industry alongside the application of adhesively bonded joints, their adequacy for primary aircraft structures remains low. Despite the advances made in this sector as well as previous attempts, the shortcomings observed were caused mainly by the absence of adequate quality assurance processes. The corresponding requirements concerning the quality assurance of the manufacturing process of load-critical CFRP structures are particularly high, as potential failures could directly affect the overall safety of an aircraft.

Considering the above-mentioned aspects, the implementation of reliable adhesive bonding processes through advanced quality assurance would lead to the increased development of highly integrated structures with an optimum combination of advanced composite materials, which would, in turn, minimise the use of the rivet-based assembly. Consequently, metallic assembly concepts would potentially be surpassed through a redesigning of the structures. The benefits of such a procedure can be crucial, especially in the field of weight saving, which may be expected to amount up to 15% in the case of the fuselage airframe. This could have further positive effects on the size and weight of other aircraft parts, such as the engines or the landing gear, causing in parallel a reduction in both the fuel consumption per passenger-kilometre and the operating aircraft costs. Furthermore, a significant reduction in greenhouse gas emissions (CO_2) would contribute to the mitigation of climate change and further improve the environmental performance of the transportation sector.

The already established quality assurance processes for adhesively bonded CFRP non-critical load structures are based on measurements using methods suitable for the detection of potential defects (pores, debonds, delaminations) in the joint area. However, using such conventional NDT methods does not facilitate a detection of any further defects of interest, such as kissing bonds, nor does it assess the weakening of a geometrically intact bondline. Thus, the development of quality assurance processes which, on the one hand, provide a correlation to the physico-chemical properties of the probed adherends and adhesives and, on the other hand, could make the adhesion properties of bonded components accessible had to be spurred. This goal also met the EASA (European Aviation Safety Agency) certification requirements for structural bonding [66]. Our research and development (R&D) in ENDT techniques aimed at establishing reproducible and reliable non-destructive inspection tools in order to ensure the manufacture of joint structures that reliably feature the required strength.

In a nutshell, our overall objective was to develop a quality assurance concept for the adhesive bonding of load-critical CFRP primary aircraft structures, which could be applicable within the whole life cycle of the aircraft to overcome the current limitations regarding the certification of composites. Therefore, we established a detailed

approach regarding in-line ENDT for CFRP materials at an increased technological readiness level (TRL), both in-process and post-process.

Applying ENDT technologies, we aimed to overcome the limitations of conventional NDT methods and allow the reliable assessment of the surface state of CFRP adherends as well as the quality of the final adhesive joint. We focused on the implementation of previously developed ENDT techniques, their assessment and, potentially, the increment of their TRL. The integration of these techniques into future adhesive bonding process chains, quality assurance concepts and material testing for maintenance processes could pave the way for the safe and reliable integration of lightweight structures into aircraft design. Applying the bonding of complex lightweight structures and the replacement of the traditional riveting method may overcome the use of CFRP as a "black metal".

Among the most important topics to which the book aims to contribute is the establishment and strengthening of the production and material testing processes at all stages of an aircraft's lifecycle using the previously mentioned quality assurance concepts. A fast and precise detection of surface contaminations and defects like kissing bonds in bondlines could help save time (up to 70% time savings using ENDT) during production, maintenance, overhaul, repair and retrofit. This way, aircraft parts could be checked for contaminants without disassembly or time-consuming steps. Also, parts of the aircraft could be replaced or fixed when necessary, resulting in up to 50% higher cost efficiency for ground operations. All of the above will significantly contribute to the competitiveness of the European aircraft sector.

The advancement of highly promising ENDT technologies was necessarily tested and demonstrated exemplarily in the frame of two fields of application, namely aircraft manufacture and in-service bonded repair. These fields of application determine the requirements in terms of the detection capabilities (e.g. of unknown contamination), applicability and robustness (i.e. TRL) that need to be met by the ENDT technologies. The maturity of the techniques will also involve approaches concerning automation and industrialisation, which means that aspects like the mobility of the measurement setup, objective and unambiguous data evaluation and interpretation were also addressed. In more detail, among the main objectives for our research and development was the incrementation of the current maturity level (TRL 3–4) to a TRL of 5–6. The aim of an increased TRL was addressed both as a measurable project result and a ground-breaking step towards the implementation of the developed ENDT techniques in real application scenarios.

The improvement of material testing during manufacturing as well as ground operations (overhaul, maintenance) will allow the automation of processes that are currently performed manually. The resulting time savings (in combination with more reliable results) should also be utilised to obtain measurable results by comparing the state-of-the-art process with the newly developed techniques. An important step was therefore the determination and improvement of the performance of ENDT in terms of the speed of inspection and data evaluation (aim: 10 min/m^2 of the inspection area at three to five times faster than the current state of the art).

In summary, a successful R&D process would enable

- The reliable and reproducible detection of unknown and potentially multiple contaminations on adherend surfaces;
- The reliable and reproducible detection of poor bond quality in bonded adhesive joints;
- A robustness of methods and a suitability for field measurements in aircraft manufacturing and repair environments in terms of detection limits and measuring speed;
- ENDT technique(s) which are validated in the relevant environments (TRL 5–6).

1.3.2 Concept and Approaches

Regarding the overall concept, the aircraft manufacturers within our project consortium provided the other partners with their demands and targets, aiming at the successful exploitation of the research activities. The sketch displayed in Fig. 1.9 summarises our overall conception of this book and its chapters:

We greatly benefited from the outcome of the EU FP7 project "Extended nondestructive testing of composite bonds—ENCOMB" [27], the results of which were detailed in the previous chapter. Launched back in 2010, ENCOMB involved a screening of potentially suitable techniques for the characterisation of CFRP adherend surfaces and adhesive bonds, whereby over 20 different non-destructive technologies were tested. Several contaminations or defects (e.g. a silicone-based release agent, hydraulic fluid, moisture, thermal degradation or poorly cured adhesive) were introduced to adhesively bonded CFRP joints in order to adapt the measuring techniques in such a way that the different contaminants and the resulting effects on the bond quality could be detected down to relevant threshold values

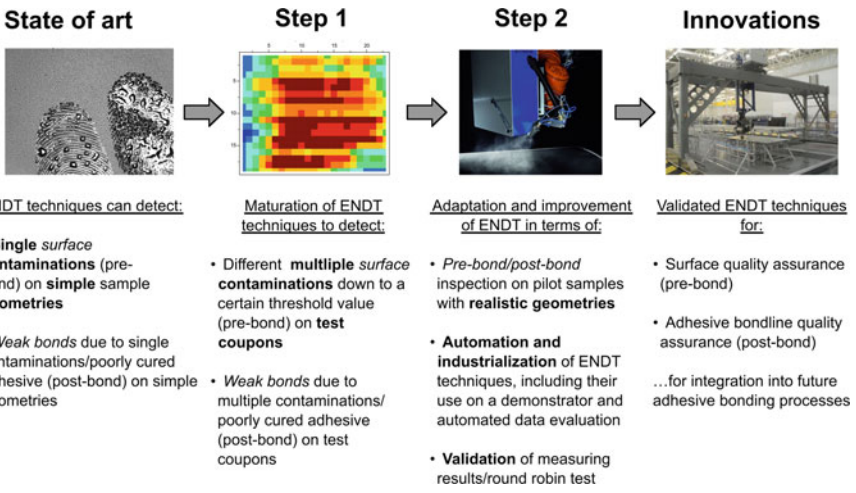

Fig. 1.9 The conception of this book and its chapters

(e.g. related to surface concentrations). Additionally, relationships were established between the degree of the pre-bond contamination and the observed degradation and the mechanical performance of the resulting adhesive joint. We briefly recall here that substantial progress was made with regard to providing the basis for an integrated approach to the quality assurance of adhesive bonding processes. Against this background, when planning the activities reported in this book, it was of strategic importance that the R&D work reported here technically and methodically enhances the most promising quality assurance concepts identified within the ENCOMB project and advances them to a TRL of 5–6.

Moreover, we aimed at additionally exploiting the knowledge gained from a series of further aeronautics and NMP projects while interacting with ongoing projects in the field that were in a parallel state of progress, e.g. CleanSky [67] and BOPACS [68]. To accelerate the further development of ENDT technologies for integration into future adhesive bonding process chains as well as allow the assessment of surface quality before bonding and the quality of the finished adhesive joint, the work within the ComBoNDT project was performed alongside test scenarios extracted from the fields of application of manufacturing and repair. Besides their relevance for manufacturing and repair, the outlined test scenarios represented as yet unanswered scientific questions, such as the effect of adherend surface contaminations on the adhesion properties, the overall bonded joint performance and the joint durability. To achieve these goals, we addressed an increase in the degree of automation in connection with a high reproducibility and an adequate measurement speed, an increase in the detection capabilities and the sensitivity of the techniques, a decrease in the costs and an adequate simplicity of handling, in particular with regard to quantifiable results.

Considering all of the above, the ENDT methods identified for further maturation in the frame of the R&D work reported here were carefully selected with respect to their suitability for the corresponding research approach. The techniques used in the project already existed in the form of laboratory setups, and their applicability was previously tested in the frameworks of other research projects. As summarised for our readers in Table 1.1, feasibility studies were demonstrated in the early phase at the beginning of this decade. To serve the book's scope, as addressed in Sect. 1.3.1 Objectives and Rationale, the selected techniques to be maturated were selected because they had previously demonstrated great applicability and effectiveness. Up to the starting point of our recent R&D work, the ENDT techniques tested met the basic requirements of a TRL up to 3 or 4. In some previously conducted projects, feasibility and accuracy were tested for some techniques, which also demonstrated capabilities of detecting and quantifying contamination and indicating failure scenarios of CFRP relevant to aeronautics (ENCOMB, ABiTAS). Among these methods, only the most promising and reliable were chosen for further investigation and improvement. Considering the objectives of this book, their accomplishment was in selecting the most promising techniques developed in previous research, as described above. Hence, the ambitious technical goal of the ComBoNDT project was to transfer the selected technologies from their current TRL state to a higher level (5 or 6). We addressed this goal through activities performed in different fields:

Table 1.1 Survey of national and international research and innovation activities connected to the ComBoNDT project

Research and innovation acronym and status	Main topics	Relation to ComBoNDT
ABiTAS [69]	Characterisation of adherend surfaces with conventional NDT with the aim of developing a robust, flexible and economic process chain for structural assembly by adhesive bonding. Surfaces after pretreatment were screened, tested and optimised	The results of in-process surface quality control of composite surfaces with the aim of achieving an increased TRL level were applied for ComBoNDT
ENCOMB [27]	Screening of more than 20 different technologies suitable for the characterisation of adherend surfaces and adhesive bonds, also those with a low TRL (1–2). Distinct contamination and degradation scenarios were introduced to the samples to test the eligibility and versatility of the techniques	Much of the knowledge from ENCOMB regarding suitable, highly promising NDT for the development of ENDT was transferred to ComBoNDT. The ENCOMB project finished in April 2014, so the full benefit of its results provided a foundation for ComBoNDT
CleanSky [67]	The influence of composite surface properties on bond durability in repair applications was studied. The pre-bond inspection of surfaces was a task in this context	The studies within ComBoNDT went beyond the work carried out in CleanSky, especially concerning the characterisation of adhesives and the testing of adhesive bonds by ENDT
BOPACS [68]	The aim of BOPACS was the weight reduction of primary aircraft structures by developing boltless adhesively bonded joints. The focus lay on the understanding of crack growth and debonding expansion mechanisms in adhesive joints with an aim of developing specific design features capable of preventing crack growth	Some partners from BOPACS were also members of the ComBoNDT consortium (Fraunhofer IFAM, Airbus Group, LTSM University of Patras). Thus, it was ensured that the findings within BOPACS were implemented in ComBoNDT

- The first step included the **test scenarios** for the project's scope as well as the sample preparation and overview of the sample measurements as previously defined by both the industrial end users and the ground operation service providers.
- The second step included the **sample preparation**, which complied with the requirements defined by the industrial partners.
- The next step was the **characterisation of pre-bond and post-bond quality** by reference methods using lab-based analytical methods. (The second and present steps were of paramount importance as a high quality of samples was imperative

to ensure reproducibility and comparability because the results of the ENDT technologies would be compared to the results of the lab methods).

- The next step included the conduction of **mechanical tests** to address the influence of contaminants on the bond strength using both established and innovative mechanical tests in samples with different levels of intentionally applied contaminants and, thus, different influences on the bond strength.
- After the completion of the mechanical tests, the next step concerned **ENDT for the quality assessment of adherend surfaces** (pre-bond inspection). The performance of the ENDT technologies was adapted and optimised regarding their sensitivity to detect the physico-chemical properties of adherend surfaces with multiple pre-bond contaminations as well as their suitability in quantifying the measuring results. This work included the further development of the technologies with regard to sensitivity, reliability, automation and mobility, the performance evaluation within real manufacturing or repair processes, and approaches for industrialisation. Another activity was performed in parallel which dealt with **ENDT for adhesive bondline quality assurance** (post-bond inspection). Within this activity, the evaluation and development of appropriate technologies with high sensitivity formed the primary interest in order to determine the bondline quality influenced by multiple pre-bond contaminations as well as to quantify the results. The sensibility, reliability, automation and mobility of the techniques were assessed by their implementation in real manufacturing or repair processes.
- A further step was the **demonstration** of the adapted and improved ENDT techniques in real application environments for both manufacturing and repair in order to reveal their suitability for future use in aeronautical industry applications.
- Another step was the **validation and technological assessment of ENDT** methods and investigations. In this part, the work was aimed specifically at the comparative evaluation of the produced innovations regarding their suitability for measurements in production or in-service environments through an assessment of their TRL (including simplicity of handling, time for data processing, detection capability, costs, lifetime, etc.), in-line capability, mobility and robustness. This activity also included probability of detection (POD) studies to evaluate the detection performance of each technique. In the frame of validation of the techniques of the project, a round-robin test was used.
- Finally, the broad **dissemination and exploitation** of the results, in parallel to the protection and safeguarding of the intellectual property rights of the partners involved in the project, was ensured, as the reader may infer from the present book.
- On the way to all these achievements, the overall **project management** was dedicated to all activities, ensuring efficient project coordination towards achieving the project's objectives.

Following the conceptualisation and throughout the course of our R&D work, distinct levels of pre-bond contamination, the influence of which was addressed via mechanical testing, needed to be previously detected and preferably discriminated by the ENDT techniques and quantitative evaluation of the quality-related data.

Table 1.2 Approaches pursued within this book, characterised by different types of test scenarios addressing the fields of application for in-plant manufacturing and in-service repair based on adhesive bonding

Sample geometry and surface state	*Fields of applications investigated*	
	ENDT for pre-bond (a) and post-bond (b) quality assurance for *manufacturing*	ENDT for pre-bond (a) and post-bond (b) quality assurance for *repair*
• Test coupons (flat surface) • Multiple contaminants	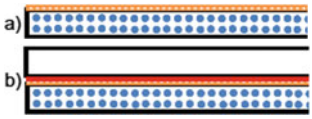	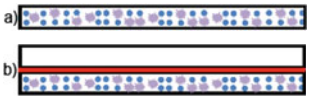
• Pilot samples (complex geometry) • Multiple contaminants	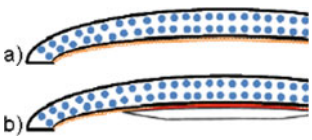	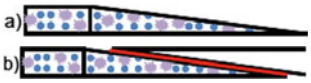
	moisture contamination release agent contamination	Skydrol© contamination adhesive bondline

From a manufacturing perspective, in the production scenarios, a contamination of adherend surfaces with, e.g. release agent and moisture was considered to be highly relevant. A variation due to the impact of moisture, hydraulic fluids such as Skydrol©, kerosene or de-icing fluid may also occur during aircraft operation. Therefore, corresponding exposures were taken into consideration for the repair test scenarios. These scenarios with contaminations, relevant for the respective field of application from manufacturing and repair, were applied to samples with increasing geometric complexity to mimic technologically relevant situations, as displayed in Table 1.2.

1.3.3 Aims and Key Aspects

The exploitation of lightweight CFRP materials for further use in aeronautic applications presupposes adhesive bonding as a very appropriate joining technology for load-critical primary structures [62] and the compliance with the appropriate certification (e.g. by the European Aviation Safety Agency, EASA). Due to the absence of an adequate quality assurance concept which can guarantee the safety of adhesively bonded joints and enable a corresponding certification, the previously mentioned exploitation was not possible. Such a quality assurance concept for adherend surfaces and the contacting bondline is crucial for load-critical bonds and must be effective. However, quality assessment exclusively involving the already existing NDT

testing methods is not considered sufficiently reliable [70]. As the major part (80–90%) of any inspection is performed visually, it is very important for advances in quality inspection that the technologically relevant effects of deviations from qualified procedures, e.g. damage, which are not accessible to human sensory perception can be sensitively detected and revealed in-process. Taking this proposition into account, a number of research projects targeted addressing and developing innovative NDT technologies in laboratory environments. These trendsetting technologies should be able to monitor the adherend surfaces and bonded joints and assess their quality-relevant features which may be affected by surface contaminations or manifest in kissing bonds. To this end, the effect of single contaminants was assessed for simple sample geometries. Nevertheless, these NDT techniques had not been tested in scenarios of multiple contaminations or on realistic three-dimensional and complex geometries.

In the frame of this book, we will highlight these tests comprising tools and procedures for in-process quality assessment using pilot samples charged with multiple contaminants; moreover, the techniques' operation and their application are demonstrated on real manufacturing and repair components. The aim is to prove their suitability and reliability for surface and bondline quality detection and compilation. This work is performed with the ultimate goal of the certification of CFRPs as the primary material in critical structural applications. Another issue is the maturation of innovative NDT methods in terms of the TRL, considering the fact that these basically had only been tested in a laboratory environment. To this end, our R&D work aimed not only at the increment of their TRL but also at building up a catalogue of criteria for an assessment of ENDT techniques applicable to adherend surfaces and bondlines of load-critical CFRP structures. In addition, within the developed concept of assessing technologically relevant quality-related features, mechanical tests of the resulting bonded joints were highlighted as necessary in order to determine the influence of contaminants up to a contamination level that shows a risk. Considering that the existing standardised methods entail a high cost and work effort, focused destructive tests providing selected specific bond strength parameters and statistics were performed. Despite this issue, the mechanical tests chosen and performed were those that appeared to be the most time and work-efficient, in addition to the most innovative ones (i.e. the centrifuge test).

Mechanical testing

More precisely, when evaluating the influence of the intentionally varied adherend surface state (clean, single or multiple contaminations) on the mechanical properties, established standardised mechanical tests like mode-I, mode-II and mixed-mode fracture toughness tests are widely used. These tests are time- and cost-consuming due to complex sample preparation, destructive single-sample testing and manual evaluation of the mechanical load and of the two obtained fracture surfaces. These limitations for standardised testing have been recognised in many previous research projects such as ENCOMB and ABiTAS. Although these significant standardised mechanical tests were knowingly chosen to be performed in the frame of our R&D work, we additionally used a new multiple sample test (centrifuge-testing) because it

was ascribed great potential to overcome the limitations of standardised tests within the BOPACS project. With this novel centrifuge test, up to eight samples can be measured within five minutes. The measured mechanical properties have previously shown accuracy with a very good precision and reproducibility. The novel testing is cost-efficient, fast and reliable, and it indeed increased the information value of mechanical testing compared to the results from standardised mechanical tests.

TRL assessment

TRLs are commonly used to evaluate the maturity of technologies (e.g. NDT techniques, pre-treatments) regarding their degree of development and applicability in industrial processes. There are several definitions of TRLs, e.g. from the EC for H2020, from the U.S. Department of Defense, NASA and ESA; however, these definitions are more general without including specific criteria for special applications. With regard to the fields of application addressed within this book (i.e. manufacturing and repair), different criteria are relevant for TRL assessment.

Establishing a satisfactory catalogue of criteria for the assessment of TRL for pre- and post-bond ENDT technologies to be used in the fields of manufacturing and repair for CFRP primary structures is a major challenge that will be elaborately assessed in this book, especially by our co-authors from industrial consortium partners experienced in manufacturing and ground services. They worked on the creation of a catalogue of requirements tailored specifically for the TRL assessment for ENDT in the chosen fields of application. With this catalogue, a distinct determination of TRL will be possible for the specific fields of application investigated within this book. With a distinct and comprehensive TRL assessment, the comparability of the test methods and the TRL improvements achieved within the project were measurable and became very clear. TRL assessment was performed according to this catalogue at the beginning (initial TRL) of our R&D work and at its end (final TRL achieved).

Monitoring of adherend surface conditions and bondline quality by in-line techniques

During the manufacturing and repair processes of CFRP materials, the quality assurance of adherend surfaces has, up to now, been performed using the water-break test for the large-area inspection of wettability properties [71]. Hydrophobic surface areas (originating from residues of, e.g. release agents or lubricants) are detected by changes in the wetting behaviour. The test is performed manually and its evaluation is done visually with an individual pair of human eyes and is, therefore, is subjective and error-prone. The water-break test is followed by time- and work-consuming drying and cleaning steps for the investigated specimens. Furthermore, water-soluble contaminants cannot be detected by this procedure (though they might have been present in the non-investigated surface regions as well), which is another disadvantage. For the inspection of small areas, contact angle or also surface energy measurements and test-inks are commonly employed. These tests only allow a monitoring of very small areas of the sample and require an additional cleaning step before bonding, and it is even recommended that they be performed adjacent to the intended bonding area, not inside it. Figure 1.10 shows a demonstrative example of applying the water-break test (left) and an ultrasonic picture of a delamination in CFRP (right).

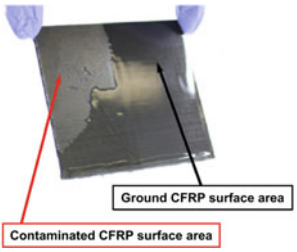

Water-break test

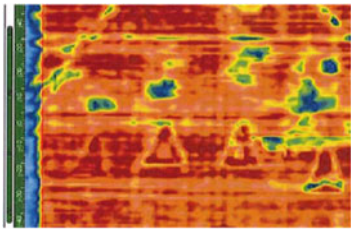

Ultrasonic picture of a delamination in CFRP

Fig. 1.10 The water-break test (left) and a state-of-the-art ultrasonic picture of the delamination (right) of CFRP

Adhesively bonded structures are also inspected by means of conventional NDT, e.g. visual inspection and audible sonic testing (tap test), to detect damages by comparing the local perception to one obtained in the vicinity or with a reference specimen. These tests are performed manually and are therefore subjective as the results depend to a great extent on the concentration, skills and experience of the operator. Furthermore, damage that is non-perceivable by unaided human senses will not be detected. More complex measuring techniques like ultrasound, thermography, shearography and radiography often need well-trained personnel and require time-consuming spectrum evaluation steps. Current conventional NDT techniques allow the detection of defects like pores, resin starvation/richness, wrinkles, discolouration (e.g. due to overheating, lightning strike), disbonding and delaminations in the joint area [72]. In addition, for ultrasound testing a couplant material such as water must be applied between the sensor and the investigated surface. Expensive re-drying and cleaning processes are therefore necessary and only single-point measurements are possible [70]. The state-of-the-art devices do not provide the necessary information for the quality assurance of adhesive joints and still have many disadvantages and shortcomings. The aforementioned state-of-the-art methods and devices are furthermore limited by the fact that defects like kissing bonds and a weakening of bonded joints cannot be detected.

Based on the results obtained within former research activities and extracted from a literature review, we carefully selected NDT technologies based on their state-of-the-art performance for further investigation in order to address these limitations. The identified technologies proved their capability to successfully detect contaminants relevant in aircraft manufacturing and in-service repair as well as to assess adhesive bond quality. All of the selected NDT techniques had the potential to reach a TRL high enough for their use in manufacturing and repair environments in order to provide quality control systems for surface and bondline inspection. The ENDT technologies that are relevant for the R&D work within this book are listed in Table 1.3 together with their main limitations in the early 2010s and the progress that was aspired to be realised within the project.

Table 1.3 State of the art, limitations of technologies and progress beyond limitations concerning ENDT for surface and bondline quality assessment contributing to quality assurance

Technology	State of the art (early 2010s)	Limitations (early 2010s)	Progress (shown in this book)
ENDT for surface quality assessment			
OSEE Optically stimulated electron emission	OSEE is a fast, contactless NDT technique to detect contaminants on surfaces. With lab setups, a detection of different contaminations is achieved	• Lab-scale for small samples; • Investigations limited to single contaminations; • Distance sensitivity and influence of surface topography unknown	Mobile detection unit for large-scale CFRP surface evaluation, influence of factors (topography, distance, mixture of contaminants) on signal rated
LIBS Laser-induced breakdown spectroscopy	Established for bulk metal and surface quality analysis Contaminations detected by spectral peak evaluation of tracer elements	• Restricted to elemental peak evaluation; • Limited to small sample sizes due to laser protection requirements; high costs	Evaluation of molecule bands including automated spectra evaluation, downsizing of the technique to reduce costs
Electronic nose	E-nose is under rapid development for gas mixture analysis, classification and quantification of components. Its suitability for ENDT purposes has been demonstrated	• Unsuitable to cope with moisture contamination; • Mixtures of contaminants not yet investigated; • High costs per device; • No onboard data analysis	Detection of contaminant mixes and water; Minimal set of sensors to lower the costs; Data analysis tools
AWT Aerosol wetting test (bonNDTinspect)	Determination of surface wetting behaviour with AWT was successfully applied for the detection of surface contaminants. Existing lab setup	• Detection of multiple contaminants not tested; • Large-area scanning and automation not yet performed	Development of automated AWT System (bonNDTinspect) for robotically operated AWT for large area scanning; Measurement of surfaces with multiple contaminants

(continued)

Table 1.3 (continued)

Technology	State of the art (early 2010s)	Limitations (early 2010s)	Progress (shown in this book)
Full-field vibrometry	Detection of cracks and delamination in CFRP demonstrated; applicable to larger samples	Applicability for surface contamination and weak bonds not yet investigated	Improvement of signal processing techniques for full wave field measurements; Signal analysis in wavenumber domain; separation of propagating wave modes; Adaptive wavenumber filtering
FTIR Fourier transform infrared spectroscopy	Used for qualitative detection of different materials; First approaches for quantitative evaluations of IR spectra by multivariate methods	Penetration depth in CFRP is restricted to the first fibre layer No experience with a combination of different contamination scenarios	Collecting absorption spectra of contaminated surfaces and evaluating the data with a multivariate method
ENDT for adhesive bondline quality assessment			
SWAT Shock waves adhesion test	Shock wave propagation used to induce localised and adjustable tensile stress within assemblies Laser shocks have proved to be efficient in a variety of samples	• Availability of shock wave generation technologies; • Difficulty to generate traction at a selected interface; • Single shock duration tests not suitable for strong bondlines	Adjustable pulsed laser and plates launcher for shock generation Numerical tool to determine adequate shock parameters
Linear and non-linear ultrasound	Linear ultrasound uses bulk and guided waves to detect changes in impedance Non-linear ultrasound relies on non-linear phenomena to detect weak bonds	• Linear ultrasound showed limitations for the detection of weak bonds • Non-linear ultrasound is hard to generate and the obtained data are difficult to interpret	Considers various guided wave modes that might be more sensitive to a lack of adhesion Considered a more powerful source. Generated non-linear effect in the kissing bond area
Electromechanical impedance	Detection of weak bonds due to release agent using piezoelectric transducer was demonstrated	• Adhesively bonding the piezoelectric transducer is required	Analysing the influence of the transducer bonding; the investigation of the proper frequency range for assessing weak bonds; the development of multivariate analysis for the features extracted from the measured electromechanical spectra; Measurement of electrical parameters without transducer

1.3.4 Impacts and Contributions

The use of CFRP as an innovative material for aircraft design has increased immensely within the few last years [22, 29, 62] (the Airbus A350 XWB is composed of up to 53% CFRP), leading to an increasing demand for both high quality and quantity of composite material and composite joints, accompanied by lower costs. Adhesive bonding as a joining technology can enable the use of the full potential of CFRP as a lightweight material for aircraft design and is already used for joining many CFRP-based aircraft parts. Admittedly, adhesive bonding has thus far not been applied for load-critical CFRP primary aircraft structures. However, it is highly desirable to facilitate adhesive bonding as a joining technology for load-critical primary structures because adhesive bonding and adhesive joints possess numerous advantages over other processes: homogeneous stress distribution, full automation capability, lightweight design, strong and even complex structure design, capability of joining two distinct materials, interesting properties in electrolytic and corrosion protection and finally high fatigue resistance furnishing a longer service lifetime compared to mechanically bonded structures.

Most of the aircraft produced nowadays contain a high amount of CFRP material and therefore require the adhesive bonding of CFRP in manufacturing, maintenance and repair [29]. From our point of view, this further emphasises the need for complete and reliable quality assurance concepts based on appropriate and resilient ENDT techniques for quality assessment. This large number of affected industry sectors leads to the huge impact of the findings and achievements reported in this book. The provision of quality assurance concepts (using ENDT techniques) for load-critical primary structures will allow the increased and optimal use of CFRP and the replacement of metallic assembly concepts resulting in weight, time and cost savings for the aeronautic and all related industries. Moreover, it directly supports the certification and continued airworthiness of repaired CFRP structures. The R&D work presented in this book is clearly aligned with this objective through the maturation, improvement and adaptation of ENDT technologies for the characterisation of, on the one hand, the CFRP adherend surface state before bonding (pre-bond) and, on the other hand, the CFRP bonded structures (post-bond) in order to establish complete and process-comprehensive quality assurance concepts. We consider this the key to overcoming current limitations for the use of CFRP in aeronautical applications.

We expect that the innovations reported in this book will result in substantial socio-economic, technical and environmental impacts. Firstly, an impact will be achieved by reinforcing the competitiveness of Europe's aircraft industry and European aircraft operators by assisting the development of high technology SMEs and by accomplishing an increment of safety resulting from more reliable components and processes, which will strengthen and augment the reputation of the European aviation and aeronautics industry. Secondly, our contributions will bring about an integration of innovative materials in aeronautics as well as automated measuring processes in combination with strong signal evaluation processes that will provide surface and structural health data and contribute significantly to the reduction of human

errors; therefore, an increment of safety will result from more reliable components and processes, weight savings of aircraft will be facilitated, and an improvement of the safety and operational capabilities of aircraft will ensue. Thirdly, a significant reduction of energy for the performance of the inspection, for the manufacturing of replacement parts and for the manufacturing of primary structures will be feasible, as will a reduction of scrapping rates during manufacture or repair and a weight reduction of aircraft.

Finally, we would like to highlight and acknowledge again the invaluable contributions resulting from the strong cooperation within the ComBoNDT consortium and promoted by the dedicated project management. The consortium consisted of eleven partners, including major European aerospace companies as well as high-level research organisations and universities experienced in aeronautics research and development. The project team consisted of aircraft manufacturers (Airbus Group; AERNNOVA Composites Illescas S.A.) in close collaboration with the research partners Fraunhofer Institute for Manufacturing Technology and Advanced Materials IFAM (IFAM), Instytut Maszyn Przepływowych im. Roberta Szewalskiego Polskiej Akademii Nauk (IMP-PAN), Centre National De La Recherche Scientifique (CNRS), Agenzia nazionale per le nuove tecnologie, l'energia e lo sviluppo economico sostenible (ENEA), University of Patras (LTSM-UPAT), and the Commissariat à l'énergie atomique et aux énergies alternatives (CEA), together with the small and medium-sized enterprises EASN Technology Innovation Services BVBA (EASN), GMI Aero SAS (GMI), and Automation W + R GmbH (AWR).

1.4 Synopsis

In this chapter, we presented a short introduction to ENDT and quality assessment in adhesive bonding processes relevant to the manufacture or repair of composite structures. We highlighted their relevance as field-level sensing systems for industrial automation and also for literally safeguarding quality in various steps of adhesive bonding processes. They will essentially contribute to quality assurance and optimisation within a manufacturing technology that we consider the most auspicious of the twenty-first century for innovations in joining functional or lightweight materials and components.

Based on a fast, firm and formal description of adhesive bonding processes and conferred to quality assurance, we determined that the analytical requirement for a monitoring process is far less complex than predicting any property of the ultimately manufactured adhesive joint, like the initial (or even final) strength or fracture toughness, which is often set as a fundamental design specification. Rather, indicating any deviations from a known, understood and qualified procedure will facilitate the timely, purposeful and precise amendments for achieving and maintaining the technologically relevant material and environment states following the requirements. All things considered, the documented compliance with documented procedures

contributes to risk reduction and safety, while also safeguarding the economic value and social acceptance of the processes and products.

We have detailed that, especially in the past decade, the monitoring of quality-relevant operand features which are characteristic for the adherend and adhesive materials has caught up with the virtually established methods and instrumentation for controlling the acting operators, i.e. process factors which effectuate changes of the operand features. A major contribution to this advance in operand QA was traced back to recent developments of ENDT tools, e.g. in the European joint research projects ENCOMB and ComBoNDT. Moreover, we explicated the layout of a concept that was developed in these interdisciplinary and applied research projects. This is based on an interdisciplinary, comprehensive and forthright analysis and a description of the supposedly controlled production environment and monitoring of deviations or events which occur when quality-relevant operator-related factors are intentionally and quantitatively altered in technologically relevant increments.

We hope that we have intrigued our readers, and we will animate this concept for ENDT and quality assessment in adhesive bonding within the subsequent chapters of this book.

References

1. Regert M (2004) Investigating the history of prehistoric glues by gas chromatography-mass spectrometry. J Sep Sci 27:244–254. https://doi.org/10.1002/jssc.200301608
2. Conard NJ, Malina M, Münzel SC (2009) New flutes document the earliest musical tradition in southwestern Germany. Nature 460:737–740. https://doi.org/10.1038/nature08169
3. Gegner J (2008) Klebtechnik – multifunktionales Fügen für den nachhaltigen Werkstoffeinsatz im 21. Jahrhundert. Mat.-wiss u Werkstofftech 39:33–44. https://doi.org/10.1002/mawe.200700228
4. Regert M, Rodet-Belarbi I, Mazuy A et al (2019) Birch-bark tar in the Roman world: the persistence of an ancient craft tradition? Antiquity 93:1553–1568. https://doi.org/10.15184/aqy.2019.167
5. Trehub SE, Becker J, Morley I (2015) Cross-cultural perspectives on music and musicality. Philos Trans R Soc Lond B Biol Sci 370:20140096. https://doi.org/10.1098/rstb.2014.0096
6. Conard NJ, Malina M (2008) New evidence for the origins of music from the caves of the Swabian Jura. In Both AA, Eichmann R, Hickmann E, Koch L-Ch (Eds), Challenges and objectives in music archaeology. Studien zur Musikarchäologie VI, Orient-Archäologie 22:13-22, Verlag Marie Leidorf GmbH, Rahden, Germany, ISBN 978-3-896-46652-5
7. Osipowicz G (ed) (2014) Kowal 14: Sepulchral and ritual place of people representing the Globular Amphora Culture. Wydawnictwo Naukowe Uniwersytetu Mikołaja Kopernika, Toruń, ISBN 978-83-231-3328-5
8. Rao H, Yang Y, Abuduresule I et al (2015) Proteomic identification of adhesive on a bone sculpture-inlaid wooden artifact from the Xiaohe Cemetery, Xinjiang, China. J Archaeol Sci 53:148–155. https://doi.org/10.1016/j.jas.2014.10.010
9. Brockmann W, Geiß PL, Klingen J, Schröder KB (2008) Adhesive bonding: materials, applications and technology. Wiley-VCH, Weinheim, ISBN 978-3-527-62393-8
10. Kozowyk PRB, Soressi M, Pomstra D et al (2017) Experimental methods for the Palaeolithic dry distillation of birch bark: implications for the origin and development of Neandertal adhesive technology. Sci Rep 7:8033. https://doi.org/10.1038/s41598-017-08106-7

11. Gross A, Lohse H (2015) Quality assurance in adhesive bonding technology—new DIN 2304 standard and its use in practice. Adhes Adhes Sealants 12–17. https://doi.org/10.1007/s35784-015-0534-4
12. Reiling JM, Middendorf P, Sindel M (2015) Quality assurance of adhesive processes in the body shop. In: Bargende M, Reuss H-C, Wiedemann J (eds) 15. Internationales Stuttgarter Symposium. Springer Fachmedien Wiesbaden, Wiesbaden, pp 1421–1431
13. Paul F (2017) Adhesive bonding roadmap—increasing trust in adhesives. DECHEMA, Frankfurt am Main
14. Encinas N, Oakley BR, Belcher MA et al (2014) Surface modification of aircraft used composites for adhesive bonding. Int J Adhes Adhes 50:157–163. https://doi.org/10.1016/j.ijadhadh.2014.01.004
15. Ledesma RI, Palmieri FL, Yost WT et al (2017) Surface monitoring of CFRP structures for adhesive bonding, 40th Annual Meeting, The Adhesion Society, St. Petersburg, Florida, USA
16. Kraft A, Brune K (2017) Assured use of release agents and adhesives in the same production process. Lightweight des Worldw 10:40–43. https://doi.org/10.1007/s41777-017-0013-5
17. Konstantopoulos S, Fauster E, Schledjewski R (2014) Monitoring the production of FRP composites: a review of in-line sensing methods. Express Polym Lett 8:823–840. https://doi.org/10.3144/expresspolymlett.2014.84
18. Hübner M, Lang W, Dumstorff G (2017) Surface integrated printed interdigital structure for process monitoring the curing of an adhesive joint. Proceedings 1:631. https://doi.org/10.3390/proceedings1040631
19. Soldatos J, Gusmeroli S, Malo P, Di Orio D (2016) Internet of Things applications in future manufacturing. In: Vermesan O, Friess P (eds) Digitising the industry: Internet of Things connecting the physical, digital and virtual worlds. River Publishers, Gistrup, Denmark, ISBN 978-8-793-37981-7
20. de Baas AF (2017) Data and documentation terminology, classification and ontology. Common terminology and classification, efficient communication. https://emmc.info/wp-content/uploads/2017/12/EMMC_IntOp2017_Cambridge_deBaas_EC.pdf
21. Gellrich A, Lunkwitz D, Dennert A et al (2012) Rule-driven manufacturing control based on ontologies. In: Proceedings of 2012 IEEE 17th international conference on emerging technologies & factory automation (ETFA 2012). IEEE, pp 1–8. https://doi.org/10.1109/ETFA.2012.6489545
22. Ullmann T, Schmidt T, Hoffmann S et al (2010) In-line quality assurance for the manufacturing of carbon fiber reinforced aircraft structures. In: NDT.net Issue: 2011-03, 2nd Int. Symposium on NDT in aerospace 2010—Tu.1.A.4
23. Dahmen T, Trampert P, Boughorbel F et al (2019) Digital reality: a model-based approach to supervised learning from synthetic data. AI Perspect 1. https://doi.org/10.1186/s42467-019-0002-0
24. Gifford C, Daff D (2017) ISA-95 evolves to support smart manufacturing and IIoT—New challenges and opportunities for manufacturing technologies and standards across industries, InTech, November/December
25. Feng SC, Bernstein WZ, Hedberg T et al (2017) Towards knowledge management for smart manufacturing. J Comput Inf Sci Eng 17. https://doi.org/10.1115/1.4037178
26. Katnam KB, da Silva LFM, Young TM (2013) Bonded repair of composite aircraft structures: a review of scientific challenges and opportunities. Prog Aerosp Sci 61:26–42. https://doi.org/10.1016/j.paerosci.2013.03.003
27. ENCOMB "Extended Non-Destructive Testing of Composite Bonds" (2010–2014) Project funded from the European Union's Seventh Framework Programme under grant agreement No 266226
28. ComBoNDT "Quality assurance concepts for adhesive bonding of aircraft composite structures by advanced NDT" (2015–2018) Project funded from the European Union's Horizon 2020 research and innovation programme under grant agreement No 636494
29. Kanterakis G, Chemama R, Kitsianos K (2020) Bonded repair of composite structures. In: Pantelakis S, Tserpes K (eds) Revolutionizing aircraft materials and processes. Springer Nature, [S.l.], pp 359–392. https://doi.org/10.1007/978-3-030-35346-9_13

30. Light GM, Kwun H (1989) Nondestructive evaluation of adhesive bond quality. State-of-the-Art Review: SwRI Project 17-7958-838, Nondestructive Testing Information Analysis Center San Antonio, Texas, USA
31. Mattmann I (2017) Modellintegrierte Produkt- und Prozessentwicklung. Springer Fachmedien Wiesbaden GmbH, Wiesbaden, Germany, ISBN 978-3-658-19408-6
32. Espie AW (1998) Quality assurance in adhesive technology: EUREKA Project EU716. Abington Publishing, Cambridge
33. DIN EN ISO 9000:2015-11 (2015) Qualitätsmanagementsysteme - Grundlagen und Begriffe (ISO 9000:2015): Deutsche und Englische Fassung EN ISO 9000:2015(DIN EN ISO 9000:2015-11)
34. Markus S, Wilken R, Dieckhoff S (2006) Fehlervermeidung durch Inline-Monitoring des Oberflächenzustandes. Adhaes Kleb Dicht 50:20–22. https://doi.org/10.1007/BF03253336
35. DIN 2304-1:2016-03 (2016) Adhesive bonding technology—quality requirements for adhesive bonding processes: Part 1: Adhesive bonding process chain (DIN 2304-1:2016-03)
36. Allotrope Foundation (2020) Data Standard | Allotrope Foundation. https://www.allotrope.org/
37. Qin SJ, Zheng Y (2013) Quality-relevant and process-relevant fault monitoring with concurrent projection to latent structures. AIChE J 59:496–504. https://doi.org/10.1002/aic.13959
38. Peng K, Zhang K, You B et al (2016) A quality-based nonlinear fault diagnosis framework focusing on industrial multimode batch processes. IEEE Trans Ind Electron 1. https://doi.org/10.1109/TIE.2016.2520906
39. Huang J, Yan X (2017) Quality relevant and independent two block monitoring based on mutual information and KPCA. IEEE Trans Ind Electron 64:6518–6527. https://doi.org/10.1109/TIE.2017.2682012
40. Huang J, Yan X (2018) Relevant and independent multi-block approach for plant-wide process and quality-related monitoring based on KPCA and SVDD. ISA Trans 73:257–267. https://doi.org/10.1016/j.isatra.2018.01.003
41. Moyne J, Iskandar J (2017) Big data analytics for smart manufacturing: case studies in semiconductor manufacturing. Processes 5:39. https://doi.org/10.3390/pr5030039
42. Berger D, Zaiß M, Lanza G et al (2018) Predictive quality control of hybrid metal-CFRP components using information fusion. Prod Eng Res Devel 12:161–172. https://doi.org/10.1007/s11740-018-0816-1
43. Wassink CHP (2012) Innovation in non destructive testing. Dissertation, TU Delft
44. Custódio J, Cabral-Fonseca S (2013) Advanced fibre-reinforced polymer (FRP) composites for the rehabilitation of timber and concrete structures: assessing strength and durability. In: Bai J (ed) Advanced fibre-reinforced polymer (FRP) composites for structural applications. Elsevier Science, Burlington, pp 814–882. https://doi.org/10.1533/9780857098641.4.814
45. DIN 6701-2:2015-12 (2015) Adhesive bonding of railway vehicles and parts—Part 2: Qualification of manufacturer of adhesive bonded materials(DIN 6701-2:2015-12)
46. Michaloudaki M (2005) An approach to quality assurance of structural adhesive joints. PhD thesis, Technical University Munich
47. Davis M (2004) Best practice in adhesive bonding. https://www.niar.wichita.edu/niarworkshops/Portals/0/BestPracticesinAdhesiveBondingMaxDavis.pdf
48. Niermann D, Gross A, Brede M et al (2005) Quality assurance in adhesive bonding technology. Adhaes Kleb Dicht 30–32
49. Niermann D, Gross A, Brede M et al (2005) Quality assurance in adhesion (Part 1): Construction phase—which general valid quality assurance measures apply to be observed? Adhaes Kleb Dicht 49:36–38
50. Niermann D, Gross A, Brede M et al (2005) Quality assurance in adhesive technology (Part 2): Production phase. Adhaes Kleb Dicht 49:28–32
51. Pirolini A (2014) Quality assurance trends in the automotive industry: an interview with Alex Koprivc. AZO Materials. https://www.azom.com/article.aspx?ArticleID=11065
52. Flämmich M, Herdin H, Kunz U, Mannschreck K, Schulze L, Straub R (2020) Guidelines for Quality Assuring Process Management in Parts Cleaning. Fachverband Industrielle Teilereinigung e.V. (FiT)

53. Ebnesajjad S, Landrock AH (2015) Chapter 13—Quality control. In: Ebnesajjad S, Landrock AH (eds) Adhesives technology handbook (Third Edition) William Andrew Pub, Norwich, NY, pp 353–374. https://doi.org/10.1016/B978-0-323-35595-7.00013-9
54. Messler SW (1993) Joining of advanced materials. Elsevier Science, Burlington
55. Breuer F, Muckel P, Dieris B (2018) Reflexive Grounded Theory: Eine Einführung für die Forschungspraxis, 3., vollständig überarbeitete und erweiterte Auflage. Lehrbuch. Springer, Wiesbaden
56. Nielsen J (1994) 10 Usability heuristics for user interface design. https://www.nngroup.com/articles/ten-usability-heuristics/
57. Kleining G, Witt H (2000) The qualitative heuristic approach: a methodology for discovery in psychology and the social sciences. Rediscovering the method of introspection as an example. Forum: Qualitative Social Research 1(1), Art. 13. http://nbn-resolving.de/urn:nbn:de:0114-fqs0001136
58. Budhe S, Banea MD, de Barros S et al (2017) An updated review of adhesively bonded joints in composite materials. Int J Adhes Adhes 72:30–42. https://doi.org/10.1016/j.ijadhadh.2016.10.010
59. Kreling S, Blass D, Wilken R et al (2017) Sauber und prozesssicher vorbehandeln — Teil 1: [Pretreating cleanly and in a process-reliable manner - PART 1]. Adhaes Kleb Dicht 61:18–23
60. Kreling S, Blass D, Wilken R et al (2017) Sauber und prozesssicher vorbehandeln - PART 2: [Pretreating cleanly and in a process-reliable manner - PART 2]. Adhaes Kleb Dicht 24–28
61. Halliwell S, Repair of fibre reinforced polymer (FRP) structures. National composites network best practice guide
62. Tserpes K (2020) Adhesive bonding of aircraft structures. In: Pantelakis S, Tserpes K (eds) Revolutionizing aircraft materials and processes. Springer Nature, [S.l.], pp 337–357. https://doi.org/10.1007/978-3-030-35346-9_12
63. Tornow C, Brune K, Noeske M (2014) Verfahren und Vorrichtung zur Bestimmung einer Oberflächengüte (DE102014209862A1)
64. Jeenjitkaew C, Guild FJ (2017) The analysis of kissing bonds in adhesive joints. Int J Adhes Adhes 75:101–107. https://doi.org/10.1016/j.ijadhadh.2017.02.019
65. Acare (2020) Acare—Advisory Council for Aviation Research and Innovation in Europe. https://www.acare4europe.org/
66. EASA (2010) Composite Aircraft Structure: Annex II to ED Decision 2010/003/R of 19/07/2010(AMC 20-29). https://www.easa.europa.eu/sites/default/files/dfu/Annex%20II%20-%20AMC%2020-29.pdf
67. Clean Sky (2020) Welcome to the Clean Sky | Clean Sky. https://www.cleansky.eu/
68. BOPACS "Boltless assembling Of Primary Aerospace Composite Structures" (2012 – 2016) Project funded from the European Union's FP7-TRANSPORT programme under grant agreement No 314180. https://cordis.europa.eu/project/id/314180/de
69. ABiTAS "Advanced Bonding Technologies for Aircraft Structure" (2006 – 2010) Project funded from the European Union's FP6-AEROSPACE programme under grant agreement No 30996
70. Esquivel O, Seibold RW (2004) Capabilities and Limitations of Nondestructive Evaluation Methods for Inspecting Components Beneath Thermal Protection Systems. AEROSPACE REPORT NO. ATR-2004(5081)-1, Cambridge, MA 02142-1093
71. ASTM F22 - 13: Standard Test Method for Hydrophobic Surface Films by the Water-Break Test. In: ASTM Volume 15.03 Space Simulation; Aerospace and Aircraft; Composite Materials. ASTM International
72. Federal Aviation Administration (2017) AMT Airframe Handbook Volume 1 (Full Version) (Faa-H-8083-31). By: Federal Aviation Administration. Aviation Maintenance Technician Handbook - Airframe, vol 1. Createspace Independent Publishing Platform

Open Access This chapter is licensed under the terms of the Creative Commons Attribution 4.0 International License (http://creativecommons.org/licenses/by/4.0/), which permits use, sharing, adaptation, distribution and reproduction in any medium or format, as long as you give appropriate credit to the original author(s) and the source, provide a link to the Creative Commons license and indicate if changes were made.

The images or other third party material in this chapter are included in the chapter's Creative Commons license, unless indicated otherwise in a credit line to the material. If material is not included in the chapter's Creative Commons license and your intended use is not permitted by statutory regulation or exceeds the permitted use, you will need to obtain permission directly from the copyright holder.

Chapter 2
Characterization of Pre-bond Contamination and Aging Effects for CFRP Bonded Joints Using Reference Laboratory Methods, Mechanical Tests, and Numerical Simulation

Konstantinos Tserpes, Elli Moutsompegka, Mareike Schlag, Kai Brune, Christian Tornow, Ana Reguero Simón, and Romain Ecault

Abstract In this chapter, the pre-bond contamination and ageing effects on carbon fiber reinforced plastic (CFRP) adherends and CFRP bonded joints are characterized by means of reference laboratory non-destructive testing (NDT) methods, mechanical tests, and numerical simulation. Contaminations from two fields of application are considered, namely in aircraft manufacturing (i.e. production) and for in-service bonded repair. The production-related scenarios comprise release agent, moisture, and fingerprint, while the repair-related scenarios comprise fingerprint, thermal degradation, de-icing fluid, and a faulty curing of the adhesive. For each scenario, three different levels of contamination were pre-set and applied, namely low, medium and high level. Furthermore, two types of samples were tested, namely coupons and pilot samples (a stiffened panel and scarf repairs). The CFRP adherends were contaminated prior to bonding and the obtained surfaces were characterized using X-ray photoelectron spectroscopy. After bonding, the joints were tested by ultrasonic testing. To characterize the effects of each contamination on the strength of the bonded joints, mode-I and mode-II fracture toughness tests, and novel centrifuge tests were conducted on the coupons, while tensile tests were performed on the scarfed samples. Additionally, numerical simulation was performed on CFRP stiffened panels under compression using the LS-DYNA finite element (FE) platform.

K. Tserpes (✉) · E. Moutsompegka
Laboratory of Technology & Strength of Materials, Department of Mechanical Engineering & Aeronautics, University of Patras, 26500 Patras, Greece
e-mail: kitserpes@upatras.gr

M. Schlag · K. Brune · C. Tornow
Fraunhofer Institute for Manufacturing Technology and Advanced Materials IFAM, Wiener Str. 12, 28359 Bremen, Germany

A. Reguero Simón
Aernnova Composites Illescas Sau, Parque Industrial y Tecnológico, Avda Barajas, 3 Illescas, 45200 Toledo, Spain

R. Ecault
Airbus Operations S.A.S., 316, route de Bayonne, B.P. D4101, 31060 Toulouse Cedex 9, France

© The Author(s) 2021

W. Leite Cavalcanti et al. (eds.), *Adhesive Bonding of Aircraft Composite Structures*,
https://doi.org/10.1007/978-3-319-92810-4_2

Keywords Pre-bond contamination · Hygrothermal aging · Fracture toughness · Centrifuge testing · Ultrasound testing · X-ray photoelectron spectroscopy

2.1 Introduction

The use of adhesive bonding in aircraft structures is increasing, both in the assembly of structural parts and when applying composite patch repairs due to the numerous advantages it offers over conventional joining techniques [1–4]. These include a more uniform stress distribution in the area of the joint, the ability to join dissimilar materials, the improved fatigue properties, and the attractive strength to weight ratio. However, the use of adhesive bonding technology is presently limited to the joining and patch repairing of secondary structures that are not load-critical. Amongst the reasons inhibiting the certification of adhesive bonding for primary structures is the sensitivity of the bondline integrity to the presence of defects, which might counteract the strength of the joints. These defects are not accessible to visual monitoring during the bonding process, and they usually are caused by a pre-bond contamination of the adherend surface during either the manufacture of the joints or their repairs. As conditions on the aircraft production line and in the maintenance/overhaul shed are different, defects are categorized as either production-related or repair-related. Table 2.1 lists the pre-bond contamination scenarios under consideration in the ComBoNDT project.

Amongst the defects that might arise during the manufacture of adhesive joints, the most critical ones are those that are not detectable by the available NDT methods. In addition to developing extended NDT (ENDT) methods capable of detecting such effects [6], evaluating their effect on the strength of adhesive joints is of equal importance. Early experimental studies conducted within the ENCOMB project [1, 7, 8] have shown that undetectable defects caused by pre-bond contamination may significantly degrade the mode-I fracture toughness of CFRP joints. In the ComBoNDT project, the experimental characterization has extended the current state of research by conducting mode-I fracture toughness tests for additional contamination scenarios, mode-II tests on the complete set of contamination scenarios (Table 2.1), and novel centrifuge tests. The centrifuge tests are fast and cost-effective tests that can be used to determine the adhesion strength of bonded joints. They serve as an alternative to the fracture toughness tests, which are more expensive and time consuming. In the test program of the ComBoNDT project, mode-II tests on aged

Table 2.1 The contamination scenarios studied in Chaps. 2 through 5 in the ComBoNDT project [5]

Production-related (P)	Repair-related (R)
Release agent (P-RA)	Thermal degradation (R-TD)
Moisture (P-MO)	De-icing fluid (R-DI)
Fingerprint (P-FP)	Fingerprint (R-FP)
	Faulty curing of the adhesive (R-FC)

joints have been also conducted with the aim of assessing the combined effect of pre-bond defects and after-bond hygrothermal aging. The material geometry tested comprises not only coupon-level samples, but also a series of samples that have more complex geometries derived from real geometries in the fields of application and are highly relevant for aerospace applications. These are the pilot samples and consist of scarfed samples and individual aerospace component parts (stiffened panels). These samples are used to evaluate the efficiency and check the applicability of ENDT methods on more complex/curved geometries with multiple contaminations in conjunction with a clean reference condition. With these samples, ENDT methods can be adapted to overcome the limitations arising from measurements on non-flat surfaces.

The debonding process is already complicated since it involves a three-material system (adherend, adhesive, and adherend/adhesive interface) as well as the geometric challenges of the parts themselves. Therefore, to determine the effects of the contaminations on the bonded joints of individual aerospace component parts, a numerical simulation was performed under compression loading using the LS-DYNA finite element (FE) platform.

The present chapter describes the respective contributions of the individual partners of the ComBoNDT consortium. The manufacturing of the CFRP adherends for the coupons and the pilot samples was performed by Aernnova Composites; the pre-bond contamination and the bonding of the samples was performed by Fraunhofer IFAM; the characterization of the adherends using X-ray photoelectron spectroscopy was performed by Fraunhofer IFAM; the ultrasound testing of the bonded plates and pilot samples was performed by Airbus; the mechanical testing of the coupons and the pilot samples as well as the aging of the coupons was performed by the University of Patras; and the numerical simulation of the stiffened panels was also conducted by the University of Patras. The datasets obtained from the mechanical testing represent design-relevant operand features. The subsequently detailed procedures offer a well-tried, step-by-step approach for compiling these features and, therefore, constitute an essential input into the framework of the applied concept for the quality assessment of adhesively bonded joints described in this book.

2.2 Materials and Sample Geometries

2.2.1 Basic Materials

Hexcel® M21E was used for the preparation of the test coupons. HexPly M21E/IMA, developed from Hexcel®'s M21 third-generation thermosetting epoxy resin system, uses an intermediate modulus fiber to balance superior strength and stiffness, and it was developed specifically for aircraft applications performed at Airbus. The matrix resin was developed to ensure an optimal translation of the carbon fiber properties whilst delivering outstanding fracture resistance. The sample plates were produced

by Aernnova Composites using the liquid water-based silicone-containing release agent Frekote® C-600 in order to obtain smooth surfaces.

Regarding the structural layout, CFRP monolithic structures were manufactured according to the Airbus AIPS 03-02-019 standard for CFRP ("Manufacture of monolithic parts with thermoset prepreg materials"). For the fracture toughness testing, the adherends consisted of eight unidirectional plies and their layup sequence was $[0_2, \pm 45]_s$ according to the AITM 1-0053 standard [9]. A release film—25 mm in length for the contaminated samples and 30 mm in length for the contaminated/aged samples—was inserted at one end of the sample prior to bonding to obtain an initial delamination for the fracture toughness tests.

The specimens used in the centrifuge tests had a stamp-to-plate configuration. The modular test stamps bonded to the CFRP adherends consisted of an aluminum (EN AW-2007) adherend screwed onto a body of mass made of copper. The CFRP adherends were manufactured from the M21E/IMA prepreg material. The layup sequence of the panels was $[(0/90/45/\text{-}45)_3]_s$.

For the adhesive bonding of the adherends, a film adhesive was used instead of a paste in order to standardize the thickness and increase the reliability of the results. Specifically, the film adhesives FM 300 K and FM 300-2 from Cytec® (0.20 and 0.25 mm thickness, respectively) were used for the production and the repair scenario, respectively.

2.2.2 Sample Geometries

2.2.2.1 Coupons

For the mode-I fracture toughness tests, a double cantilever beam (DCB) specimen was used to mirror the relevant geometry and the loading of the adhesive joint. A DCB specimen consists of rectangular adherends bonded along their length, incorporating a region of non-adhesive release film at one end for the introduction of the initial crack in the bondline during testing (Fig. 2.1a). For the mode-II fracture toughness tests, an end notched flexure (ENF) specimen was used. Similar to the DCB specimens, ENF specimens also consist of rectangular adherends, but with a longer pre-crack that is embedded through the width at the end of the specimen to accommodate the sliding deformation of the adherends that result from the flexural loading (Fig. 2.1b). In order to provide crack growth stability, the initial crack length was considered to be equal to 70% of $L/2$ [10, 11]. The test specimens were cut from the residual part of the mode-I specimens.

Finally, the specimen for the centrifuge tests comprised a rectangular composite plate (adherend) bonded to a metallic cylindrical stamp using a technically relevant adhesive system. The test stamps had a diameter of 10 mm on the bonding face. The samples were cut to the desired size by dry diamond cutting. The final dimensions of the CFRP adherends were 25 mm × 25 mm × 4.4 mm.

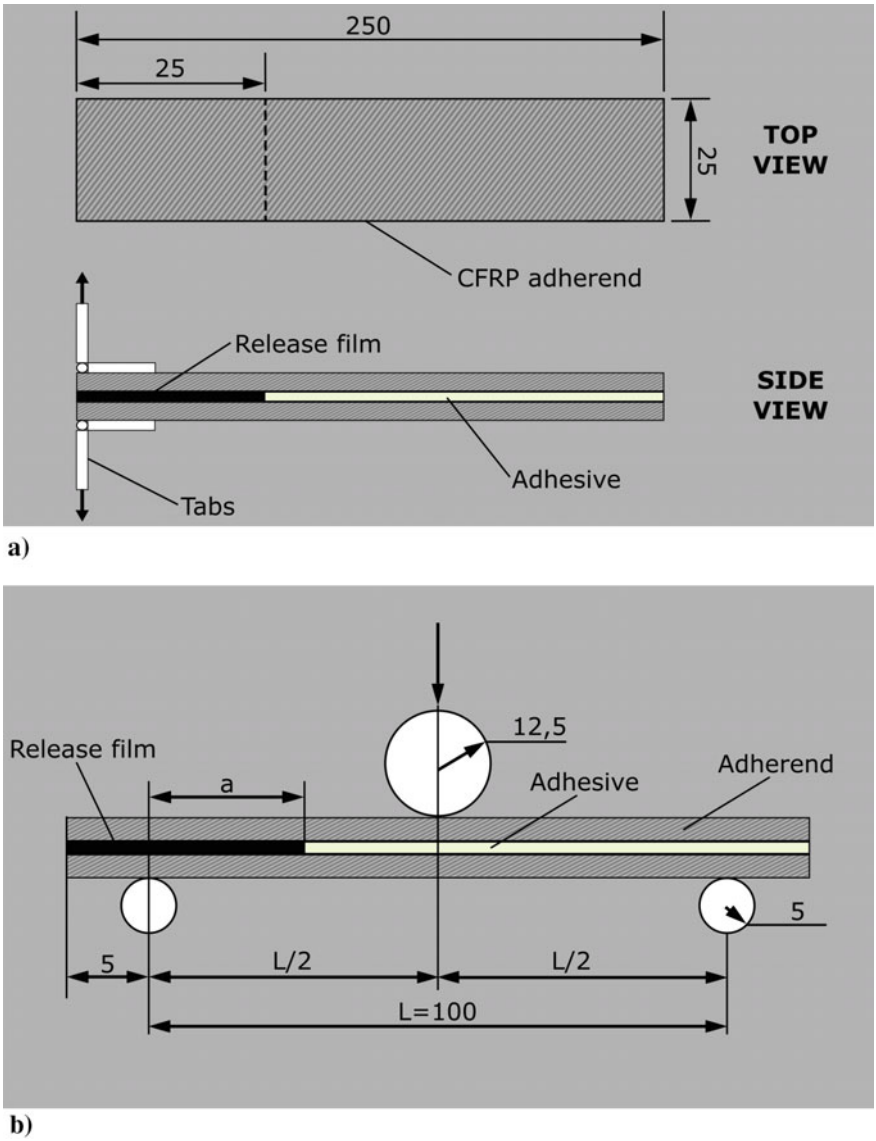

Fig. 2.1 Geometry, dimensions and boundary conditions of **a** DCB coupon and **b** the ENF coupon

2.2.2.2 Scarfed Samples

As already stated, the two main relevant scenarios for CFRP adhesive joint quality assurance are manufacturing, when the joints are first bonded during aircraft construction, and maintenance, when aerostructures are repaired. Scarfed joints were used for the second scenario. When damage is detected, the aircraft part is locally scarfed

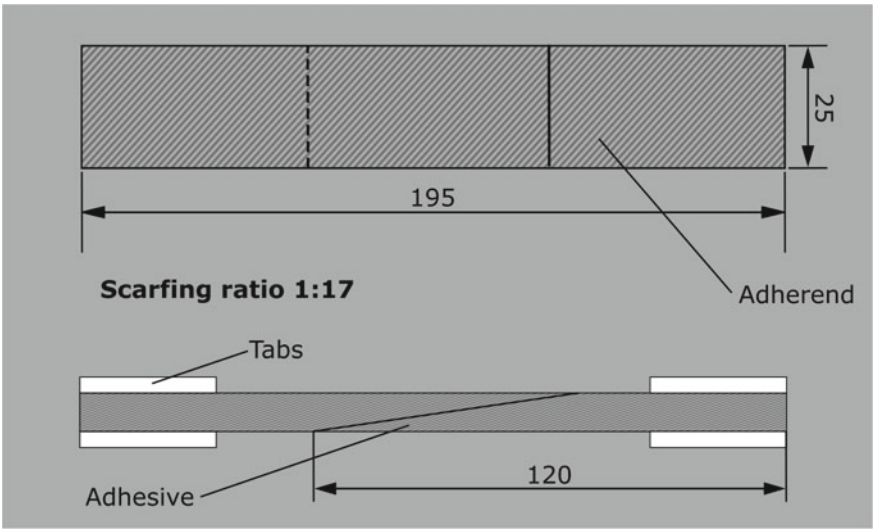

Fig. 2.2 Geometry and dimensions of the scarfed sample

to remove the damaged outer layers, which are then substituted with a patch that is bonded over the scarfed area in order to restore the load-carrying capacity.

The scarfed samples used in this work were rectangular and consisted of two CFRP plates scarfed by milling with a ratio of 1:17 (Fig. 2.2).

2.2.2.3 Panels

The individual aerospace component parts considered here were two stiffened panels: A flat panel with a laminated skin and two laminated T-stringers for the production scenario, and a curved panel with a laminated skin and two laminated Ω-stringers for the repair scenario. The stringers were spaced at equal distances on the panels.

The dimensions of the panel and the T-stringers are given in Fig. 2.3. The dimensions of the Ω-stringers are 800 mm × 100 mm × 33 mm (Fig. 2.4).

2.3 Manufacturing

2.3.1 Adherend Manufacturing

The CFRP laminates for the coupons were manufactured using the automated tape laying (ATL) technique (Fig. 2.5a). The diagram showing the applied vacuum bag

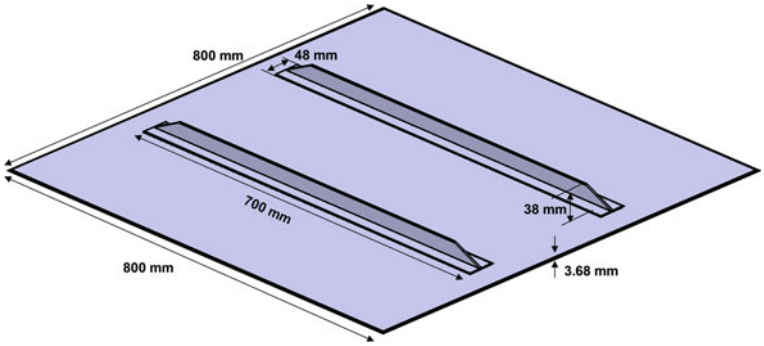

Fig. 2.3 Geometry and dimensions of the flat stiffened panel

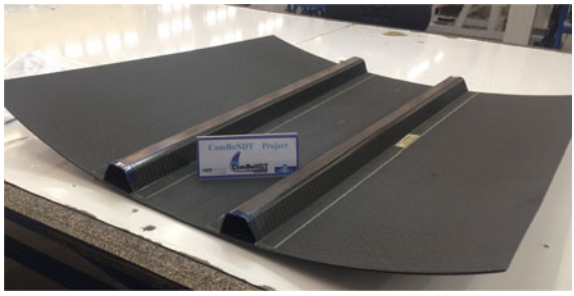

Fig. 2.4 Curved stiffened panel with a laminated skin and two laminated Ω-stringers

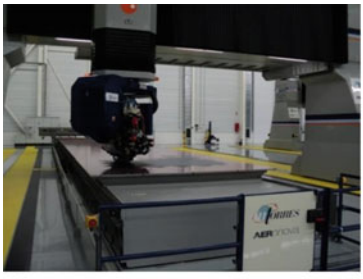

a)

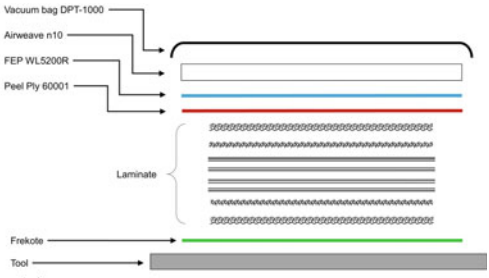

b)

Fig. 2.5 **a** Photograph showing the automated tape laying process of the laminated panels; **b** diagram of the vacuum bag

is given in Fig. 2.5b, while Fig. 2.6 shows the panels placed inside the autoclave as well as the cutting of the panels.

The CFRP material for the scarfed samples was also manufactured by Aernnova Composites, as described previously, and was then delivered to Fraunhofer IFAM. The CFRP plates were scarfed with a ratio of 1:17 by milling and were then manually ground and cleaned with methyl ethyl ketone (MEK) to remove any handling

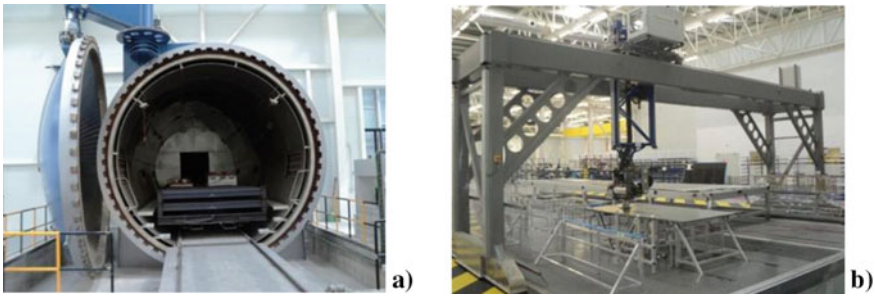

Fig. 2.6 Photographs showing **a** the panels inside the autoclave and **b** the cutting of the panels

contamination from thermoplastic residues resulting from the milling process. Lastly, the samples were cut to the final size using dry diamond cutting (Fig. 2.7).

The laminated skin for the flat panels (Fig. 2.8a) was manufactured using the same process as was applied for the laminates of the coupons. For the manufacturing of the T-stringers, the web was shaped by joining two C-shaped preforms that had been manufactured using the ATL technology. First, a flat panel was laminated and placed on a hot-forming tool to obtain the C-shape. After that, both C-shaped preforms were joined. Finally, the stringer was trimmed to obtain the six T-stringers with the required dimensions. The T-stringers are shown in Fig. 2.8b.

In the curved stiffened panels, the Ω-stringers were first manufactured using a specific shaping tool (Fig. 2.9). As the skin was curved, a difference in the orientation

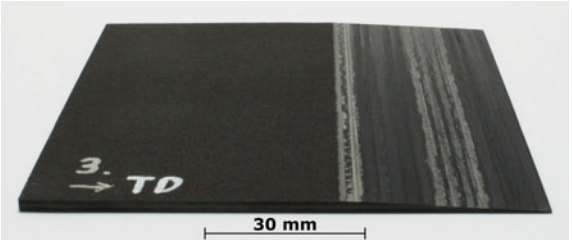

Fig. 2.7 Overview of scarfed sample after milling

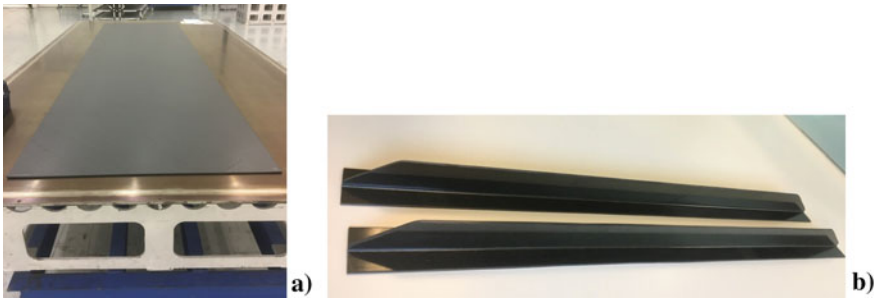

Fig. 2.8 Photographs showing **a** the flat laminated skin before being placed into the autoclave and **b** the T-stringers

Fig. 2.9 Photograph showing the Ω-stringers inside the shaping tool

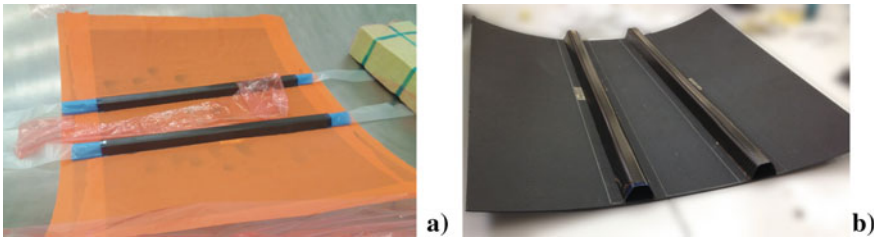

Fig. 2.10 Photographs showing **a** the preparation of the final curing for the curved panel and the Ω-stringers and **b** the curved and stiffened panel

of the Ω-stringers was considered. The bonding of the Ω-stringers with the skin was done immediately after the manufacturing of the skins. Once the stringers had been placed in their respective positions, the preparation for the final curing cycle started. In addition to the added tubular bags, the panel needed to be protected before entering the curing cycle (Fig. 2.10a). Special attention was paid to the adaptation of the complicated geometry parts to the vacuum bag during the pre-compaction. The curved and stiffened panel is shown in Fig. 2.10b.

2.3.2 Adherend Pre-bond Contamination

Implementing the concept for quality assessment during joining processes, e.g. as applied in the ComBoNDT project, requires the development of ENDT technologies for their integration into adhesive bonding process chains in aircraft production as well as for in-field repair. Such implementation is based on the identification and definition of all test scenarios to be considered and investigated; therefore, possible quality-relevant contaminants with high relevance for all, or at least for

the majority, of aerospace applications must be identified. Following this decision, a detailed description of the sample preparation, including the surface contamination, was prepared in order to guarantee a precise and reproducible sample preparation process, which is an important key element in the success of the entire approach, as highlighted during the ComBoNDT project. Table 2.2 presents more details on quality-relevant scenarios affecting CFRP adherends or adhesive layers in adhesive joints investigated during the ENCOMB [8] or ComBoNDT [5] projects; a more detailed description is provided in the following sections.

2.3.2.1 Production Scenarios

Most aircraft produced nowadays contain a significant number of components made of CFRP, and therefore require the adhesive bonding of CFRP in manufacturing, which further emphasizes the need for complete and reliable quality assurance concepts using ENDT techniques. Three different contaminations were investigated in detail, namely release agent (scenario RA), moisture (scenario MO) and (human) fingerprint (scenario FP).

During the molding process of the composite panels, silicone (Si)-based release agents are used to facilitate the easy removal of the component from the mold. A Si-containing contamination on the CFRP surface caused by release agent residue hinders the adhesion of the adhesive to the substrate [1, 4, 7].

The release agent used was Frekote® 700NC. This is an Si-based liquid that needs to be removed from the CFRP surface before the bonding process because it prevents wetting and adhesion. Therefore, it is necessary to detect possible residues on surfaces prior to adhesive bonding. The release agent was applied to the CFRP surfaces by dip-coating with fixed immersion times and fixed withdrawal speeds. Different concentrations of Frekote® 700NC in heptane were used to yield different degrees of contamination. After the dip-coating of the adherend, the polymerization of the release agent was allowed to occur by drying for 30 min under ambient conditions followed by a heat treatment for 60 min in an oven at 80 °C. The first tests used to yield the desired amounts of Si-containing contaminations on the surface were conducted with solutions of Frekote® 700NC in heptane with the following concentrations (vol%): 1, 2, 3, 4, 5 and 8%. Based on the results of the preliminary tests (X-ray photoelectron spectroscopy measurements and mechanical tests with lap shear specimens), one of the two CFRP adherends per joint was intentionally exposed using dip-coating solutions with the following volumetric concentrations: 1, 2, and 4% of Frekote® 700NC in heptane.

Pre-bond moisture penetration into a composite adherend can occur via either air humidity or direct contact with liquid water. CFRP panels often undergo several pre-treatment procedures, such as wet abrasion and the water brake test, to ensure the effectiveness of the cleaning procedure [4, 7]. Although precautionary measures are implemented, such as using large autoclaves to remove moisture by heat-drying, the problem persists due to the ubiquity of water, e.g. in the surrounding atmosphere, and the limitation of water removal from the bulk of the CFRP thermoset resin through

Table 2.2 Quality-relevant scenarios affecting a CFRP adherend or an adhesive layer in an adhesive joint as assessed in the European joint research projects ENCOMB [8] and ComBoNDT [5]. In each scenario, the formation and properties of at least one interphase region (close to one of the adherends) is impaired as compared to a joint prepared following the qualified joining process

Quality-relevant scenario	Technological implementation and denotation		Affected joint region	Comment
	ENCOMB [8]	ComBoNDT [5]		
Reference (during production of the joint)	**X ("RE")** grinded down to fibers	**X ("RE")** grinded	Following the qualified bonding process	ComBoNDT [5]: P-RE (slightly grinded) and R-RE (grinded down to fibers) for production and repair scenarios, respectively
Release agent (during production of the joint)	**X ("RA")** higher amount	**X ("RA")** lower amount	CFRP surface covered by nanoscale film	Same silicone-containing agent used in ENCOMB and in ComBoNDT
Moisture (during production of the joint)	**X ("MO")**	**X ("MO")**	CFRP surface covered by nanoscale water film; moist CFRP bulk	
Fingerprint (during manufacture of the joint)	–	**X ("P-FP")** (following DIN ISO 9022-12)	CFRP surface covered by (dried) aqueous film	Artificial hand perspiration solution, according to DIN ISO 9022-12 [12]
Thermal impact (during joint application; repair scenario)	**X ("TD")** (thermo-oxidative)	**X ("TD")** (thermal)	CFRP surface thermo-oxidatively affected during application; CFRP bulk thermally affected	Removal of oxidatively affected surface region by grinding only in ComBoNDT
Exposure to components of hydraulic oil (during joint application; repair scenario)	**X ("HF")** (immersion in aqueous extract of oil)	**X ("R-FP")** (fingerprinting of hydraulic oil)	CFRP surface covered by a film	Different liquids used in ENCOMB and ComBoNDT
De-icer (during repair of the joint)	–	**X ("DI")**	CFRP surface covered with salt particles	De-icer liquid based on potassium formate

(continued)

Table 2.2 (continued)

Quality-relevant scenario	Technological implementation and denotation		Affected joint region	Comment
	ENCOMB [8]	ComBoNDT [5]		
Faulty curing of adhesive (during repair of the joint)	–	**X ("FC")**	Adhesive layer; interphases to adherends	Initiated by selective pre-curing of the adhesive

diffusion as it is intercepted by the fiber layers. Moisture uptake mainly affects the properties of the matrix, resulting in swelling and the development of stresses large enough to pull the matrix away from the fiber [4, 7, 13]. Moreover, moisture also affects the adhesion properties [13]. CFRP can absorb moisture by up to 1.5–2.0 wt%. The range for concern at production sites often goes up to 0.5 wt%. A higher moisture uptake needs to be avoided because it negatively influences the adhesion properties and leads to a loss of performance of both the CFRP as well as the adhesive bond.

The preparation of moist CFRP samples was performed following two different procedures with different environmental conditions: One for use in the development of ENDT monitoring technologies for the quality assurance of adherend surfaces and the second one for the measurement of the mechanical properties of the bonds and for the further development and adaptation of ENDT technologies for the quality assurance of adhesive bondlines. Regarding the first category, the samples were contaminated in a defined climate that was established in small boxes in an oven at 70 °C. The humidity in the boxes was adjusted using beakers of demineralized water (MO-3) and saturated salt solutions (MO-1 and MO-2), which were placed in the boxes together with the samples until a constant weight of the samples had been achieved. The beakers in the boxes contained the following aqueous liquids in terms of saturated salt solutions: $MgCl_2 * 6H_2O$ saturated solution for MO-1, resulting in an approximately 30% relative humidity (RH); NaCl saturated solution for MO-2, resulting in an approximately 75% RH; and pure demineralized water for MO-3, resulting in an approximately 99.5% RH.

Clean CFRP samples were dried at 80 °C until they had achieved a mass constancy resulting in the dry weight. Afterward, they were stored in the respective boxes with moist atmospheres until the weight was constant (at least 40 days) and then taken out directly prior to the measurement with the respective surface inspection method. With this method, the following mass uptake of water was achieved:

- 0.4 (±0.2) mass% water for MO-1
- 0.8 (±0.1) mass% water for MO-2
- 1.4 (±0.2) mass% water for MO-3

For the second MO conditioning, the samples were prepared using a different procedure. These adherends were dried in an oven at 80 °C until mass constancy.

They were then stored in a climate chamber (70 °C and with the respective and well-defined relative humidity) for two weeks prior to bonding. After the removal from the climate chamber, the samples were directly bonded. The following RH conditions were adjusted in the chamber:

- 30% RH for MO-1
- 75% RH for MO-2
- 98% RH for MO-3

All the results presented in this chapter refer to the second MO conditioning.

Contamination by fingerprints can occur due to inadequate cleaning of a bonding surface or inappropriate handling after the cleaning process [14, 15]. Fingerprint contamination leads to the formation of thin contaminant films on the bonding surfaces and, ultimately, to a lower adhesion quality [15]. This may occur during both production and repair processes. Even though the occurrence of fingerprints seems to be easily avoidable, they are often responsible for adhesion failures, and therefore the detection of fingerprints is an essential requirement for an appropriate quality assurance approach.

Concerning the samples with fingerprint contamination to be investigated for the production scenario, the preparation was performed using a standardized salty fingerprint solution (artificial hand perspiration solution) according to DIN ISO 9022-12 [12]. This liquid formulation contains sodium chloride, urea, ammonium chloride, lactic acid, acetic acid, pyruvic acid, and butyric acid dissolved in demineralized water. Samples were prepared by manually applying this solution onto a surface area of the samples that correspond to the size and extent of a wet fingerprint. Different degrees of contamination were achieved by using different dilutions (with demineralized water) of the FP solution:

- 10% FP solution for P-FP-1
- 50% FP solution for P-FP-2
- pure FP solution for P-FP-3

Finally, in addition to the single contamination cases described above, the occurrence of a combined contamination case was also considered. Combined contaminations for the production scenario included the combination of release agent and fingerprint contaminations (RA+FP). Two levels of contamination were investigated:

- Low-level contamination (RA1+FP3): level RA-1 of release agent followed by the application of level FP-3 salt-based fingerprint solution.
- Medium-level contamination (RA2+FP3): level RA-2 of release agent followed by the application of level FP-3 salt-based fingerprint solution.

2.3.2.2 Repair Scenarios

In the second field of feasible application scenarios, distinct composite "repair" cases were defined, implemented, and examined. Hereby, the effects of contacting adherend surfaces with either of the two contaminant materials de-icing fluid or hydraulic oil

(applied in a fingerprinting process) were examined in detail. The third scenario dealt with thermally degraded CFRPs and aimed to account for CFRP parts that may have been exposed to heat (fuselage parts or alighting gear, for example, or aircraft structures that affected by lightening impact) and are then subjected to a mechanically abrasive surface pretreatment process. A fourth scenario that was investigated comprised a faulty curing of an adhesive that is then applied to distinct pretreated adherend surfaces. In the following, these technologically relevant contamination issues will be assessed in more detail.

In winter, airports use a de-icer to maximize runway friction during plane taxiing. Runway de-icing fluid is one of the most commonly encountered fluids to which aircraft structures may be exposed, as it can be swirled up from the runway and onto the outer parts of the aircraft [16]. During the patch repair of composite parts, inadequate cleaning can result in residues or the transfer of de-icing fluid onto adherend surfaces. After drying, potassium formate, which is present in the de-icing fluid, forms a thin layer on the CFRP part, thus affecting the bonding quality.

The de-icer used (DI scenario) was SAFEWAY® KF from CLARIANT, which contains potassium formate (KF) as the freezing point depressant. It was diluted with demineralized water to obtain solutions with the following concentrations in vol%: 2, 5, 7, 10, 30, and 50%. It was applied to the surfaces by dip-coating in the respective aqueous solution; finally, drying was performed in an oven for 2 h at 40 °C in air. Subsequently, acclimatization at room temperature was allowed for at least 24 h.

With the aim of narrowing the applied range of de-icer solution concentrations, three lap shear specimens comprising one contaminated adherend each were manufactured for each of these DI concentrations, and these were then used for adhesive bonding and subsequent mechanical testing. A significant loss in bond strength was observed for contamination levels characterized by surface concentrations of approximately 4 at.% potassium as measured by XPS. The fracture pattern also showed an impact when potassium surface concentrations of approximately 4 at.% were present. Based on these preliminary tests, it was decided to assess such samples in more detail; these were obtained using de-icer dip-coating solutions with the following concentrations for the ComBoNDT final coupon level samples: 2, 7, and 10% de-icer in demineralized water.

Moreover, CFRP aircraft parts may be exposed to high temperatures during service, for example, when fuselage parts are exposed to lightning [17], which causes local overheating and damage to the matrix or the wing parts situated close to the engines. Damage can also be caused by an overheating of an aircraft part by an external source of heat (gas, liquid, beam, etc.) that has inadvertently been placed near the aircraft. Besides affecting the mechanical properties of the structural parts, the thermal impact on and resulting degradation of the CFRP parts might also affect bonding in a repair situation.

For the sample preparation, all thermal impact treatments were carried out in an oven with air circulation. The samples (subsequently denoted as TD samples) were placed inside the oven and then underwent the heating phase at different temperatures. Once the indicated temperature was reached, the samples remained inside the oven for 2 h. Prior to both the surface inspection and the subsequent steps of the bonding

process, all samples were grinded down to the fibers (using Si-free sandpaper, grit size 120). A significant loss in bond strength (lap shear specimens) was observed for the samples treated with 280 °C. In a comparison with joints prepared from adherends that had not suffered such a thermal impact, the fracture pattern demonstrated an impact from a heat treatment of 260 °C. Based on these results, the following three different temperatures were used to realize three different levels of thermal impact (TD):

- 220 °C for TD-1
- 260 °C for TD-2
- 280 °C for TD-3

Concerning a further feasible contamination scenario, oily fingerprints can accidentally be applied to CFRP bonding surfaces when, for example, a worker wears gloves while working in an area where hydraulic oil is used and afterwards touches a bonding surface. Even though this contamination scenario seems easily avoidable, it is nevertheless of great importance in the field of aircraft repair because such a transfer of oil is unlikely to be detected during a visual inspection. Concerning the sample preparation for the repair scenario, fingerprints containing Skydrol 500B-4 hydraulic oil from Eastman were applied to the surfaces using a plastic finger. The oil was diluted in heptane to obtain formulations with the following contamination concentrations in vol%:

- 20% for a low level (denoted as R-FP-1)
- 50% for a medium level (R-FP-2)
- 100% for a high level (R-FP-3)

In order to achieve adequate adhesive bonding processes, it is important that all adhesive-related parameters, like pot life and curing times, comply with regulations as well as the specifications of the qualified bonding process. If the adhesive is out of specification with respect to its pot life due to, e.g., too high temperatures in the working area, the result can be weak or kissing bonds in the resulting joint. In this scenario, the bonded joint does not contain any foreign materials or contaminants that have erroneously remained after the cleaning, pretreatment, or conditioning steps. Instead, the loss of performance of the bonded joint is due to irregularities affecting the adhesive material that was used in the manufacturing process of a limited number of joints.

Regarding the sample preparation, a faulty curing of the adhesive was initiated through a selective pre-curing of an adhesive that was subsequently introduced into the bonding process. In the resulting selected and pre-cured areas, the bond strength may be reduced drastically, possibly due to its impeding any force transfer. This scenario will represent the cases of weak and kissing bonds. Three levels of pre-curing resulting in a faulty curing (FC) of the adhesive were realized:

- a slight pre-curing for FC-1
- a medium pre-curing for FC-2
- a strong pre-curing for FC-3

Finally, besides the single contamination cases described above, a combined contamination case was also considered. Combined contaminations in the repair scenario include the combination of thermal degradation and de-icing fluid (TD+DI), whereby two levels of contamination were investigated:

- Low level of contamination (TD1+DI1): Thermal degradation at 220 °C for 2 h followed by dip-coating in the DI1 concentration of the de-icing fluid solution.
- Medium level of contamination (TD1+DI2): Thermal degradation at 220 °C for 2 h followed by dip-coating in the DI2 concentration of the de-icing fluid solution.

2.3.3 Bonding

For the production scenarios, the samples described in this book were bonded in an autoclave using the adhesive FM® 300 K (0.2 mm) from Cytec® following the curing cycle shown in Fig. 2.11. The heating rate (starting from room temperature) was 3 K/min up to 175 °C. The pressure was 3 bars and the final temperature of 175 °C was held for 1 h.

Plates with the dimensions 30 cm × 30 cm and 30 cm × 15 cm were bonded and afterwards cut into the desired sizes for measurements with the respective measuring techniques as well as for mechanical testing in the specified geometries. The cutting was performed dry (diamond cutting) to prevent any contamination of the cleaned surfaces as might be the case when using cooling liquids. After cutting, the surfaces were cleaned again with isopropanol (IPA) soaked tissues. Figure 2.12 shows the preparation of the samples for bonding in the autoclave (at Fraunhofer IFAM facilities).

For the repair scenarios, all the samples were bonded in the autoclave using the adhesive FM® 300-2 (0.25 mm), which is specially designed for bonded repair. The

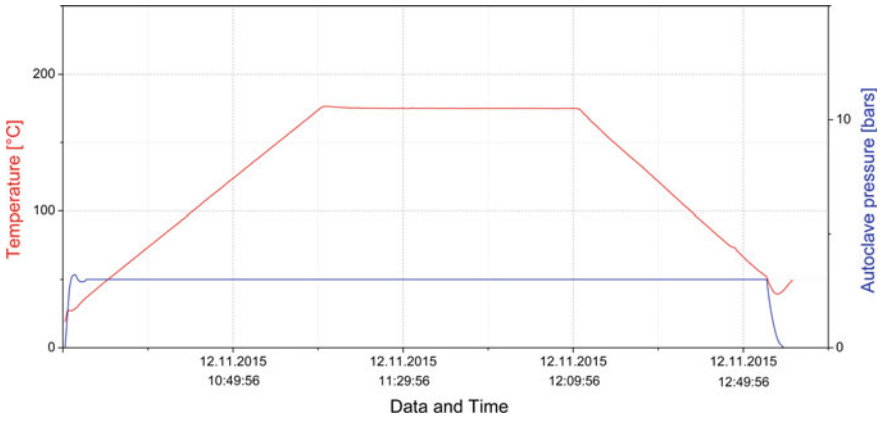

Fig. 2.11 Autoclave thermal and pressure cycle for bonding production samples with adhesive FM® 300 K

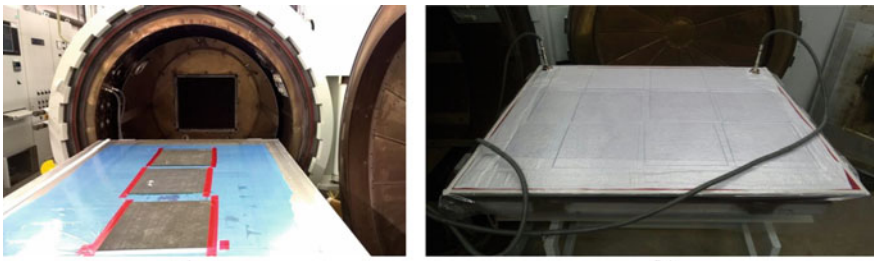

Fig. 2.12 Photographs showing the preparation of samples for bonding **a** in the autoclave and **b** using a vacuum bag

respective curing cycle is shown in Fig. 2.13. The CFRP plate sizes and the cutting of the samples into the final sizes after the bonding were as described for the production of the samples.

For the bonding of the centrifuge samples (Fig. 2.14a), the film adhesive was hole-punched to a diameter of 10 mm and then deposited onto the test stamp (cleaned by sonication for 5 min in isopropanol), which was then placed onto the CFRP sample (Fig. 2.14b). The production samples bonded with the FM 300 K adhesive were cured in an autoclave using a custom-made curing device at 3 bars and 175 °C for 60 min (heating up to 175 °C in 60 min, cooling down to room temperature in 60 min). The repair samples bonded with the FM 300-2 adhesive were cured at 2 bars and 121 °C for 90 min (heating up to 121 °C in 30 min, cooling down to room temperature in 60 min).

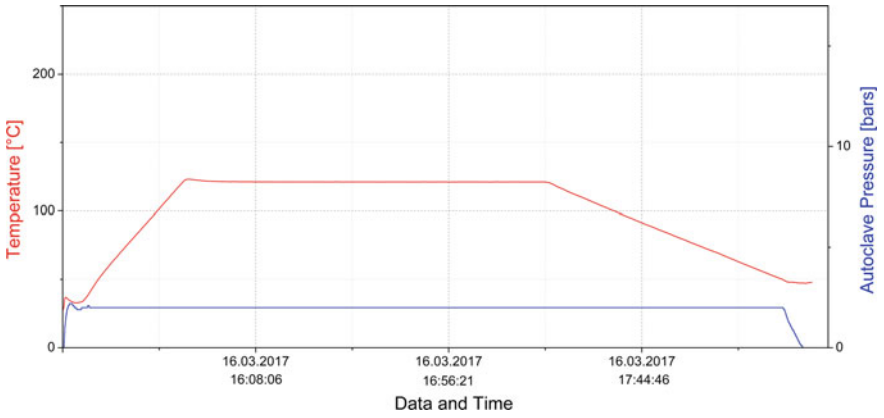

Fig. 2.13 Autoclave thermal and pressure cycle for bonding repair samples with the adhesive FM® 300-2

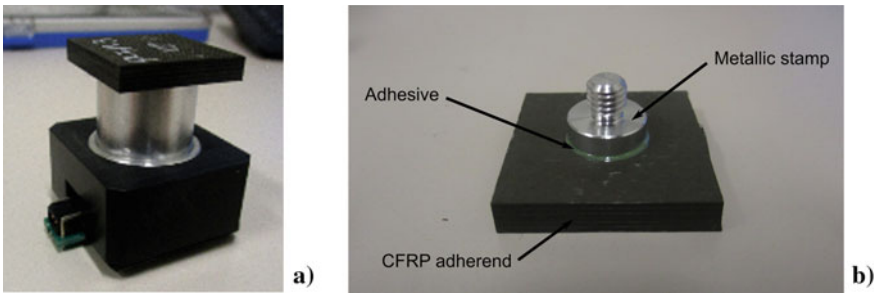

Fig. 2.14 Photographs showing the stamp-to-plate specimen used in the centrifuge tests; **a** full specimen configuration and **b** metallic stamp bonded to the CFRP adherend

2.4 Experimental Procedure

2.4.1 Characterization of CFRP Adherend Surfaces by Reference Methods

Spectroscopic surface characterization was performed on the CFRP adherends before the adhesive bonding to verify the contamination level obtained by the contamination procedure. X-ray photoelectron spectroscopy (XPS) was used as a spectroscopic reference method, and XPS measurements were performed on detached and cut plates in the state "as delivered" on three different surface positions.

X-ray photoelectron spectroscopy (XPS) is a widely used surface analysis method for the characterization of the elemental and chemical composition of a sample surface, which is positioned inside a vacuum system. XPS is based on the photoelectric effect and enables the study of the energy distribution of the photoelectrons emitted by X-ray irradiated compounds [18]. Monochromatic soft X-rays irradiate the sample surface, and upon interaction with the sample material electrons are emitted, mainly from the atomic core levels. These ejected electrons have discrete kinetic energies, and the portion of electrons passing the electron energy analyzer is detected within the photoelectron spectrometer. Signal intensities are given by the number of emitted photoelectrons as a function of the photoelectron kinetic energy. A high vacuum environment is required to enable the emitted photoelectrons to be analyzed without interference from gas-phase collisions, and in cases of electrically non-conducting surfaces special care is taken to control electrostatic surface charging.

2.4.2 Characterization of CFRP Bonded Samples by Reference Methods

Ultrasonic testing is considered a conventional NDT technique for the quality control of components. This technology is widely used for composite material inspection in aeronautics as well as in other domains. It is thus considered as a standard method by end users.

Within the ComBoNDT project, the aim of the ultrasonic inspection was to check the integrity and quality of the produced bonded samples. Indeed, according to the literature and also with regards to the context of the project, a "weak bond" is not expected to be detectable by conventional NDT methods. Otherwise, a common interpretation of the obtained data is that such a bond is considered a bond with defects (such as voids, porosity, gap-like disbonding) rather than as a possible weak bond. Therefore, within the framework of the characterization using ultrasonic testing as a reference method for the bonded samples, one issue was proving that the contamination and bonding processes do not lead to such defects. This information, in combination with the results of the terminal destructive mechanical testing (i.e. strength and fracture pattern), is required in order to consider the respective joints as samples with weak bonds.

Three categories of samples were investigated:

(a) Coupons were widely used by all the project partners in order to develop their ENDT technology, and thus it is of great importance that the quality of these samples is known. The obtained dataset comprises results from more than 360 samples.
(b) Multi-contaminated samples were used to increase the maturity of the ENDT technologies.
(c) Curved specimens were also tested. In this case, the curvature of the samples led to challenges in the signal reception, which rendered the inspection of these samples more prospective than quantifying.

The ultrasound-based inspections were performed in the Airbus laboratory using an M2M ultrasonic generator and a 6-axis mechanism (Fig. 2.15b, c). The immersion configuration was selected to maximize the signal quality. Samples were placed in consistent groups in the water tank on metal beams (Fig. 2.15d). The water path for passing the oscillation from the sonotrodes to the sample, i.e. the distance between the probe and the samples, was set to 40 mm on average. Two different phased array probes were used for the inspection (Fig. 2.15a). The characteristics are given below, with the trajectory parameters for each:

– 5 MHz linear probe, 64 elements, 1.0 mm pitch, 64 mm of aperture, 10 mm elevation, flat focusing; linear scanning; scanning step: 2 mm (standards), increment 30 mm
– 10 MHz linear probe, 64 elements, 0.5 mm pitch, 32 mm of aperture, cylindrical focusing (R = 40 mm); scanning step: 1 mm, increment 20 mm (i.e. 33% overlap)

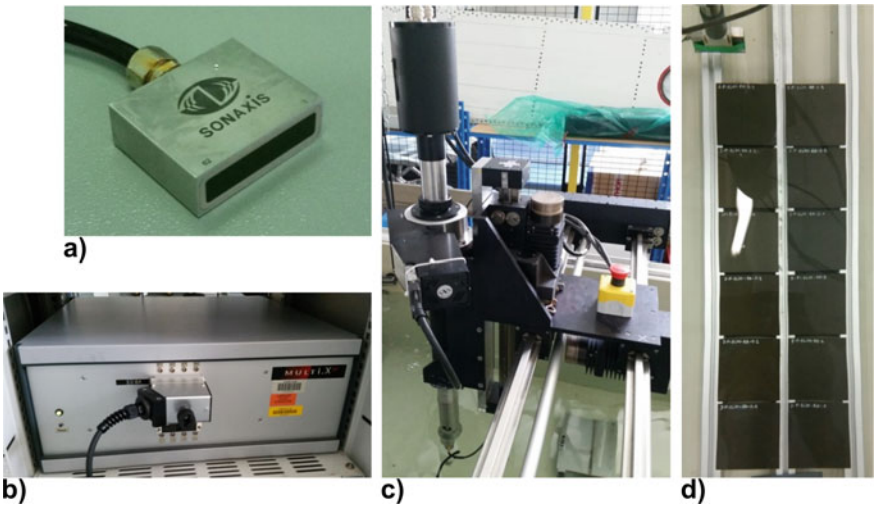

Fig. 2.15 Overview of the ultrasonic inspection setup; **a** example of a phased array probe; **b** ultrasound generator for emission and reception (M2M MultiX); **c** water tank and the 6-axis mechanism used to scan the parts; and **d** typical placement of the samples in the water tank for the inspections

The 5 MHz probe corresponds to Airbus standards. It was important to check that it is not possible to highlight any contamination-induced defects using current production tools. The 10 MHz probe was chosen because it is more accurate due to its higher central frequency and the smaller element size.

For each probe, different settings were used for the production samples and the repair samples. The global gain of the signal and the time correction gain (TCG) are slightly different between scenarios. This is mainly due to the bond material, which is different in each case and thus induces different ultrasonic responses.

In order to display ultrasonic cartographies, software settings (or gates) are necessary. A typical B-scan and A-scan are given in Fig. 2.16a with the gate display. Three main echoes can be observed, namely the front wall echo (with the gate or, respectively, obtained signal dataset denoted as "FWE"), bond echo ("Bond") and back-wall echo ("BWE"). All gates are synchronized using a synchronization gate tracking the entry echo. These gates can subsequently be used for the analysis. The respective details are

- "FWE" is the maximum of the front wall echo. It can be used to check the acquisition quality and to highlight surface defects.
- "g+" records the highest echo after FWE. In this case, it is typically the bond or the back-wall echo. The signal from this gate is particularly useful to compare the echoes.
- "Bond" is centered on the bond echo and tracks its maximum.
- "BWE" is centered on the BWE and tracks its maximum.

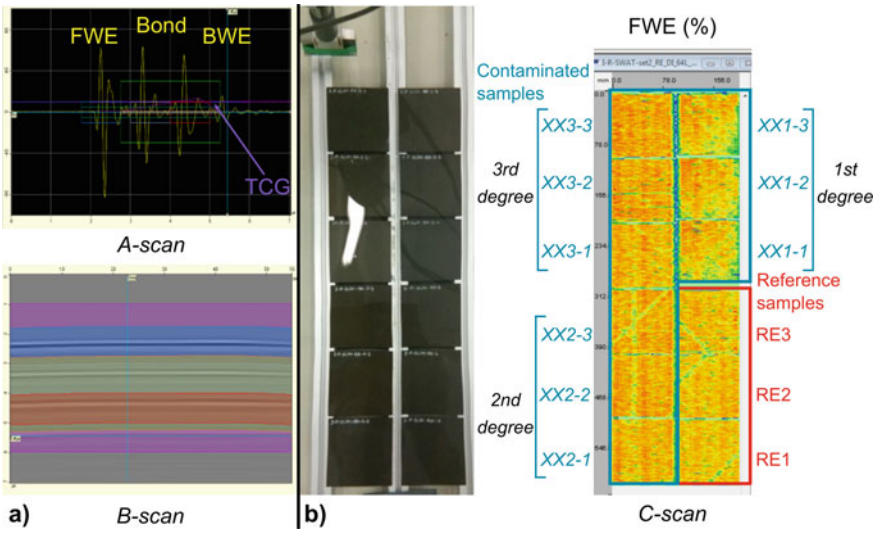

Fig. 2.16 Use and display of the ultrasound results from gates related to the front wall echo (FWE), bond echo (Bond), and back-wall echo (BWE); **a** typical A-scan and B-scan with gates setting display and **b** example of cartographies in amplitude for bonded coupon coupons with the corresponding sample positions

These gates are used to generate cartographies, also called C-scans, where the amplitude (given in %) or the time-of-flight (TOF, given in μs) of the recorded echo is displayed on the inspection plan (for an example of amplitude cartography see Fig. 2.16b). Samples are always placed in the same way with the references situated on the bottom right and the contaminated samples in the remaining spaces. For each set of samples, the origin is taken at the top left corner for the defect positioning.

In order to be complete, there must be precision on the phased array acquisition mode. Two different pulse-echo modes were used:

- The linear scanning (LS) mode, which consists of emitting a group of elements (E10 typically) and then receiving the same group of elements (R10). This configuration increases the scan accuracy. A single point focusing (SPF) can be added to direct the ultrasonic beam along the bondline, for example.
- The PaintBrush (PB) mode with the additional surface adaptative ultrasonic laws (SAUL) option, which consists of emitting with all the elements (E64) and then summing the responses by groups of elements (R10 for the 5 MHz probe and R16 for the 10 MHz probe). Such an investigation is faster but can lead to "strip-like" marks within the cartographies. The SAUL algorithm was also used in some specific cases. This option is particularly interesting for curved parts or to achieve a higher tolerance to a misalignment between the probe and the coupons.

2.5 Mechanical Testing

2.5.1 Fracture Toughness Testing

2.5.1.1 Mode-I Testing

Mode-I fracture toughness tests were conducted with double cantilever beam specimens according to the standard AITM 1-0053 [9] using a Tinius Olsen H5KT universal testing machine with a load cell of 5 kN under ambient conditions (25 °C, 55% RH) and under constant displacement control. Loading was applied to the DCB specimen via metallic piano hinges bonded to the adherends at one end. In order to avoid any influence of the incorporated release film, the specimen was preloaded until an initial crack length of 10–15 mm was achieved. The pre-cracked specimens were then loaded continuously by opening forces until a total propagated crack length of 100 mm was reached. After that, the test was stopped, and the specimen was unloaded. Six specimens per scenario were tested in this manner. During the crack propagation, the load and crosshead displacement of the test machine was recorded continuously. A traveling microscope was used to facilitate the visual measurement of the crack length. Figure 2.17 illustrates the mounting of a specimen onto the tensile testing machine during the mode-I test.

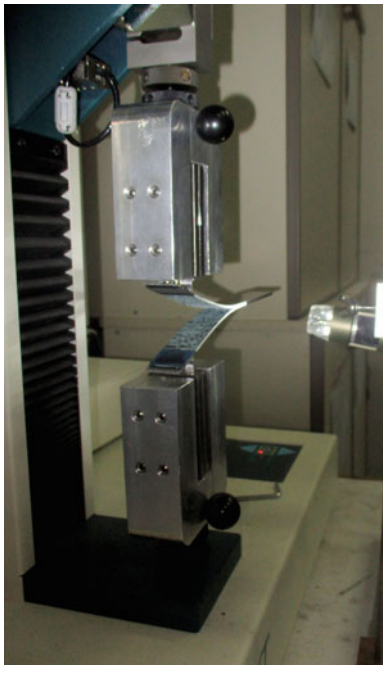

Fig. 2.17 Photograph showing a DCB specimen under mode-I loading

The AITM 1-0053 standard specification specifies the area method to determine the mode-I fracture toughness energy G_{IC} of CFRP bonded joints [9]. The crack extension is related directly to the area enclosed between the loading and unloading curves:

$$G_{IC} = \frac{A}{a \times w} \times 10^6 \left(J/m^2\right) \tag{2.1}$$

where

A is the energy required to achieve the total propagated crack length (J) (integration of the area of the load-crosshead displacement diagram)
a is the propagated crack length (mm) ($a = a_{final} - a_{initial}$)
w is the width of the specimen (mm)

The most popular approach to investigating delamination mechanisms in mode-I tests is the examination of fracture surfaces. Therefore, in order to accurately assess the causes of bondline failure, the fracture patterns were examined after the tests based on a visual inspection supported by photography. The classification, identification, and characterization of the failure mode of the CFRP bonded joints were conducted according to the ASTM D5573 standard [19]. For increased accuracy, a grid drawn on a clear film placed over the failure surface was used and the square areas showing a certain type of fracture pattern were counted, providing input to calculate the area percentage attributed to each failure mode. The main failure modes that were observed for the tested CFRP adhesive joints are schematically described in Fig. 2.18:

a. Adhesive (ADH) failure, which occurs when a separation takes place at the adhesive/adherend interface (respectively, within the three-dimensional adhesive/adherend interphase).
b. Cohesive (CO) failure, which results when a separation takes place within the adhesive.
c. Fiber tear (FT) failure, which is perceived when a failure occurs exclusively within the matrix of the CFRP adherend, resulting in the appearance of fibers on both fracture surfaces.
d. Light fiber tear (LFT) failure, which follows when a failure occurs within the adherend, near the interface characterized by a thin layer of the matrix on the fracture surface with few or no fibers transferred from the substrate to the adhesive.
e. Thin layer cohesive (TLC) failure, which is observed when the separation takes place within the adhesive in proximity to one adherend and not around the mid-thickness area of the adhesive layer.

Usually, a mixed failure occurs and symptoms of several failure modes are observed simultaneously for each tested specimen.

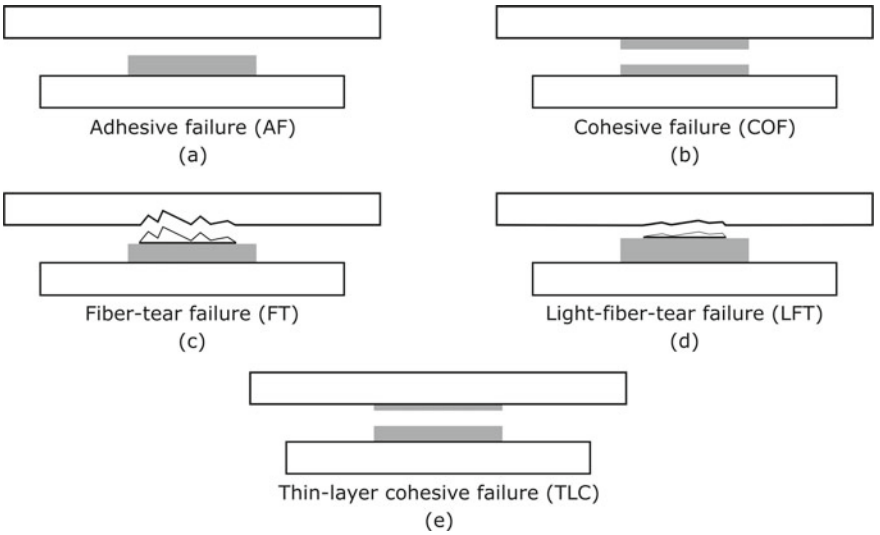

Fig. 2.18 Schematic representation of the main failure modes of CFRP bonded joints observed after destructive mechanical testing

2.5.1.2 Mode-II Testing

Since there is currently no standardized mechanical test to measure the fracture toughness energy of bonded joints under pure mode-II loading, we decided to use the ENF test, which we have identified as the most convenient mode-II fracture toughness test [16]. Figure 2.19 provides a schematic representation of the ENF test,

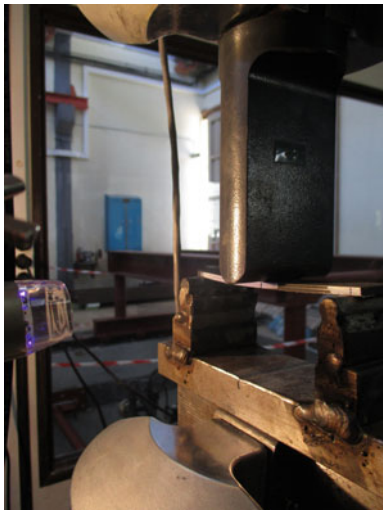

Fig. 2.19 Photograph showing an ENF specimen under mode-II loading

wherein a pre-cracked specimen is loaded into a three-point bending fixture until the crack propagation onset occurs.

Mode-II tests were conducted according to the AITM 1-0006 standard [20] under a constant displacement rate of 1 mm/min using an MTS universal testing machine with a load capacity of 100 kN. The test specimens were cut from the residual parts of mode-I specimens so that a pre-crack of 35 mm was achieved. Three specimens were tested for each condition within the considered scenarios. In order to facilitate the optical observation of the crack tip and the detection of the crack propagation onset, a digital microscope was used, and a thin layer of white ink was applied to the longitudinal side faces of the specimen.

Both the load applied to the specimen and the crosshead displacement of the test machine were continuously recorded during the test. To calculate the G_{IIC} fracture toughness energy, the following formula was used [20]:

$$G_{IIC} = \frac{9 \times P \times a^2 \times d \times 1000}{2 \times w \times \left(1/4 \times L^3 + 3 \times a^3\right)} \left(\mathrm{J/m^2}\right) \tag{2.2}$$

where

d is the crosshead displacement at onset of the crack propagation (mm)
P is the critical load to start the crack propagation (N)
a is the initial crack length (mm)
w is the width of the specimen (mm)
L is the span length (mm)

2.5.1.3 Centrifuge Testing

Standardized methods only allow the testing of specific bond strength parameters, and the achieved statistics are often limited due to the high cost and work effort required. Additionally, the respective measurements are time and cost-consuming due to complex sample and fixture preparation, single-sample testing, and manual evaluation of the mechanical load and fracture surfaces. Against this background, the novel centrifuge test is introduced in order to overcome these limitations.

Up to eight samples can be measured within 5 min and the measured mechanical properties have a defined accuracy with very good precision and reproducibility. The novel testing is cost-efficient, fast, and reliable. In the ComBoNDT project [5], the information value of mechanical testing was increased as compared to the results obtained from the abovementioned standardized mechanical tests.

The centrifuge testing principle for bonded joints is illustrated in a schematic diagram in Fig. 2.20 [21]. The centrifuge test is based on the physical law of inertia of a body [22]. Due to rotation, a progressively increasing radial centrifugal force is applied synchronously to each of the specimens being tested. The load increase is adjusted through a variation of the rotor's rotational speed.

Across the bondline, the axial centrifugal force acts as a normal tensile force. If the applied load exceeds the tensile strength of the joint, a rupture occurs, and the

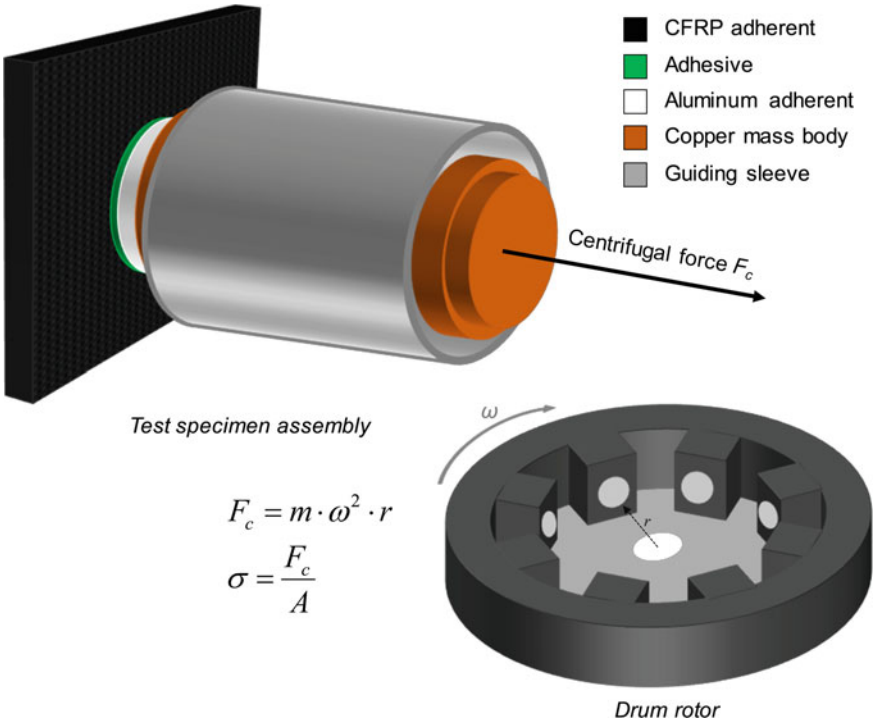

Fig. 2.20 Diagram highlighting the measurement principle of the centrifuge test

test stamp changes its position within the guiding sleeve. The detachment of the test stamp from the CFRP adherend at the moment of rupture is automatically detected and a position-coded infrared signal is sent from the turning rotor, transmitting the current rotor speed as well as the rupture time [23].

The centrifugal force F_c (N) is derived from

$$F_c = m \cdot \omega^2 \cdot r \tag{2.3}$$

where m (kg) is the mass of the stamp, r (m) is the distance of the test stamp to the rotational axis, and ω (rad/s) is the angular velocity related to frequency v by

$$\omega = 2 \cdot \pi \cdot v \tag{2.4}$$

Dividing the centrifugal force F_c (which is effective at the time of the adhesive fracture) by the area of the bondline A (mm^2), the tensile adhesion strength σ (MPa) is derived:

$$\sigma = \frac{F_c}{A} \tag{2.5}$$

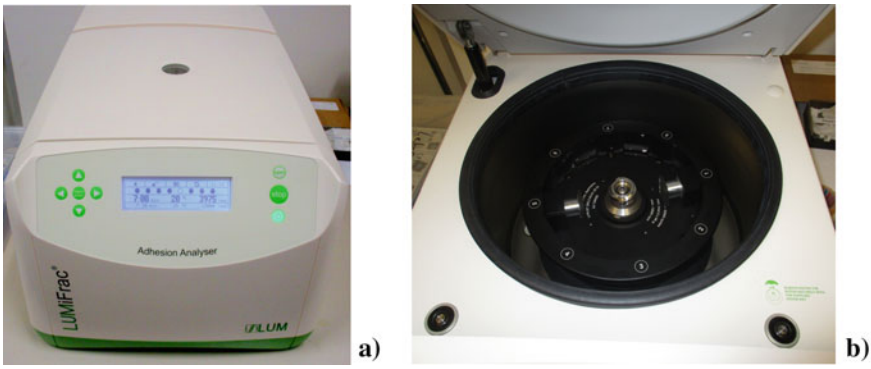

Fig. 2.21 Photographs displaying the setup for the centrifuge test; **a** the LUMiFrac desktop analyzer and **b** stamp-to-plate test specimens inside the drum rotor

For the preparation of the thus investigated joints, the composite substrates were subjected to contamination with the release agent, moisture, fingerprint, thermal degradation, or de-icing fluid before being bonded to the metallic stamp. The centrifuge tests were carried out using a LUMiFrac desktop adhesion analyzer equipped with an LSFR-ST: 200.42 drum rotor with up to eight testing units (Fig. 2.21). The fully loaded rotor allows for a maximum rotational speed ω of 13,000 rpm, corresponding to a centrifugal acceleration of 13,715 g [23].

By means of the SEPView software, the desired load-controlled testing sequence was realized. To achieve compatibility with conventional testing machines (in load-controlled mode), the increase in the rotational speed of the rotor was designed to be quadratic. According to Eq. (2.3), a square root-like increase in the rotational speed is accompanied by a linear increase in the centrifugal force [24]. Subsequently, the rotor and centrifuge lid were closed, and the testing procedure was initiated. The duration of each test lasted from 6 to 20 s on average, depending on the contamination scenario. The rupture event was detected online outside the centrifuge using a position-coded and rpm-correlated infrared data transmission from the inside of the testing units mounted in the drum rotor. After testing, high-resolution microscopy images of the failure surfaces of both the CFRP adherend and the test stamp's side were taken and examined with the aim of characterizing the failure patterns.

2.5.1.4 Tensile Testing

Scarfed samples were loaded under ambient conditions (25 °C/48%RH) by tensile stress using an MTS universal testing machine with a load capacity of 100 kN under a constant crosshead speed of 0.5 mm/min (Fig. 2.22) until a final failure (separation) of the two scarfed adherends occurred. Aluminum end tabs (30 mm × 25 mm × 2 mm) were bonded to the ends of the specimens using a two-part adhesive (PM Mega Cryl) in order to achieve a successful and smooth introduction of the load into

Fig. 2.22 Photograph showing a scarfed specimen under tensile loading

the specimen. Moreover, the end tabs prevented gripping damage to the adherends or premature failure as a result of a significant discontinuity. The load and crosshead displacement were recorded using a computerized data logging system. A total of four tests were performed for each contamination scenario and the failure load was the mechanical feature used for comparing the tested specimens.

Additionally, after the tensile tests, the failure surfaces were examined in order to accurately assess the causes of adhesive joint failure. The ASTM D5573 [19] standard was followed.

2.5.1.5 Environmental Aging

The procedure given in the EN 2823 [25] standard was used to determine the effects of after-bond exposure of the joints to a humid atmosphere on the mechanical characteristics of the contaminated joints. The specimens were exposed without mechanical loading to conditions of 70 °C and 85% RH until the moisture saturation point, which was reached after approximately 65 days of aging.

The specimens to be aged were placed inside an environmental chamber with an embedded pre-crack (Fig. 2.23), which was created a priori through mode-I tests conducted according to the AITM 1-006 standard [20]. Reference and contaminated specimens were subjected to hygrothermal aging using an ESPEC SH-641 environmental chamber for a period of 64–74 days, ensuring that the saturation point was reached.

Fig. 2.23 Photograph showing CFRP joint specimens inside the chamber during environmental aging

During the hygrothermal aging period, the weight of the specimens was measured at weekly intervals. After the hygrothermal aging, the specimens were stored in sealed containers and tested under mode-II loading conditions within 72 h according to the DIN EN 2823 standard [25].

As a measure of the absorbed moisture, the percental normalized weight gain $M(t)$ was used:

$$M(t) = \left(\frac{w_t - w_0}{w_0}\right) \times 100 \tag{2.6}$$

where

w_0 is the initial weight (g)
w_t is the weight at exposure time t (g)

The weight gain achieved with these hygrothermal aging conditions was 0.49–0.71%. Fick's law was used to define the equilibrium conditions in composite materials [25]. The diffusion coefficient D of water is derived from the slope of the linear part of $M(t)$ curve as

$$D = \pi \times \left(\frac{h}{4 \times M_\infty}\right)^2 \times S^2 \left(\frac{\text{mm}^2}{2}\right) \tag{2.7}$$

where

M_∞ is the water uptake at saturation (wt%)
h is the specimen thickness (mm)
S is the slope of the $M(t)$ curve $\left(1/s^{0.5}\right)$.

2.6 Experimental Results

2.6.1 Spectroscopic Surface Characterization

To prepare the clean reference samples from the delivered CFRP plates, a thorough cleaning procedure was followed to remove any contaminations or residues remaining from the manufacturing process (Fig. 2.24). Each step was monitored using X-ray photoelectron spectroscopy (XPS) analyses to measure the amount of release agent on the plate surface:

1. Pre-cleaning of the plates with isopropanol (IPA) soaked tissues to remove part of the release agent and any other soluble contaminations, e.g. fingerprints, remaining from the manufacturing process. XPS measurements performed on the "as delivered" plates on three different positions showed an inhomogeneous distribution of Si-containing release agent on the CFRP surface (Table 2.3). The XPS results for the cleaned plates showed that pre-cleaning with IPA is effective in that the amount of release agent on the CFRP surface can be reduced to 0.5–1.4 at.% within the information volume of the investigation. This indicates the

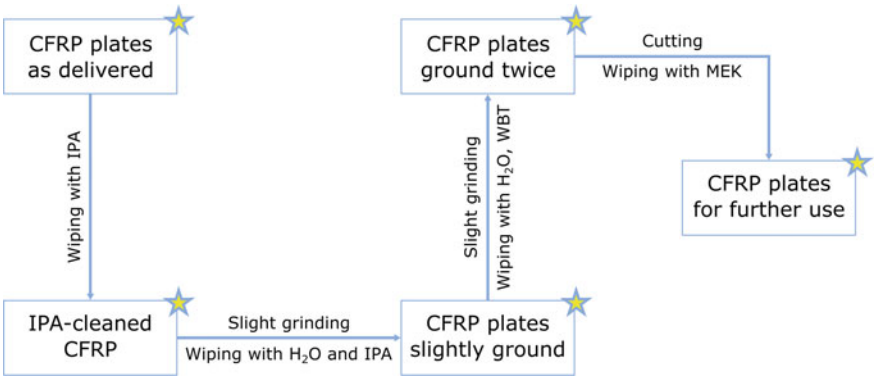

Fig. 2.24 Process of the cleaning of as-received CFRP plates by moist wiping with water, isopropanol or methylethylketone soaked tissues and grinding with sandpaper

Table 2.3 Surface Si concentrations (in at.%) from XPS investigations performed for the CFRP sample plates following the given cleaning steps with isopropanol (IPA)

CFRP plates	Si (at.%)
CFRP "as delivered" sample plates	5.3 ± 1.3
CFRP sample plates after IPA cleaning	0.9 ± 0.5
CFRP sample plates after IPA cleaning and slight grinding	0.3 ± 0.2
CFRP sample plates after IPA cleaning and two slight grinding steps with cleaning in between	0.1 ± 0.04

amount of dehesive material that can easily be removed by a subsequent abrasive grinding step without significant smudging.
2. Slight grinding of the surfaces to remove residual release agent that had penetrated or was incorporated into the topmost resin layers, and afterward wiping with demineralized H_2O and IPA to remove the dust from the grinding, which comprised the inhering residual silicone. Further XPS measurements showed that a small amount of silicone remained on the surface (Table 2.3).
3. A second slight grinding step followed by wiping off the dust with demineralized water and IPA. On these samples, XPS measurements showed a very clean surface Table 2.3.

After the cleaning steps, the sample plates were wiped with methylethylketone (MEK) soaked tissues prior to performing the intentional contamination (corresponding to the respective scenario) and the subsequent adhesive bonding.

For the release agent contamination scenario (RA), the first and last dip-coating samples for each dip-coating solution (labeled RA-1, RA-2, or RA-3) were used for the XPS measurements; these were conducted on three positions (top, middle, bottom) on each sample. The results are shown in Table 2.4.

Based on these results, samples with the final concentrations of Si on the CFRP surfaces were obtained, as shown in Table 2.5.

For the production fingerprint contamination, three samples with each FP concentration were prepared for the XPS measurements. The results are shown in Table 2.6.

Based on these results, the concentrations of Na and Cl on the CFRP surfaces for each contamination level could be determined, as described in Table 2.7.

For the repair fingerprint scenario (FP), the locally applied Skydrol has the tendency to spread over the surrounding surface, thus no clear fingerprints can be observed after some time. Systematic XPS measurements were not conducted for this contamination scenario since most of the oil evaporates in the vacuum of the analysis chamber.

Since the de-icer contains potassium formate, the potassium content on the surface is taken as a measure for the degree of de-icer contamination. Dip-coating of the final de-icer contaminated samples was performed using solutions of 2, 7, and 10% de-icer in demineralized water. The samples for XPS control were dip-coated together with these samples. The XPS results are shown in Table 2.8.

Based on these results, the final concentrations of potassium on the CFRP surfaces for each contamination scenario were determined (Table 2.9).

Table 2.4 XPS results (indicating the surface concentrations of the main elements [in at.%] as obtained) for CFRP plates after dip-coating in Frekote solutions (following RA-1, RA-2, RA-3) with different concentrations

Samples	C (at%)	O (at%)	N (at%)	Si (at%)	S (at%)	Na (at%)
RA-1 start, top	69.7	19.6	6.8	2.6	1.2	<0.1
RA-1 start, middle	67.1	22.2	5.2	3.6	1.4	<0.1
RA-1 start, bottom	66.6	20.5	6.6	5.1	0.8	<0.1
RA-1 end, top	70.0	19.2	6.9	2.5	0.9	0.2
RA-1 end, middle	70.4	18.6	7.1	2.6	1.1	0.1
RA-1 end, bottom	69.9	19.1	7.1	2.6	1.0	0.2
RA-2 start, top	67.3	20.9	6.5	4.3	1.1	<0.1
RA-2 start, middle	64.9	22.1	6.1	5.6	1.0	<0.1
RA-2 start, bottom	66.1	20.8	6.9	5.2	0.7	<0.1
RA-2 end, top	68.4	19.2	7.2	4.2	0.8	<0.1
RA-2 end, middle	65.4	21.3	6.6	5.2	0.9	0.1
RA-2 end, bottom	65.2	21.1	6.5	5.9	0.7	0.3
RA-3 start, top	66.0	20.4	6.9	5.8	0.7	<0.1
RA-3 start, middle	63.2	23.1	5.7	6.4	0.9	0.3
RA-3 start, bottom	64.8	21.0	6.6	6.6	0.6	<0.1
RA-3 end, top	65.3	22.2	5.0	6.3	1.1	<0.1
RA-3 end, middle	65.4	21.0	6.5	6.1	0.7	<0.1
RA-3 end, bottom	64.5	23.0	4.8	6.2	1.1	<0.1

Table 2.5 Average concentration of Si on CFRP surfaces (obtained by XPS) for the RA contamination scenario

Scenario	Si (at.%)
RA-1	3.2 ± 1.0
RA-2	5.1 ± 0.7
RA-3	6.2 ± 0.3

Table 2.6 XPS results indicating the surface concentrations (main elements) of three CFRP plates contaminated with different (salty) solutions (FP-1, FP-2, FP-3) applied as a fingerprint

Samples	C (at%)	O (at%)	N (at%)	Si (at%)	Zn (at%)	Cl (at%)	S (at%)	Na (at%)
FP-1, sample 1	74.6	15.3	8.5	0.2	0.1	0.4	0.6	0.2
FP-1, sample 2	74.5	16.6	6.3	0.2	0.2	0.8	1.0	0.3
FP-1, sample 3	74.7	16.6	6.8	0.2	<0.1	0.3	1.0	0.2
FP-2, sample 1	74.0	15.0	8.8	<0.1	<0.1	0.9	0.7	0.5
FP-2, sample 2	73.2	16.8	7.3	<0.1	<0.1	0.9	1.0	0.6
FP-2, sample 3	74.5	17.2	5.2	0.2	<0.1	0.9	1.4	0.5
FP-3, sample 1	73.8	16.0	7.5	0.1	-	0.9	1.1	0.6
FP-3, sample 2	73.3	15.3	8.5	0.1	<0.1	1.2	0.8	0.8
FP-3, sample 3	73.3	16.1	7.4	0.1	-	1.2	1.1	0.8

Table 2.7 Selected average surface concentrations (from the XPS results) of CFRP samples treated with differently concentrated solutions (FP-1, FP-2, and FP-3) applied as a fingerprint

Scenario	Na (at.%)	Cl (at.%)
P-FP-1	0.2 ± 0.1	0.5 ± 0.3
P-FP-2	0.5 ± 0.1	0.9 ± 0.0
P-FP-3	0.7 ± 0.1	1.1 ± 0.2

2.6.2 Ultrasound Results

2.6.2.1 Coupons

In this section, the results from the two different phased array probes used are presented, depending on the highlighted feature. Various types of defects were observed over the complete set of samples; these can be grouped into the three categories detailed below. The first one contains observations of a minor defect due to manufacturing; the second one comprises slight deviations from the reference; and the third one is the category of obvious defects with possible consequences for the ENDT measurements. Illustrations are given in the following sub-sections.

Table 2.8 Final XPS results indicating the surface concentrations at distinct positions (pos.) for CFRP samples contacted with different de-icer dip-coating concentrations (DI1, DI2, DI3)

Samples	C (at%)	O (at%)	K (at%)	S (at%)	Si (at%)	Cl (at%)	N (at%)	Na (at%)
DI-1 sample 1, pos. 1	58.4	28.5	8.9	0.8	0.3	0.3	2.6	0.3
DI-1 sample 1, pos. 2	62.5	25.9	6.2	0.9	0.3	0.3	3.7	0.2
DI-1 sample 1, pos. 3	64.1	25.7	4.3	0.9	0.3	0.3	4.3	<0.1
DI-1 sample 2, pos. 1	61.9	26.2	8.4	1.0	<0.1	0.5	1.8	0.1
DI-1 sample 2, pos. 2	65.0	24.3	5.2	0.9	<0.1	0.2	4.2	<0.1
DI-1 sample 2, pos. 3	63.5	25.0	5.6	0.6	<0.1	0.2	4.7	<0.1
DI-2 sample 1, pos. 1	55.7	30.5	11.0	0.6	1.0	0.2	0.8	0.2
DI-2 sample 1, pos. 2	51.8	32.9	12.8	0.5	0.6	0.2	0.8	0.3
DI-2 sample 1, pos. 3	51.5	31.8	13.8	0.6	1.0	0.2	0.9	0.2
DI-2 sample 2, pos. 1	63.8	24.9	7.4	1.0	<0.1	0.2	2.6	0.1
DI-2 sample 2, pos. 2	62.6	24.4	10.2	0.6	0.3	0.2	1.5	0.1
DI-2 sample 2, pos. 3	63.9	23.3	10.0	0.6	0.4	0.2	1.5	0.2
DI-3 sample 1, pos. 1	52.3	31.9	13.0	0.4	0.6	0.2	1.1	0.2
DI-3 sample 1, pos. 2	55.2	30.5	11.2	0.6	1.1	0.1	1.1	<0.1
DI-3 sample 1, pos. 3	55.7	29.2	11.8	0.6	0.9	0.2	1.3	0.3
DI-3 sample 2, pos. 1	57.5	28.7	11.9	0.5	0.4	0.2	0.4	0.3
DI-3 sample 2, pos. 2	57.3	29.6	9.9	0.9	0.2	0.1	1.7	0.2
DI-3 sample 2, pos. 3	53.8	29.3	14.0	0.6	0.6	0.1	0.8	0.2

Table 2.9 Average concentration of potassium on CFRP surfaces for the DI contamination scenario

Scenario	K (at.%)
DI1	6.4 ± 1.8
DI2	10.9 ± 2.3
DI3	12.0 ± 1.4

First category of defects: Minor defects due to sample manufacturing

The defect types within this category can be itemized into three groups. These are most likely due to the sample manufacture and are expected to have no impact or a low impact on the ENDT measurements:

- Bending of the bonded specimens (Fig. 2.25a). This defect type was particularly observed for the repair reference samples as well as some of the samples within the TD scenario. The observed curvature is evidenced on the FWE amplitude cartography with the 5 MHz probe, as shown in Fig. 2.25a. In fact, a phased array measurement was only possible using the SAUL option to partially compensate for the curvature and the induced misalignment of the probe with the sample along its

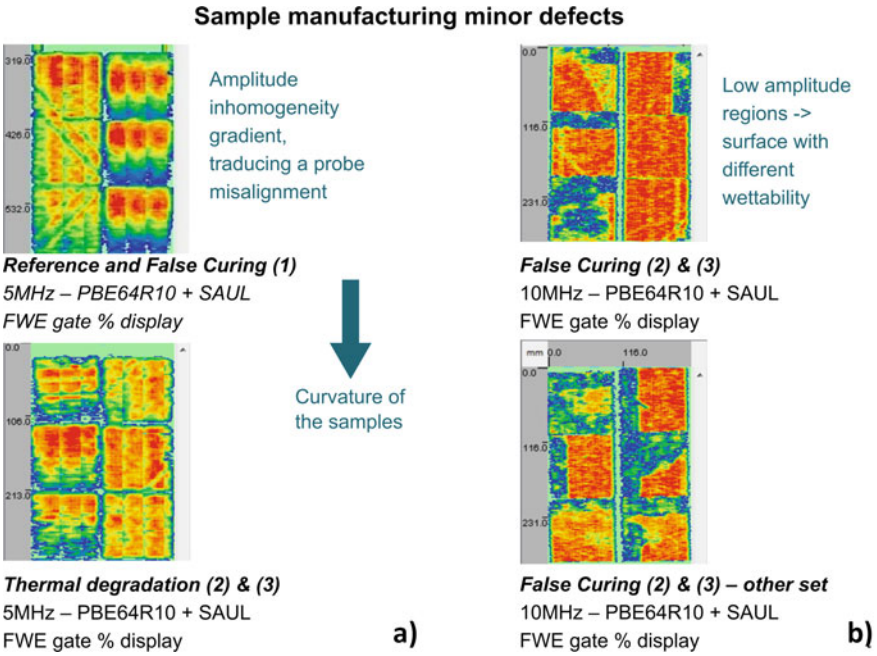

Fig. 2.25 Overview of the minor manufacturing defects observed during the ultrasonic inspection of CFRP specimens, with typical examples of **a** the bending of samples and **b** the surface quality problem

length. However, even if this defect has an effect on the ultrasonic measurements, it should have no consequences for the ENDT investigations.

- Bad quality of the composite surface (Fig. 2.25b). This defect type was evidenced using the 10 MHz probe on the FWE amplitude cartographies. Indeed, the cylindrical focusing of the probe increases the sensitivity to such surface defects. These were generally located on edges and were probably due to marks left by the adhesive tape used during the manufacture. In these areas, wettability with the ultrasound coupling medium is probably different, thus leading to low amplitude regions. In other rare cases, the wall surface was covered, probably due to resin leakage.

Second category of defects: Minor deviation from the reference, potentially due to contamination

Other sample inspection results presented a significant deviation from the reference measurements, albeit without clear evidence of a defect (Fig. 2.26). Specifically, in case of CFRP samples from the P-MO and P-FP scenarios, the bond echo amplitude is of approximately the same order of magnitude as the BWE, whereby this is not the case for the reference and other contaminated samples (as shown by the release agent samples in Fig. 2.26). This observation could be due to higher bond impedance or lower back composite skin impedance. In other words, it could be a sign of bond alteration or composite alteration (especially in the case of moisture). This was evidenced using g+gate TOF cartography, which displays the position of

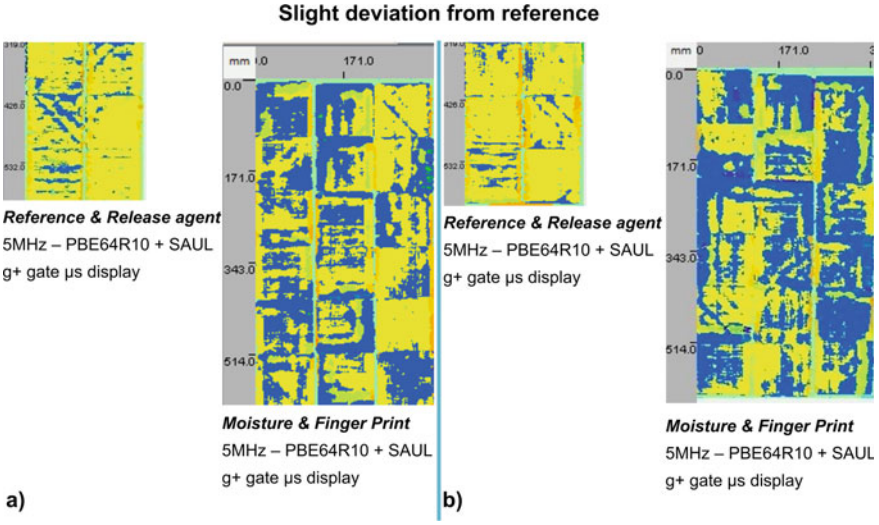

Fig. 2.26 Example of ultrasonic inspection results for CFRP specimens showing a slight deviation from the reference, taking the "g+" gate display for the reference and release agent scenario or for the moisture and fingerprint combined contamination scenario; **a** first sample set as an example and **b** second sample set as an example

the maximum echo in the sample thickness. Referring to the color coding used for displaying the results of the ultrasound investigations, blue corresponds to the bond echo, and yellow to the BWE. A mix between blue and yellow means that the echoes are of approximately the same order of magnitude, while only yellow means that BWE dominates. Two examples are given in Fig. 2.26a for the first set of samples, while Fig. 2.26b shows the second set. This effect is so far neither well defined nor explained, but it might be due to contamination. However, this does not prevent these samples from being considered as weak bonds.

Third category of defects: Obvious defects due to "contamination"

Finally, more sizeable and obvious defects with a potentially highly detrimental effect on the future ENDT measurements were observed, namely delamination and disbonding. CFRP specimens having undergone faulty curing or thermally degraded samples are the main concerns here. In these cases, the state of the joint of the samples cannot be considered as presenting as a weak bond but rather as a bond with defects. All the observed defects are presented in Figs. 2.27 and 2.28.

In the FC-1 samples (Fig. 2.27), the regions showing the effects of debonding are evidenced in the middle of each plate. A defect signature is visible in the bond amplitude and TOF cartographies. The highest amplitude and a small shift in TOF, respectively, show debonding with a high contrast. Consequently, defects are also visible on the BWE amplitude gate, with a low amplitude region, and in the "g+" TOF cartography. The sizes of the debonding regions vary depending on the samples but are usually above 1 cm and up to 5 cm. These debondings are located in the middle of the bonded coupons and, thus, they could have a significant impact on the ENDT measurements. Note that some small debonding spots (smaller than 1 cm) are also observed in some of the FC-2 samples. These defects were probably induced by the way the samples were manufactured.

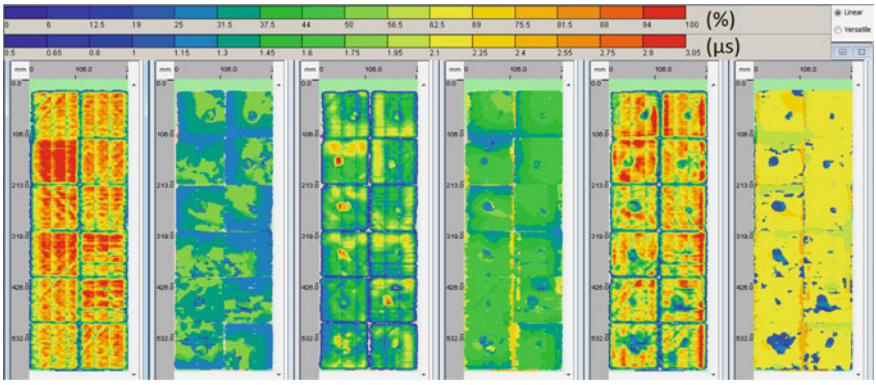

Fig. 2.27 Results of the ultrasound investigations for samples within the FC-1 scenario—observation of disbonding in all the samples with defects showing a size range of 1–5 cm

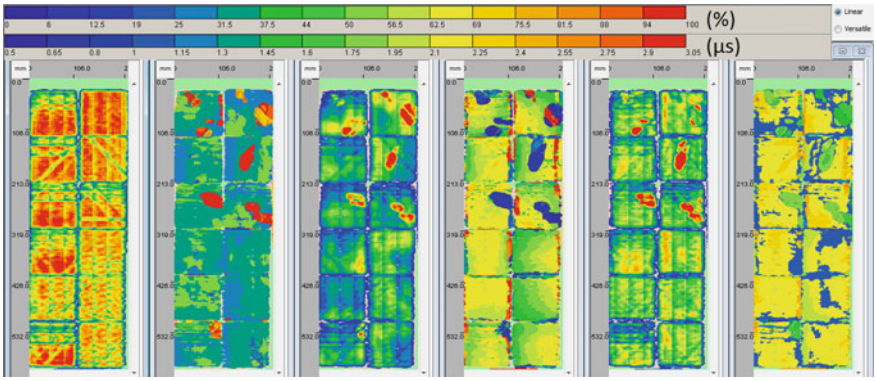

Fig. 2.28 Results of the ultrasound investigations for all samples within the TD-3 scenario—observation of delamination, in some samples with a size in the range of 2–5 cm

For the TD-3 samples, important delaminations were highlighted by ultrasonic inspection (Fig. 2.28), however not for all samples. The delaminations are evidenced by all the gates because they are located on the first composite skin, i.e. the one that has been thermally affected. This is confirmed by the "g+" TOF cartography (cf. light green color coding in the figure of Table 2.10). Therefore, the defect signature enters the bond gate and has consequences on all the other gates. Because of their considerable size (several centimeters) these delaminations could have a strong influence on results obtained using ENDT techniques.

The most profound investigations were achieved using a post-treatment tool. In this work, the NDTKit analysis software was used to obtain the ultrasound data for the CFRP samples (the commercial version of this software is named Ultis), whereby "defect detection" was enabled to size some of the defects. An example of a case of faulty curing is presented in Table 2.10, together with the main characteristics typical for disbonding and described according to the parameters of position on the plate, surface, outline surface, length, and mean value (for TOF). We note that the origin of the defect is at the top left-hand corner of each plate.

2.6.2.2 Combined Contamination Coupons

Multi-contaminated samples were also investigated using the same methodology and the same instrument settings as described above. Essentially, the same kinds of defects were observed for these samples, which is as expected since their manufacturing and contamination procedures were the same. Some examples are given in Fig. 2.29, and are these are further detailed below.

Minor defects were also observed; in this case, they are attributed to clamp marks, as shown in Fig. 2.29a. These are located on the edges and occur during the sample manufacture (probably while stabilizing the plate for bonding). On the ultrasound data acquisitions, they are visible on the bond amplitude C-scan as well as on the

Table 2.10 Example of an ultrasound-based defect detection result for CFRP coupons prepared within the faulty curing scenario, indicating the position in the plate, surface, outline surface, length, and mean value (for TOF)

Defect detection	Names (centers)	Surface (mm^2)	Outline (mm^2)	Length (mm)	Mean (μs)
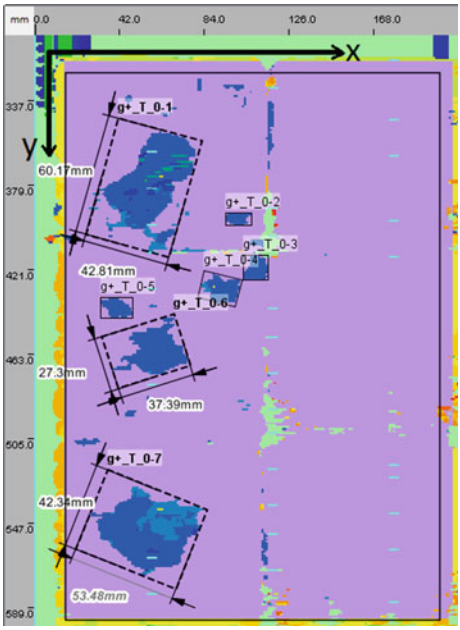	g+_T_0-1 (X = 43, Y = 62)	1328.0	2575.6	60.2	1.08
	g+_T_0-2 (X = 92, Y = 81)	57.0	78.0	13.0	1.08
	g+_T_0-3 (X = 98, Y = 7)	115.0	144.0	12.0	1.09
	g+_T_0-4 (X = 80, Y = 20)	174.0	260.2	19.2	1.12
	g+_T_0-5 (X = 28, Y = 27)	108.0	160.0	16.0	1.08
	g+_T_0-6 (X = 49, Y = 49)	517.0	1020.9	37.4	1.07
	g+_T_0-7 (X = 44, Y = 44)	1350.0	2264.3	53.5	1.12

FWE gate. Indeed, this type of defect is often associated with a bond material leakage on the composite surface (due to bond creep). Therefore, the composite surface is also modified. Note that these areas are also often associated with a bond thickness reduction. Moreover, slight deviations from the reference can also be evidenced in the case of the "release agent+fingerprint" scenario. The effect is in this case probably the same as the one explained in the previous section, namely that a higher bond impedance may have been induced by the contamination. Since this effect was not observed when considering the release agent contamination alone, it might mean that additionally applying the fingerprint is causal for this signature in the combined contamination samples.

2.6.2.3 Curved Specimens

Finally, the curved specimens were tested. Compared to inspecting the flat samples using ultrasound, these inspections are more challenging because of the geometry of the part. The echo entry face reverberates almost all the incoming energy in a divergent beam. Therefore, it is very hard to inspect such a type of geometry with

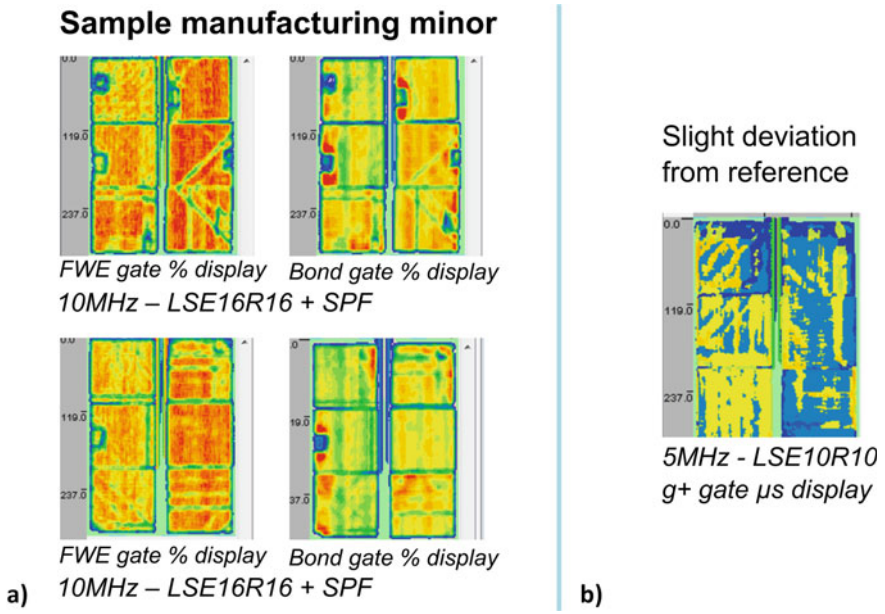

Fig. 2.29 Overview of the defects observed by ultrasound investigations of CFRP samples from the combined contamination scenarios, especially the scenario "release agent+finger print"; **a** minor manufacturing defect and **b** minor deviation from reference

a regular phased array setting. An example of an inspection result when using a conventional linear scanning configuration is shown in Fig. 2.30. Only one small part of the sample appears in the cartography for the curved specimen. The thus inspected region corresponds to the place where the sample surface is oriented closest to parallel to the probe, plausibly in the middle of the curved specimen. Everywhere else, no echo was measured, which is attributed to the fact that all the waves were reflected away from the probe.

To solve this issue, the SAUL algorithm was used. The idea is to first describe the surface geometry by using the ultrasonic phased array like a radar, whereby the

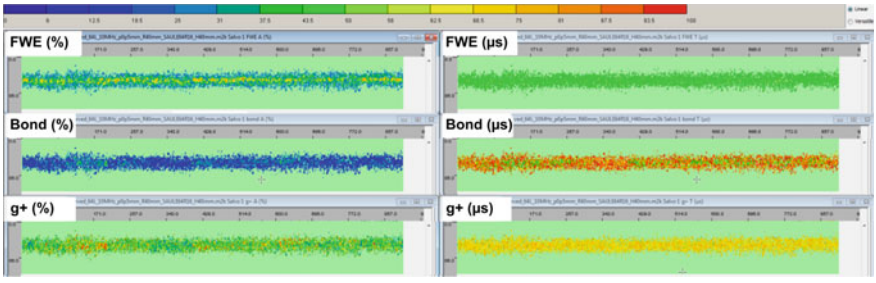

Fig. 2.30 Inspection results for a curved CFRP when using a linear scanning configuration

distance to each element of the probe is detected. Subsequently, the delay laws are calculated to generate an ultrasonic wavefront that will fit the sample geometry. In Fig. 2.31, an example based on a CIVA numerical simulation is presented in order to explain the principle. The elements on the edges are shot first, while those in the middle are shot in the last position.

The curved CFRP sample inspections when applying SAUL are presented in Fig. 2.32. The results show that the specific algorithm helps to complete the inspection. We did not notice any lack of data acquisition in any region of the specimen, and the echo-wall "ew" amplitude was more or less homogeneous. Inspections were thus possible thanks to SAUL, and the obtained signal could be used to make a statement

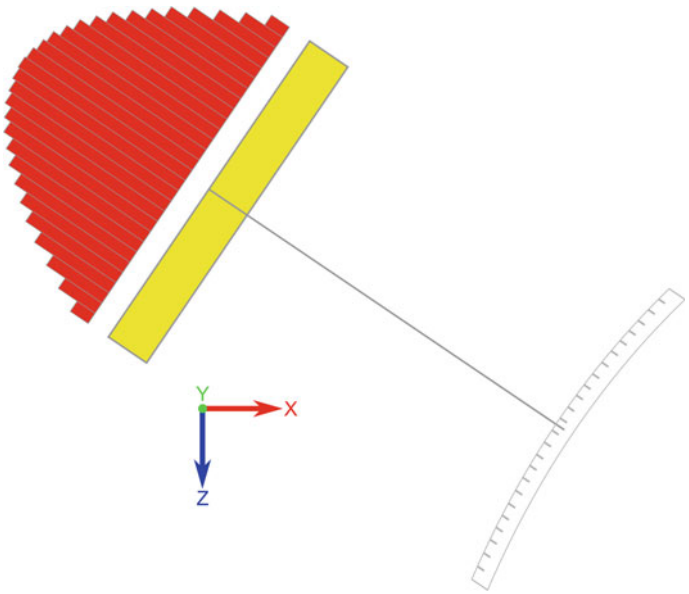

Fig. 2.31 Sketch showing an example of a SAUL (surface adaptative ultrasonic laws) calculation applying CIVA software

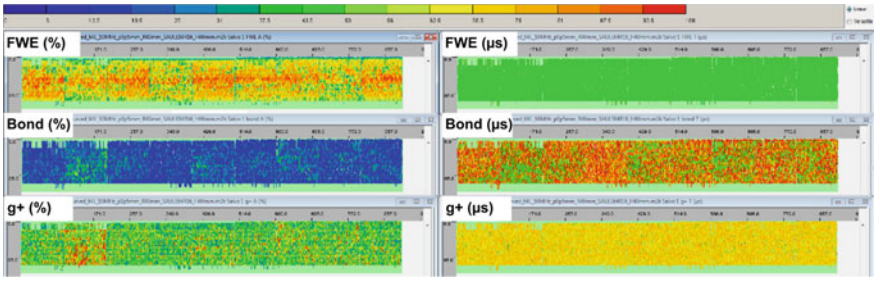

Fig. 2.32 Ultrasound inspection results for a curved CFRP specimen using a SAUL configuration

about the material quality, which appears to be very poor. Indeed, the amplitude of the BWE turned out to be very low. The TCG had to be significantly increased in order to receive a signal from the back wall. This necessary increase in the gain is an indication of strong attenuation, probably due to a high porosity content. Thus, it is difficult to give a clear statement on the bond quality, since the quality of the composite adherends might be the main issue.

2.6.3 Fracture Toughness Results

As presented in the previous sections, pre-bond contamination was systematically arranged and intentionally performed on CFRP adherends, and the adherend surfaces as well as the resulting CFRP bonded joints were then characterized by means of reference laboratory non-destructive testing (NDT) methods. Subsequently, the results from the destructive testing regarding the respective joint strength are reported and the effects of the carefully adjusted deviation from the qualified bonding process are evaluated based on the observed joint strength and fracture pattern, which are a common design quantity constituting a joint specification. Using the terminology introduced in Chap. 1 for the concept of quality assessment in adhesive bonding suggested in this book, in the aircraft production this strength is considered a design-relevant operands feature.

2.6.3.1 Mode-I Testing

The average G_{IC} values of the specimens manufactured within the production and repair scenarios are presented and compared in the compendious histograms in Fig. 2.33 and Fig. 2.34, respectively. The reference category samples denoted as

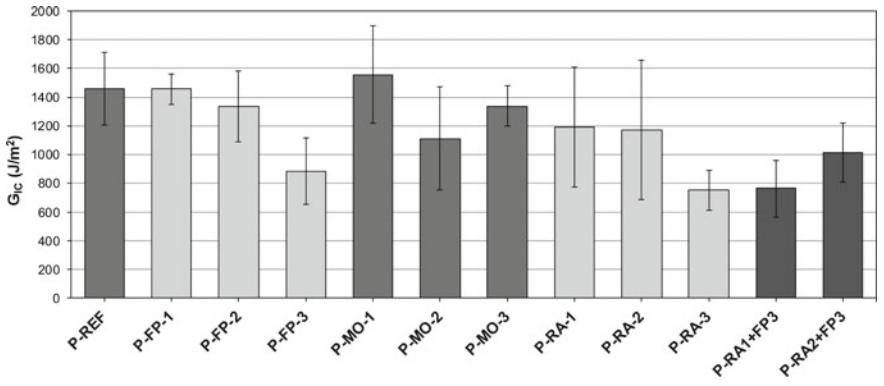

Fig. 2.33 The average G_{IC} values for bonded CFRP joints in a comparison of the production (P) scenarios

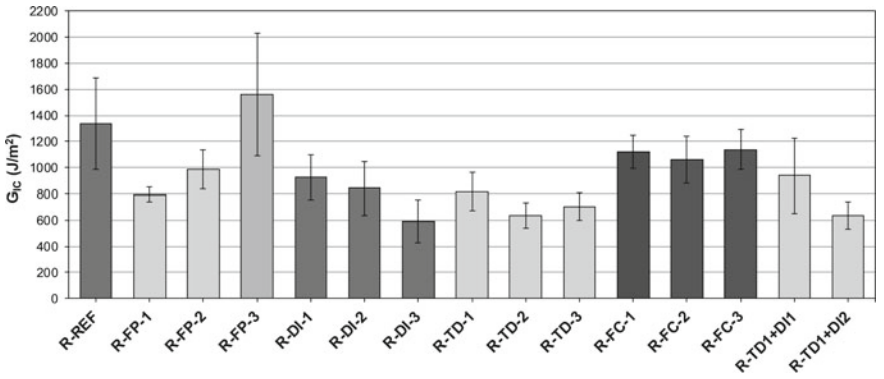

Fig. 2.34 The average G_{IC} values for bonded CFRP joints in a comparison of the repair (R) scenarios

P-REF and R-REF exhibited the highest fracture toughness values while the experimental results indicate a mainly negative effect of the contamination introduced in the respective scenario.

The characterization of the failure mode observed for the respective fracture surfaces showed that adhesive failure was the dominant failure for all the production-related scenarios regardless of the contamination case or level. The adhesive fracture occurred for both the intentionally contaminated substrates in the production and the repair scenarios, but in a different way for each specimen (the pattern and amount of separated adhesive differ), contributing to the large scatter effect observed in the G_{IC} values. In the repair reference samples, a mixed-mode failure was observed (Fig. 2.35), with the dominant failure being a light fiber tear failure, at 50%.

When investigating the joints manufactured following the production fingerprint contamination scenario (P-FP), the respective observed G_{IC} values decreased as the level of contamination by the artificial hand perspiration solution increased. Specifically, for the joints prepared following the P-FP-1 deviation from the qualified production process used for the set of reference joints, the average G_{IC} value was the same as obtained for the reference joints. This indicates that a low concentration level of the FP contamination does not affect the performance of the bond. For P-FP-2, the average G_{IC} decreased by 8%, while for the high contamination level P-FP-3 the G_{IC} fracture toughness of the joints decreased significantly, by 39%. These findings show the detrimental effect of FP contamination on bond performance.

Regarding moisture contamination, for the joints produced following MO-1, the average G_{IC} values show an almost 7% increase compared to the reference category. Considering the observed mixed-fracture pattern, such a finding might be attributed to a modification of the CFRP material by a moderate water uptake, which causes plasticization of the polymeric matrix due to dispersing water molecules. However, in the MO-2 production scenario, the average G_{IC} value was reduced by 24%, and in the MO-3 by 8% as compared to the reference value. Considering the large standard deviation observed, especially for the MO-2 samples, extrapolating a straightforward

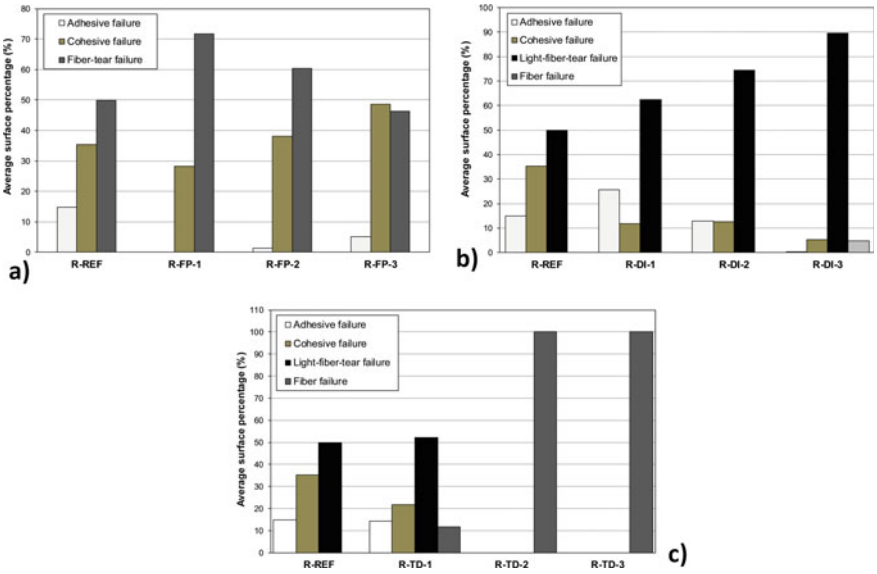

Fig. 2.35 Average percentages of fracture modes obtained after mode-I testing of the joints manufactured within the repair scenarios **a** R-FP, **b** R-DI, and **c** R-TD

structure-property relationship regarding the effect of a medium or high level of moisture contamination on bondline integrity is hindered. In any case, observing a changed average value or a higher standard deviation for the findings related to the design quantity fracture toughness indicates that moist CFRP adherends should be considered an issue for the quality assessment of the resulting bonded joints.

Evaluating the effects of applying even small amounts of release agent to CFRP adherend surfaces within the RA scenario indicates that there are substantial effects on the observed fracture toughness for the thus produced adhesive joints. When the production follows the low-level contamination RA-1 scenario, the average G_{IC} values show an almost 18% reduction compared to the reference category, and for RA-2 the average G_{IC} is reduced comparatively clearly by 20%. The large scatter of the G_{IC} values of the RA-1 and RA-2 samples denotes that there is no statistically significant difference between the effects of the RA-1 and RA-2 contaminations; however, the negative effect of the release agent contamination on the fracture toughness of the bonded joint is evident when compared to the joints produced following the qualified process. For RA-3 the fracture toughness of the joints degrades significantly, by 43%, demonstrating the detrimental effect of the release agent on bond performance. Moreover, the mixed-fracture pattern indicating a weak bond is observed in this case, in clear contrast to the fracture pattern of the joints produced following the P-REF scenario.

Finally, the effects of following a combined contamination scenario with release agent and fingerprint during the production process were investigated with respect to the fracture toughness. The results indicate a significant reduction of the G_{IC} value

of the bonded joints that is greater than the reduction caused by each contaminant separately, indicating that the combination of contaminations may be more detrimental to the composite bonded joints' performance. Specifically, the G_{IC} values in the RA1+FP3 and RA2+FP3 scenarios decreased by 48% and 30%, respectively, compared to the reference category values. It is worth mentioning that a consecutive combination of the contamination RA2+FP3, i.e. first a contamination as for RA2 and then as for FP3, led to a smaller G_{IC} reduction than the nominally lower contamination level of RA1+FP3. This finding may indicate that the interaction of a high RA level with FP3 affects the fracture toughness of the bondline less than the interaction of a low RA level with FP3. With both the release agent and the artificial hand perspiration solution resulting in filmy deposits on the CFRP surface upon drying, the supposed interaction between the contaminations is attributed to the effect that the hydrophobic and barely water-soluble release agent film exercises on the transfer and/or film formation of the aqueous solution, which finally dries on top of it.

Subsequently, we discuss the G_{IC} findings displayed in Fig. 2.34, meaning that the focus will be on the mechanical characteristics of joints manufactured according to a repair scenario. The evaluation of the, respectively, obtained fracture pattern is presented in Fig. 2.35. In contrast to the deleterious effect of films from the artificial hand perspiration solution observed for joints prepared within the P-FP category, for the R-FP scenario the contamination with a Skydrol fingerprint seems to have a different scaling effect on the mechanical performance of the joint. We refer to the finding that although R-FP contamination degrades the mode-I fracture toughness of the joint, a reduced decrease in the G_{IC} values was surprisingly observed for samples provided with higher contamination levels. This phenomenon was also supported by the failure mode presented in these samples, whereby an increasing cohesive failure mode was observed (Fig. 2.35a). While a discussion based on additional findings from the surface characterization will not be initiated here, intuitively such a trend would hardly be expected if—in an analogy to the RA scenario—an increasingly thicker inert film with a low cohesion were formed on CFRP surfaces upon contact with increasingly concentrated Skydrol formulations.

Returning to Fig. 2.34 and moving on to the contamination scenario based on depositing residues from a drying aqueous solution of de-icing agents onto CFRP adherends, the fracture toughness results indicate a detrimental effect of dried de-icer fluid on the bond performance as G_{IC} is reduced for all three contamination levels (up to 56% for the DI3 contamination level). The large scatter of G_{IC} values is attributed to the complexity of the adhesion mechanisms and the failure mechanisms (unstable crack propagation, varying failure modes) and possibly to a non-uniformity of the contamination [1, 17]. Considering the respective fracture patterns, it was observed that when increasing the contamination level there is an increase in the percentage of areas exhibiting LFT failure (Fig. 2.35b), which is a clear sign that contact with de-icing fluid degrades the tensile strength of the matrix.

Concerning the TD scenarios, thermal impact and degradation constitute an external influence on a well-characterized material rather than a contamination, e.g. by deposited substances. High temperatures can cause local overheating, damage the CFRP resin and even affect the fiber/matrix interaction due to the differences in

thermal elongation between matrix and fiber. The average G_{IC} was reduced by 39%, 53%, and 58% for the joints prepared following the TD-1, TD-2, and TD-3 cases, respectively, as compared to the reference category. However, the G_{IC} value obtained following an exposure of the adherends to the higher degradation temperature (TD-3) was not significantly lower than that observed after an exposure to the temperature of the TD-2 scenario. Although the opposite might be expected, it should be noted here that in some cases [17, 26, 27] it has been reported that high temperatures can cause oxidation, especially at the surface of the resin, which, due to the formation of carbonyl surface groups, may even improve adhesion. This aspect is expected to be less relevant when comparing the effects of the TD-2 and TD-3 scenarios because the thermo-oxidatively affected CFRP surface region had been removed in a grinding process prior to the bonding step. In any case, thermally affected CFRP adherends are clearly an issue for the quality assessment of adhesively bonded joints. Based on the fracture pattern evaluation, the dominant failure was the LTF failure and its percentage increased as the temperature to which the CFRP adherends were exposed increased, with LTF portions reaching up to 100% of the fracture surface area for joints prepared following the TD-2 and TD-3 scenarios (Fig. 2.35c). This indicates that considerable damage was caused to the CFRP adherends due to thermal degradation.

When inspecting the G_{IC} values of the joints with the faulty curing of the adhesive and comparing them with those obtained for the reference joints, it is evident that there was a degradation of 15–21%. Evidently, the non-proper curing of the adhesive in a joint can be very detrimental. Considering the rather large scatter between the fracture toughness values of the joints with the faulty curing of the adhesive, a significant distinction between the effects of the three contamination levels within the TD scenario was not found.

Finally, a contamination scenario that combined the thermal impact on the CFRP adherends and a deposit of dried de-icer was studied and a loss of the bond quality—mirrored by a lower fracture toughness—was observed. Specifically, the G_{IC} values for samples of the combined scenarios R-TD1+DI1 and R-TD1+DI2 decreased by 30% and 52%, respectively, compared to the values observed for joints from the reference category. Especially for the higher level of combined contamination, i.e. TD1+DI2, the G_{IC} reduction was greater than the reduction that each contamination scenario induced separately.

2.6.3.2 Mode-II Testing

The average G_{IIC} values of the samples prepared either following the qualified production and repair processes or after intentionally introducing process deviations during production or repair are presented and compared in the histograms displayed in Fig. 2.36 and Fig. 2.37, respectively. Subsequently, we will present and discuss our findings beginning with the tested as-bonded specimens and then regarding the effects of environmental aging for specimens that underwent a hygrothermal exposure prior to testing the mode-II fracture toughness.

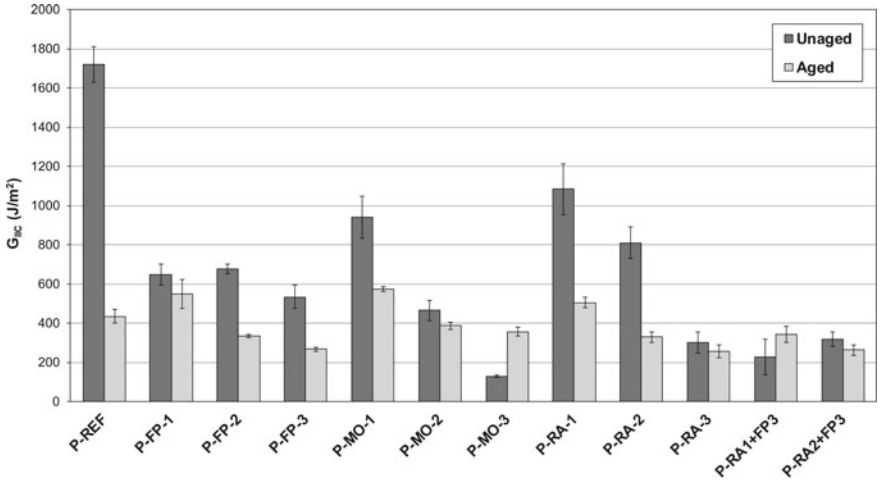

Fig. 2.36 Comparison of the average G_{IIC} values for bonded CFRP joints in the production scenarios before and after hygrothermal environmental aging

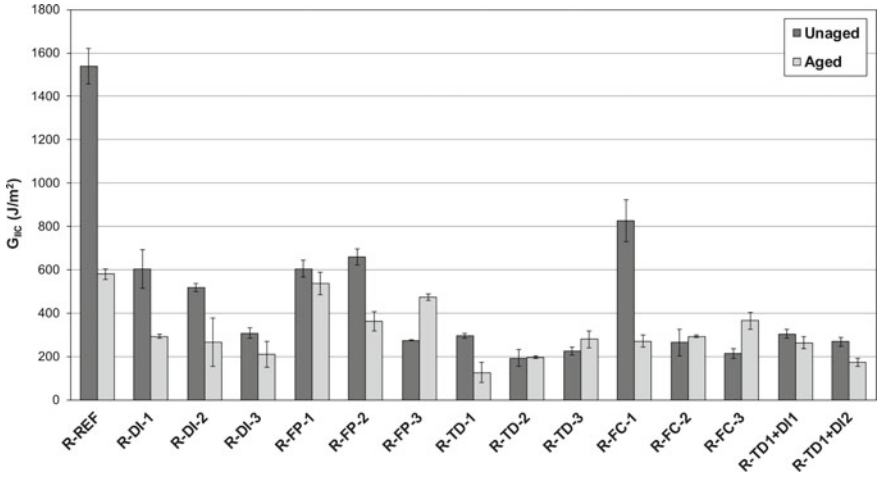

Fig. 2.37 Comparison of the average G_{IIC} values for bonded CFRP joints in the repair scenarios before and after hygrothermal environmental aging

As was observed for the average G_{IC} values of the unaged specimens, the reference category samples exhibited the highest fracture toughness values, also with mode-II characterization. Implementing any of the previously described contamination scenarios during production or repair cases caused a decrease in the G_{IIC} fracture toughness. The observed reduction, as compared to the values found for specimens from the P-REF and R-REF scenarios, respectively, was always greater than the decrease of the G_{IC} values that was observed for the correspondingly prepared sample

sets. This finding indicates that the composite bond is more sensitive to contamination when loaded in mode-II (shear-induced crack propagation).

Starting with the G_{IIC} tests of the unaged specimens, a detrimental impact of fingerprinting the CFRP adherend surface prior to bonding in the P-FP scenario was observed, also for the mode-II fracture toughness. When intentionally applying increased contamination levels for further sample sets within this scenario, this highly significant adverse effect was confirmed and a further reduction of the value of G_{IIC} was found. Specifically, for both the P-FP-1 and the P-FP-2 cases a reduction of 61% was observed regarding the reference values, while for P-FP-3 the reduction reached 69%.

Clearly exceeding the effects observed the in mode-I test results, a profound impact of implementing the moisture contamination scenario for the adherends before bonding was revealed in the mode-II tests. An increase of the moisture concentration in the atmosphere applied during the storage of the adherends even caused a further G_{IIC} reduction. Specifically, a reduction by 45% and 73% compared to the reference values was observed for the MO-1 and MO-2 cases, respectively, while for MO-3 the reduction reached 93%. These findings clearly reveal the detrimental effect of moisture absorption on CFRP adherends in the mode-II fracture toughness of the composite bonds. Moisture significantly lowers the quality of adhesion, and it also leads to a loss of performance in the CFRP material itself and, by extension, causes a loss of performance of the adhesive bond [1].

Concerning the mode-II investigations of specimens prepared from adherends intentionally contaminated by release agent, a detrimental effect on the fracture toughness was observed, which corresponds to the findings of the mode-I tests. Increasing the release agent concentration causes an even stronger G_{IIC} reduction. Specifically, for RA-1 a reduction of the G_{IIC} value by 37% was observed with regard to the reference values, while for RA-2 the corresponding value was 53% and for RA-3 the reduction reached 82%.

Finally, it was also observed that the combined contamination with release agent and fingerprint resulted in a pronounced reduction of the G_{IIC} values for the sets of bonded joints. The decrease in fracture toughness was greater than the reduction caused by each contaminant separately, indicating that the effect of successively implementing two deposit-forming combination scenarios of contaminations may prove even more deleterious to the performance of bonded composite joints. Specifically, the G_{IIC} values which were found after having applied the combined contamination RA1+FP3 and RA2+FP3 on the CFRP adherends during the manufacture of the joints were decreased by 87% and 82%, respectively, compared to the reference category values. As in the mode-I tests, the combination RA2+FP3 did not lead to a more distinct reduction of the G_{IIC} value than the RA1+FP3 combination, in which a fingerprint was applied using the same diluted artificial hand perspiration solution but on top of a thinner release agent film.

The following will cover the results of G_{IIC} tests performed with adhesive joints prepared following the distinct repair scenarios and presented in Fig. 2.37.

Intentionally applying runway de-icing fluid to the CFRP adherend surface before bonding has a similar impact on the mode-II fracture toughness of the resulting

joints as was observed in the mode-I fracture toughness testing. An increase of the de-icing fluid concentration used for the intentional CFRP surface contamination caused a further G_{IIC} reduction. Specifically, when following the DI1 scenario a reduction of 56% was observed with regard to the reference values, while for DI2 the corresponding value was 62% and for DI3 the reduction reached 80%.

With respect to specimens from the R-FP contamination scenario, it was observed that the mode-II fracture toughness of the joints was drastically reduced. Specifically, applying R-FP-1 and R-FP-2 contamination levels caused a reduction of approximately 61%, while introducing R-FP-3 reduced the G_{IIC} even further to 82% compared to the R-REF category. For all the tested joints a mixed-fracture image was found. Basically, this reduction in bond strength could be attributed to the fact that the FP contamination, with the hydraulic fluid transferred by fingerprinting, led to poor adhesion between the adhesive and the adherend, whereby kissing bonds were formed. However, the observed decrease in the fracture toughness as compared to the R-REF specimens and the obtained adhesive fracture image contrast with the findings for the joints based on correspondingly contaminated CFRP surfaces that were subjected to mode-1 testing and which, in the case of the R-FP-3 scenario, yielded increased G_{IC} values as compared to the R-REF scenario as well as an adhesive fracture image. Therefore, we essentially highlight once again that, under mode-II loading, the composite bond is strikingly more sensitive with respect to the applied contamination than under mode-I loading.

Concerning joints prepared from adherends that had experienced thermal impact before being bonded within the TD scenario, an increase in the exposure temperature caused a further G_{IIC} reduction. The average G_{IIC} was reduced by 81%, 88%, and 86% for the TD-1, TD-2, and TD-3 cases, respectively, compared to the reference category. Again, the reduction for the TD-3 case was lower than for the TD-2 thermal degradation. The scatter hinders any clear distinctions to be made between the effects of applying the TD-2 and TD-3 scenarios on the adhesive composite bond integrity.

As in the mode-I tests, the mode-II tests revealed that the intentionally applied faulty curing of the adhesive within the repair scenario of CFRP joints can be detrimental to their resulting properties. Specifically, for the FC-1 scenario a reduction of 46% was observed with regard to the reference values, while for FC-2 and FC-3 the reduction was even more drastic, amounting to 83% and 86%, respectively.

Finally, applying the more complex repair scenario, which comprises a combination of thermal impact and degradation with an application of de-icing fluid contamination on the CFRP adherends before being bonded, results in a reduction of the G_{IIC} value of the joints by 80% and 83% for the R-TD1+DI1 and R-TD1+DI2 cases, respectively. These effects are greater than the reduction of the G_{IIC} value caused by each contaminant separately. These findings indicate that monitoring effects of successively applied contaminations is a task in the quality assessment of adherend surfaces as well as the performance of the resulting joints.

Aging Effect

Exposure to a hygrothermal environment is reported to be a critical issue regarding the durability of adhesively bonded joints whenever the applied demands are characterized by a combination of elevated temperature, moisture, exposure time, and mechanical loading [28]. For example, elevated parameter settings are applied in scenarios for highly accelerated life tests (HALT), which are used in the development of a joint design to quickly achieve indications of weak points [29] or to identify the functional operating limits exceeding the operational area defined by the product specifications [30]. Against this background and aiming at a comprehension of feasible deviations from the qualified bonding process in the development phase of an adhesive joint, we have decided to include such elevated hygrothermal parameter settings in the concept of the quality assessment for the manufacturing processes of CFRP composite adhesive joints. The effect of the externally applied environment in terms of moisture and temperature has been thoroughly investigated [31–33], essentially indicating a significant loss of the bond strength of joints subjected to aging, especially after reaching a moisture saturation in adhesive joints that were exposed to a high relative humidity or water immersion.

The combination of a pre-bond contamination of adhesive composite joints and after-bond exposure to hygrothermal aging leads to a drastic reduction of the G_{IIC} (Figs. 2.36 and 2.37). In the majority of the investigated scenarios, the effect of applying the combination of pre-bond contamination and after-bond long-term hygrothermal aging to a set of bonded joints is more severe than the effect of applying either of the two scenarios separately.

The drastic reduction of the G_{IIC} values ascertained when comparing the findings for sets of aged and unaged CFRP joints coincides with the fact that the onset of crack propagation was observed at the side of the specimen where the moisture concentration and thermal effect are higher [34]. Additionally, the crack propagation occurred near the adhesive region, and diffusion through the adhesive is regarded as the primary access route for moisture to enter a joint [35].

For example, the aging procedure resulted in a reduction in the mode-II fracture toughness of the R-REF samples by 62% compared to the unaged repair reference scenario (Fig. 2.37). Additionally, for all of the aged specimens of any of the applied contamination scenarios, the observed G_{IIC} values of the aged samples were drastically reduced for all contamination levels compared to the respective unaged reference REF category. Surprisingly, it was observed that there were some sets of joint specimens for which the G_{IIC} values after the hygrothermal aging were higher than for the respective set that was destructively tested before aging, namely for the sample sets prepared following the MO-3, RA1+FP3, R-FP-3, FC-2, and FC-3 scenarios. We attribute this finding of increased fracture toughness after hygrothermal aging to a plasticization caused by the swelling of the adhesive layer and the CFRP matrix due to a specific water uptake. Additionally, that the Skydrol contained in the R-FP series is known to react with the water from the environmental chamber, producing phosphoric acid [36]. Discriminating between such effects or deriving more detailed

insights into effects caused by reversible water uptake, e.g. a plasticization of polymeric material, or by irreversible chemical reactions with moisture, e.g. the hydrolysis of phosphoric acid esters, might be possible if re-dried aged specimens were investigated in addition to unaged and aged specimens.

2.6.4 Tensile Testing

In this section we present and discuss the load–displacement curves and the respective fracture patterns observed when performing a tensile testing of adhesive joints prepared from scarfed CFRP adherends. The results obtained for specimens prepared following the reference scenario or by implementing distinct scenarios characterized by introducing contaminations during the manufacturing process are presented in Fig. 2.38. In all the contamination cases, one of the adherends was contaminated while the other was intentionally left in the respective reference state, a setup intended to replicate the real-life application of repair patches.

During tensile testing, it was observed that prior to the final failure (i.e. the separation of the two adherends), all specimens presented an initial failure revealed by a first load drop in the region of the load–displacement curves, which corresponds to plastic deformation. This failure was localized at the edges of the scarfed area and is attributed to stress concentrations at this point as well as to edge effects. Having overcome this marginal fracture, the initial failure propagated along the scarfed area and led to the final separation of the two adherends.

For the specimens prepared following one of the contamination scenarios, we observed that all samples of the II-R-REF+TD1 scenario presented a higher failure

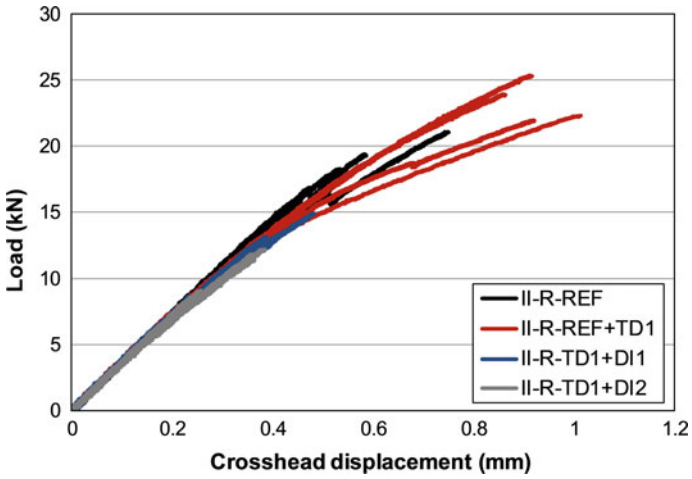

Fig. 2.38 Load–displacement curves for adhesive joints manufactured from scarfed CFRP adherends that were prepared following the reference and contamination scenarios

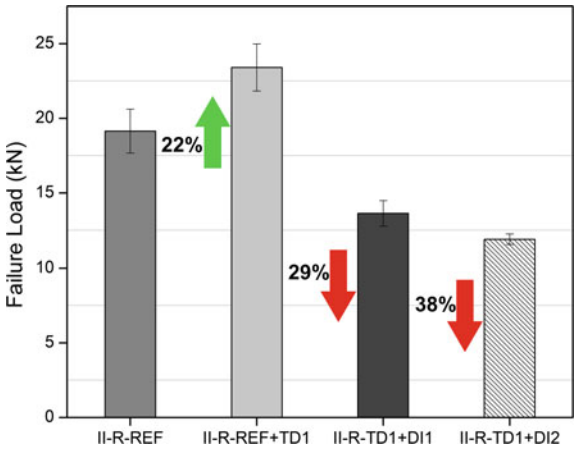

Fig. 2.39 Failure load comparison for the scarfed samples

load, by 22%, than the reference samples (Fig. 2.39). Although the exposure of flat CFRP adherends to an elevated temperature following the TD-1 scenario decreased the fracture toughness tested in mode-I and mode-II loading, such a decrease was not prominently observed in the tensile testing of the joints prepared from scarfed CFRP adherends. Even though heat usually damages the CFRP structure or causes chemical changes in the matrix, there have been reports that high temperatures can cause oxidation of the resin which may improve adhesion due to the formation of carbonyl groups at the surface [17, 26, 27].

When implementing scenarios comprising the successive application of two contamination cases, the obtained results revealed that the contamination combining thermal impact and deposits of dried de-icing fluid had a negative effect on the mechanical performance of the scarfed repair joints, reducing the failure load as compared to specimens prepared following the reference scenario. Specifically, for samples from the TD1+DI1 scenario, the reduction of the failure load was 29%, while for the TD1+DI2 scenario the reduction reached 38% (Fig. 2.39).

Additionally, the failure surfaces of the joints were examined after the tensile tests in order to characterize the failure modes and correlate them with the tensile test results. Figure 2.40 depicts the representative fracture surfaces of each contamination scenario studied, showing the main failure modes observed in the tensile specimens.

The percentages of the different failure modes are compared for the different sample sets in Fig. 2.41. For the reference samples, a mixed-mode failure was observed, with the dominant failure being the FT failure, at 63% of the surface area, while adhesive (ADH) failure was observed for 37% of the surface area. In contrast, the tested samples prepared following the II-R-REF+TD1 case presented a higher amount of CO failure (30%), while FT failure and the ADH failure modes showed a reduction (43 and 27%) as compared to the reference samples. This change of the fracture pattern coincides with the increase in the failure load observed for the specimens prepared from scarfed adherends that had been exposed to elevated

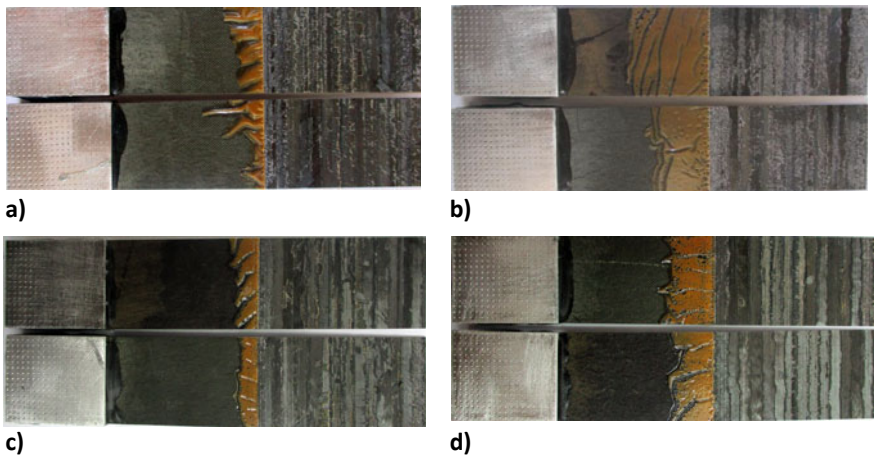

Fig. 2.40 Images showing the representative fracture surfaces of the joints prepared from scarfed CFRP adherends obtained after loading in tension, sorted according to the contamination scenario; **a** II-R-REF; **b** II-R-REF+TD1; **c** II-R-TD1+DI1; and **d** II-R-TD1+DI2

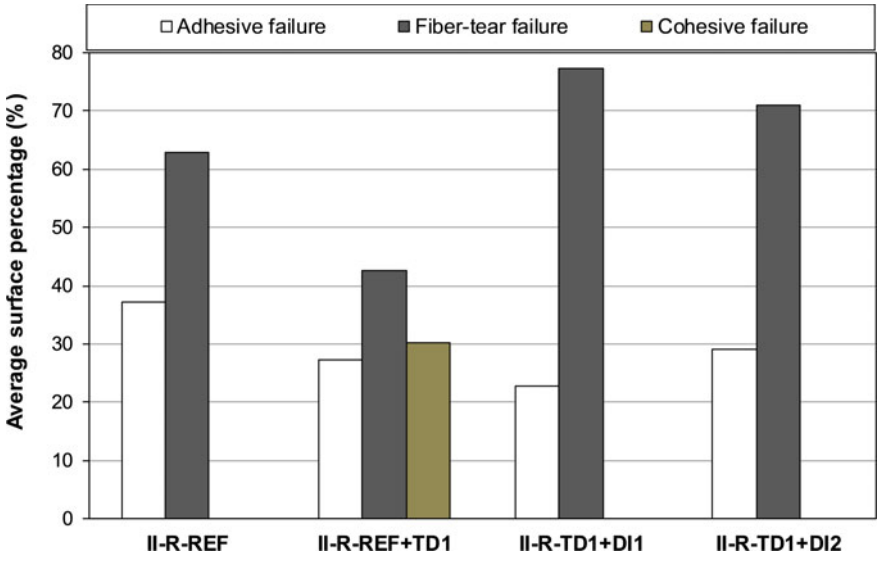

Fig. 2.41 Average percentages of the failure modes presented in the tensile tested scarfed joints, sorted according to the contamination scenario

temperatures following the II-R-REF+TD1 scenario. When discussing these observations, the effects should be considered in relation to the loading geometry of the scarfed specimens or the performed scarfing and subsequent cleaning processes. It is plausible, according to the occurrence of a CO failure, to infer a greater amount

of energy required for a crack to develop and propagate than that required to cause an ADH or FT failure. As a consequence, an increase in the failure load is observed.

Inspecting the fracture patterns obtained for the II-R-TD1+DI1 samples, we found that the FT remained the dominant failure. The observed increase of the area percentage by 77%, as compared to samples prepared following the REF scenario, indicates that the combined successive contamination with TD1 and DI1 had a deleterious impact mainly on the behavior of CFRP adherends under tensile loading. Finally, after testing the II-R-TD1+DI2 set, the FT failure showed a slight reduction compared to the findings for II-R-TD1+DI1. Specifically, 71% of the surface area with an FT failure was observed, while ADH failure increased to 29%. These findings indicate that the TD1+DI2 combined contamination affects mainly the bondline performance (the interphase between the adherends and adhesive).

2.6.5 Centrifuge Test Results

In this section, the effect of pre-bond contamination scenarios related to production and repair processes on adhesion strength between the intentionally contaminated CFRP surface and the adhesive layer is assessed based on investigations by means of the novel centrifuge testing technology. The plots shown in Fig. 2.43 and Fig. 2.45 display the average adhesion strength values, as derived from Eq. (2.5) for the applied geometry used in the tests, for the production-related and repair-related samples, respectively.

Figure 2.42 depicts representative microscope imagery revealing the different failure modes observed for the various samples. Meanwhile, Figs. 2.44 and 2.46 display the evaluated average surface area percentages of the failure modes for specimens prepared following the different production and repair-related contamination scenarios.

For all the intentionally implemented deviations from the qualified manufacture process for CFRP adherend surface preparation by applying contaminations defined for production scenarios, the results showed a decrease in the adhesion strength. This decrease was small for the low and medium contamination levels; however, for the high contamination level a more profound decrease was found. The lowest adhesion strength values were obtained for the specimens prepared following the P-MO-3 case (98% RH). The standard deviation is also considerable, but within acceptable limits for revealing the described trends. Remarkably, for all the sets of samples prepared with contaminated adherends, a significantly higher standard deviation of adhesion strength values was observed than for the P-REF specimens (Fig. 2.43).

Considering the specimens for the production-related scenarios, all the investigated fracture patterns revealed ADH and LFT failure modes (Fig. 2.44). The adhesive mainly remained on the metallic stamp, which is an indication of a stronger bond between the metallic stamp and the adhesive as compared to between the adhesive and the CFRP adherend. This stands for all cases of ADH failure here. The P-REF samples showed a much higher adhesion strength (almost double) than that of the

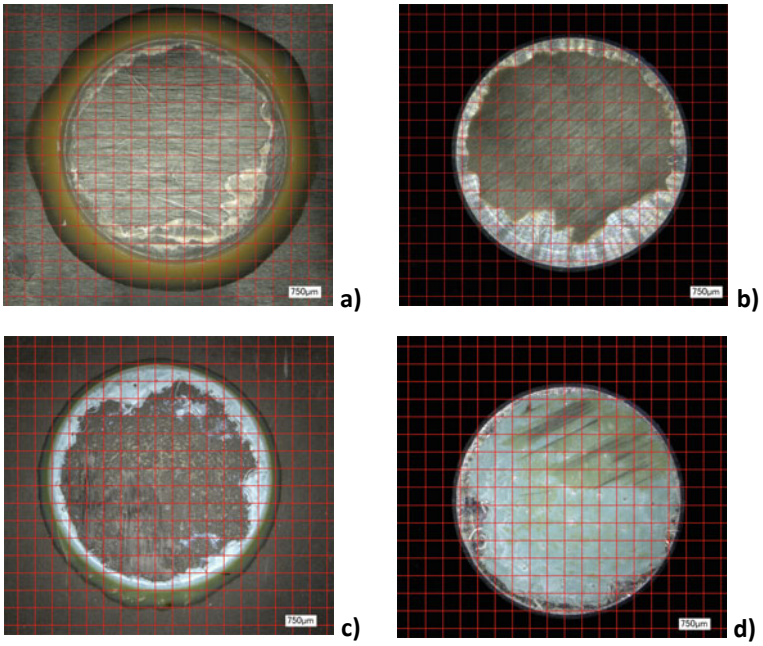

Fig. 2.42 Representative microscopy images revealing the failure modes of centrifuge-tested CFRP samples; **a** ADH+FT for R-TD sample (CFRP side); **b** ADH+FT for R-TD sample (stamp side); **c** ADH+LFT for P-MO sample (CFRP side); and **d** ADH+LFT for P-MO sample (stamp side)

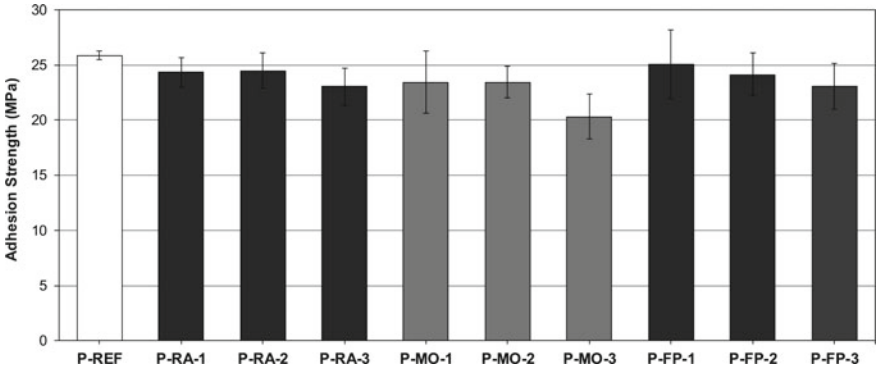

Fig. 2.43 Adhesion strength values obtained upon centrifuge testing specimens of the production-related scenarios

R-REF samples (Fig. 2.45), which is due to the different type of adhesive used and the different curing conditions applied.

Regarding the specimen sets prepared and tested within the repair scenario, the R-REF samples (Fig. 2.45) showed a much lower adhesion strength (almost half) than

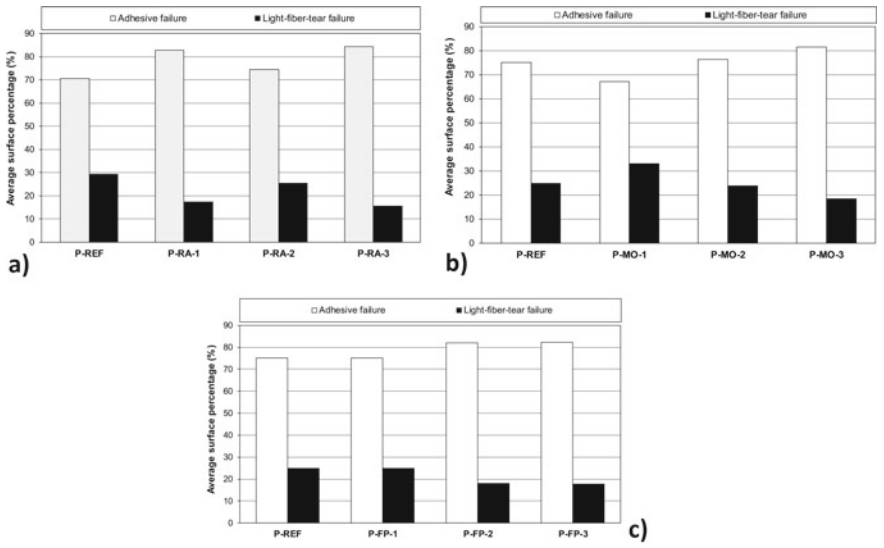

Fig. 2.44 Average surface percentage for the different failure modes of the centrifuge-tested samples **a** P-RA, **b** P-MO, and **c** P-FP

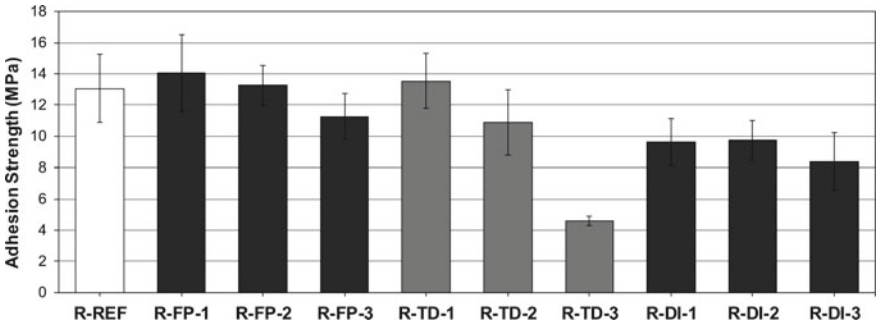

Fig. 2.45 Adhesion strength values for the repair-related sample categories

the P-REF samples. A significantly higher relative standard deviation of the measured strength values was found for the reference scenario R-REF as compared to in the P-REF scenario. These findings are attributed to the different types of adhesive used and the different curing conditions applied.

Against the background, quite insignificant effects of the implemented deviations from the reference joining process were found. Concerning the specimens from repair-related contamination scenarios, (except for R-FP-1 and R-TD-1), a decrease of the adhesion strength was generally observed (Fig. 2.45) as compared to the specimens prepared following the R-REF scenario. For the Skydrol-based R-FP scenario, there seemed to be a slight increase in the adhesion strength for the R-FP-1

case, while an insignificant variation in the adhesion strength was observed for the R-FP-2 case and a decrease of the adhesion strength for the R-FP-3 case. However, a robust conclusion cannot be drawn for the R-FP-1 and R-FP-2 cases due to the very high standard deviation of the results for these two cases and the R-REF case. Only for the R-FP-3 case was there a considerable decrease in the adhesion strength.

The percentages of the failure modes in Fig. 2.46a reveal a similar failure behavior for the R-FP-1 case and the R-FP-2 and R-FP-3 cases, namely a decrease of the LFT failure and an increase of the ADH—which is an indication of a weak bond—and TLC failure modes.

Bearing in mind that the TD scenario mimics effects of a thermal impact on the CFRP adherends, we may assume from the finding that for specimens of the R-TD-1 case a similar behavior in terms of adhesion and failure modes is observed as for the R-REF case (Fig. 2.46b). In contrast, the R-TD-2 and R-TD-3 cases present a lower adhesion strength, and this is attributed to the degradation of the polymer matrix, which becomes effective in the first layer of the CFRP adherend because of the increased temperature, which causes the FT failure mode. The lowest adhesion strength for this set of scenarios was measured for the R-TD-3 case (corresponding to one of the CFRP adherends experiencing a pre-bond exposure of 280 °C).

Finally, for the R-DI scenario, a detrimental effect of the presence of dried de-icer was revealed for the adhesion strength of the joint. The failure mode percentages (Fig. 2.46c) show that an increase in the DI concentration causes an increase of the ADH failure mode, as the deposition of a thin layer by the de-icer acts as a barrier during the bonding of the adhesive and the CFRP adherend. However, in contrast to

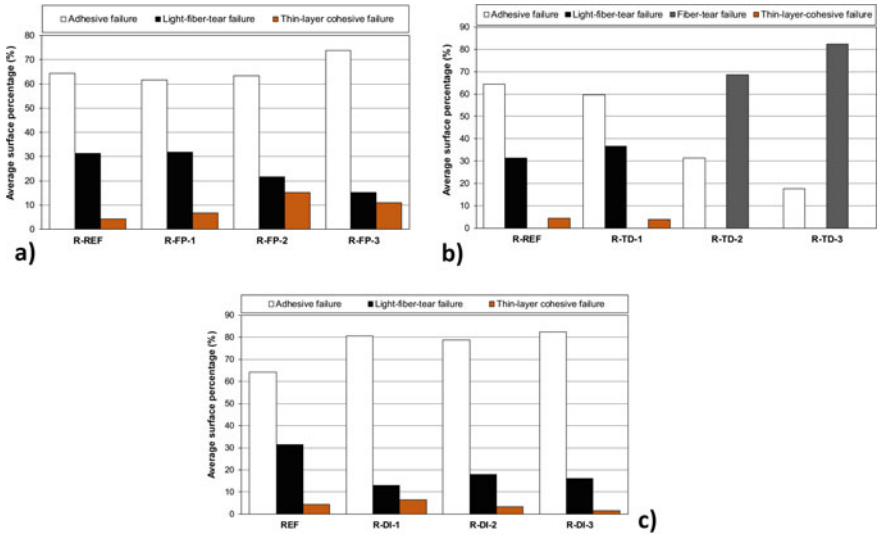

Fig. 2.46 Average surface percentages of the different failure modes for the **a** R-FP **b** R-TD and **c** R-DI centrifuge samples

the adhesion strength, there is not a clear differentiation regarding the failure mode percentages between the different concentrations of the dried de-icer.

2.7 Numerical Simulation

2.7.1 FE Model

A composite panel, stiffened with two stringers, was simulated under compression using the LS-DYNA FE platform. Besides the reference panel, all contamination scenarios were simulated, and their maximum load-bearing capacity was compared to the reference panel. Debonding growth was simulated using the cohesive zone model (CZM) method. This method has been widely used in the last decade to simulate the delamination progression in composite materials and the debonding progression in bonded joints, mainly due to its ease of use as it has been implemented in many commercial FE codes.

For the analysis, the linear elastic/linear softening (bilinear) traction-separation law was adopted. The constitutive law described in Fig. 2.47a is for the tension loading and separation of the adherends in the normal direction (mode-I). The mixed-mode behavior is described by the mixed-mode bilinear traction shown in Fig. 2.47b. The first region (until point 1) corresponds to the elastic part of the material's response. In this region, the material remains undamaged and the unloading at point 1 follows the elastic line. The region from point 1 to point 2 represents the material softening (damage growth) area. Once the loading has progressed beyond point 2, the material has suffered some damage (damage parameter is greater than zero but less than one), however, there is no adherend separation yet. This occurs at point 2, where the adherends separate permanently (damage parameter has reached unity). The total area under the triangle represents the energy required to debond the adherends and is known as the fracture energy. In LS-DYNA, the fracture energy

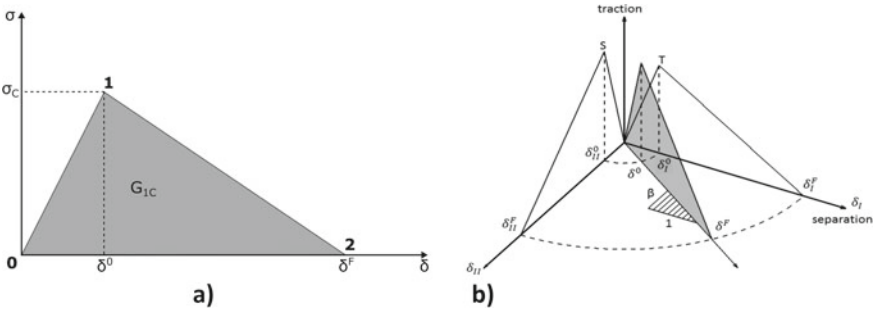

Fig. 2.47 Schematic representation of **a** the bilinear traction-separation law for the mode-I load case and **b** the bilinear traction-separation law for the mixed-mode load case [37]

is an input parameter. It has units of energy/area. In addition, the elastic stiffness (slope) and the peak stress (point 1) are required to completely define the bilinear law.

The progressive damage modeling method was adopted to simulate the damage in the composite adherends. To this end, the material model MAT_162 of the LS-DYNA was used, which has the capacity to predict several modes of damage to the composite material. The specific material model automatically implements the progressive damage modeling method by combining a set of strain-based Hashin-type failure criteria for predicting several failure modes like tension/shear fiber failure, compression fiber failure, perpendicular matrix failure, and delamination [38].

To this end, skin, cap, and web components were modeled using standard eight-node solid elements with three degrees of freedom per node (ELFORM = 1) and MAT_162_COMPOSITE_MSC_ DMG. In addition, MAT_162 automatically applied a property degradation module to simulate the damage effects.

FE mesh was created using ANSYS Workbench and imported into the LS-DYNA FE platform. All analyses were performed using LS-DYNA. The imported mesh is depicted in Fig. 2.48.

The adhesive layer was modeled using eight-node cohesive elements with three degrees of freedom per node (ELFORM = 19) and MAT_138_COHESIVE_MIXED_MODE, which applied a mixed-mode CZM with bilinear traction-separation law to the cohesive elements. Furthermore, the debonding growth was predicted using the B-K power law.

The FE model was loaded in compression by applying displacement and the nodes were fully supported at the end of panel, as can be seen in Fig. 2.48. In addition, in order to reduce the extensive out-of-plane deformation that would cause a buckling to the panel, the nodes that are depicted in Fig. 2.48 were also supported. These nodes represent a possible anti-buckling device that could be used during mechanical tests.

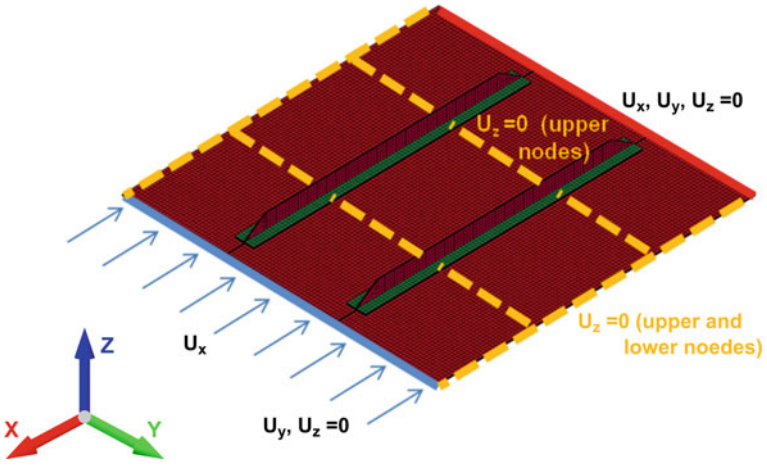

Fig. 2.48 Applied compression and boundary conditions on a flat stiffened panel

2.7.2 Numerical Results

The resulting load–displacement curves for all contamination scenarios are depicted in Fig. 2.49.

The comparison concerning the maximum load for all contamination scenarios is presented in Fig. 2.50, wherein it can be observed that all contamination scenarios have a negative influence on the load-bearing capacity of the stiffened panel.

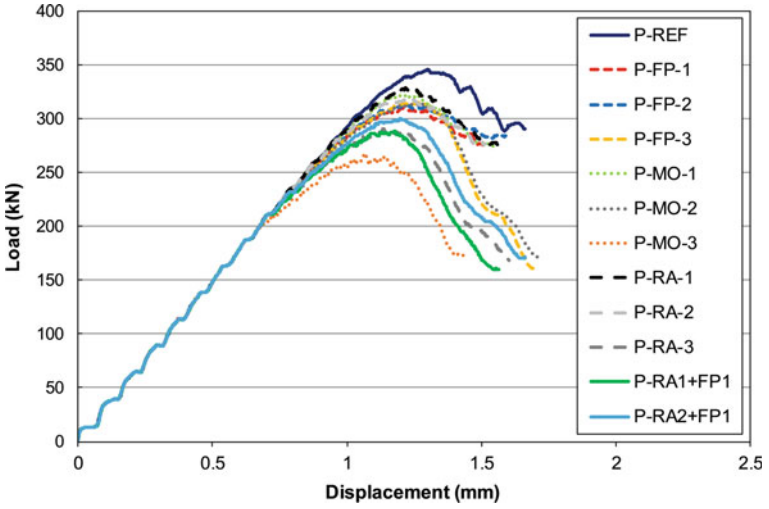

Fig. 2.49 Load–displacement curves under compression for all contamination scenarios

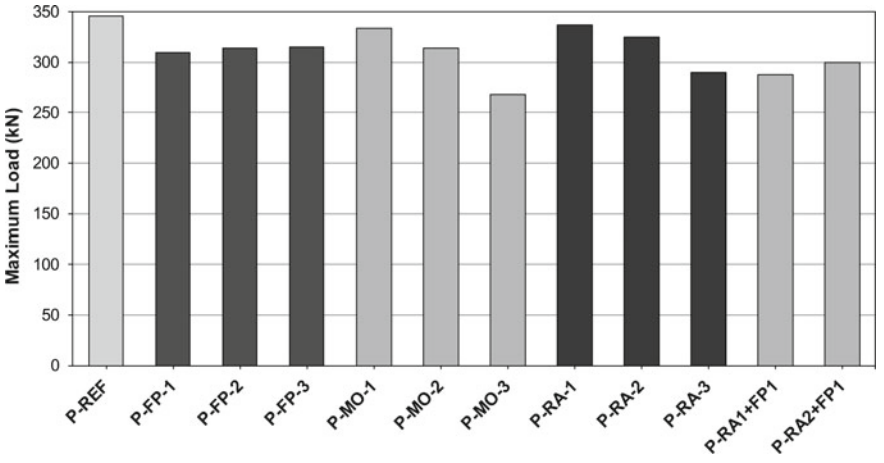

Fig. 2.50 Predicted maximum compressive load for all contamination scenarios

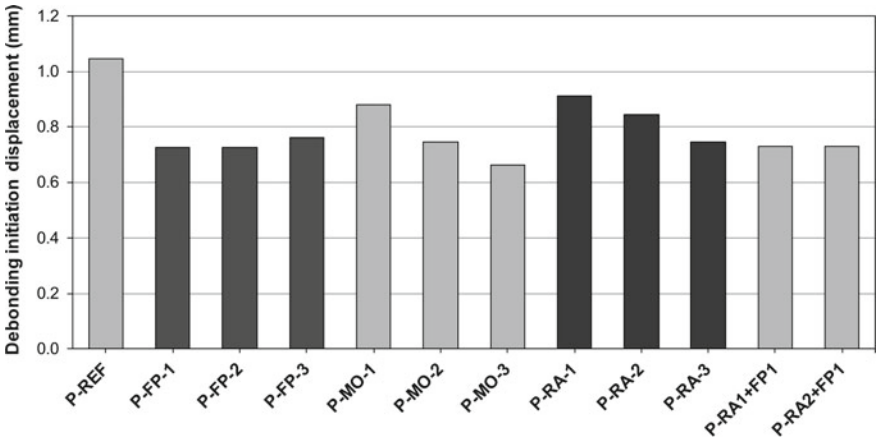

Fig. 2.51 Predicted debonding initiation for all contamination scenarios

In Fig. 2.51, the debonding initiation displacement is presented and compared for all contamination scenarios. It is clear that all contamination scenarios have a negative impact on debonding initiation, as in all scenarios the debonding initiates earlier than in the reference case.

2.8 Conclusions/Synopsis

With our objective in mind of providing the reader with a feasible concept for quality assessment in adhesive bonding technology that complies with the ten heuristics and systematics described in Chap. 1, in this chapter we detail procedures to introduce disturbances from one or even several operator-related process features in scheduled ways and to test quantitative and design-relevant joint features by applying pre-process or post-process methodologies. Hereby, the exemplification is based on identifying, defining, and intentionally implementing pre-bond contamination on carbon fiber reinforced plastic (CFRP) adherends in gradational levels quantified with spectroscopic laboratory methods and identified with respect to a reference state given by the respective qualified bonding process.

The contaminants investigated within this project have a high relevance for the majority of aerospace applications. The test scenarios cover two fields of application for the adhesive bonding of primary structures, namely aircraft manufacture and in-service bonded repair. The identification of all feasible (or, pragmatically, all imaginable) disturbances of process features resulted in the definition of production and repair scenarios, yielding distinct reference surface states differing in the depth of abrasion accomplished by the CFRP grinding process. For the relevant adherends, three sample geometries were defined, namely smooth coupon samples, scarfed samples, and curved panels. The production-related disturbances comprised

the impact of release agent, moisture, or saliferous fingerprints and, with respect to repair-related disturbances, thermal impact, dried de-icing fluid, or a fingerprint with hydraulic fluid on the adherend surface; a faulty curing of the adhesive was also considered. For each of these identified and technologically crucial scenarios, we implemented discrete levels differing in the dimension of the applied contamination. Moreover, we accounted for the effects of hygrothermal aging before determining the joint strength using mode-I or mode-II testing of the fracture toughness as well as through a novel centrifuge test. In particular, specifications defined by the users of CFRP adhesive joints are often based on safeguarding adequate G_{IC} values. Exceeding the respective standards, we show that joint quality is supportively and sensitively mirrored by mode-II testing of the fracture toughness as well as by the novel centrifuge test.

The present chapter describes in detail the manufacturing of the adherends for all the sample geometries (Aernnova Composites), the pre-bond single and multiple contamination and bonding of the samples (Fraunhofer IFAM), the characterization of the adherends and the joints using the XPS method (Fraunhofer IFAM), the ultrasound testing of the bonded samples (Airbus), the mechanical testing and the after-bond contamination of the samples (University of Patras), and finally the numerical simulation of the stiffened panels (University of Patras).

The manufacture of the CFRP adherends for the coupons, scarfed samples, and stiffened panels was performed under consideration of the specifications and surface quality requirements determined by the internal procedures of the manufacturing company and end users. In order to obtain a high level of repetitiveness and quality, the process of the sample preparation was carried out under aeronautical specifications and in a controlled environment.

Following the identification of the relevant three production-related and four repair-related contamination scenarios, for each scenario three levels of contamination concentration were applied, namely a low level, a medium level, and a high level. In addition, a combined contamination case for each process field was realized. The contamination of the adherends was realized by Fraunhofer IFAM and investigated using XPS analyses to measure the amount of contamination on the adherend surface and to determine the exact contaminant concentration. After the contamination procedure, the adherends were bonded in the autoclave.

The resulting joints manufactured from intentionally contaminated adherends were inspected using conventional NDT. The objective was to make a statement on the sample quality as well as on the weak bond status. All the samples were investigated using two different probes (5 and 10 MHz). For the contaminated coupons and the multi-contaminated flat samples, three different kinds of defects were observed:

1. Manufacturing defects with a marginal impact on the use of the sample for ENDT evaluation, e.g. bending of the bonded specimens, adherend surface quality issues.

2. Minor deviation from the ultrasound reference signal in the case of moist CFRP samples or sample surfaces contaminated by fingerprints (including multi-contaminated specimens). This effect could be due to contamination if only compared to the reference signal, but no further proof has been found so far.
3. Contamination-induced defects such as disbonding (faulty curing) or delamination (thermal degradation). They might have a detrimental effect on future ENDT measurements.

Conjointly with the mechanical testing results, the status of weak bonds could then be confirmed for most of the samples. Finally, curved samples were successfully tested thanks to SAUL (surface adaptive ultrasonic laws) configurations. The inspection results revealed a very low-quality sample material, probably due to the CFRP composite adherend itself. Results obtained from such samples should be evaluated and interpreted carefully.

In order to evaluate the influence of the surface state (clean, single, or multiple contaminations) of one adherend on the mechanical properties on adhesively bonded joints, established mechanical tests like mode-I and mode-II fracture toughness tests as well as tensile and centrifuge tests were conducted by the University of Patras. Mechanical testing demonstrates the contamination level that affects the mechanical strength of a bond; the results can be correlated with the results from the reference analysis methods and ENDT methods.

We shortly highlight that for each of the investigated disturbances we found significant effects on the resulting CFRP composite joint strength for at least one level of contamination applied during the bonding process. Moreover, in many cases, the lowest applied level only caused a decrease in the joint strength as compared to production or repair procedures performed following the respectively qualified process. In this way, the prepared sets of specimens encompass two challenges for the aspired process monitoring procedures: On the one hand, (the effects of) the contaminations will need to be detected, and on the other hand, the measured values will need to facilitate the discrimination between more and less relevant levels of contamination.

Specifically, the reference category exhibited the highest fracture toughness values, while for almost all cases, except from R-FP-3, the presence of the contaminant proved to be detrimental for the fracture toughness of the joints. The higher the contamination level, the higher the decrease of the joints' performance. A combined contamination results in a reduction of the fracture toughness of the bonded jointed that is greater than the reduction caused by each contaminant separately, indicating that a combination of contaminations may be more detrimental to the composite bonded joints' performance.

Additionally, a novel test was used that is both time and cost-efficient, namely the centrifuge test, whereby the adhesion strengths of all the bonded joints were measured. Besides the rather large scatter presented in some scenarios, in almost all contamination scenarios, except for R-FP-1 and R-TD-1, there was a decrease of the adhesion strength. By evaluating the centrifuge test's experimental process and results, it can be concluded that the centrifuge testing technology has great potential

to be established as a test method for the characterization of bonded joints as it is a fast testing process that generates repeatable tests capable of describing the strength of the joints.

In order to evaluate the combined effect of the pre-bond contamination and after-bond exposure to hygrothermal environment on the mode-II fracture toughness of CFRP bonded joints, the contaminated samples underwent aging inside an environmental chamber. Mostly, there was a negative effect of the contamination. After-bond hygrothermal aging significantly degrades the mode-II fracture toughness of the composite bonded joints. The decrease is larger for the contaminated samples, which reveals that the combined effect is more severe than that of the two effects separately.

Furthermore, the results of the tensile mechanical testing performed by the University of Patras revealed the effect of each contamination scenario in the tensile performance of the scarfed samples. A single contamination of an adherend with TD-1 proved to be beneficial since the sample presented a higher failure load than the reference samples. This was attributed to the enhancement of the matrix properties due to its oxidation and the formation of carbonyl groups at the surface. However, the negative effect of the combined contamination was also demonstrated. The results showed that a combined contamination of thermal degradation and de-icing fluid has a negative effect on the mechanical performance of the scarfed repair joints, reducing the failure load by up to 38%.

In total, 378 test coupons were tested using mode-I and mode-II fracture toughness tests, while 136 samples were tested using a centrifuge and tensile tests, resulting in a total of 514 tested specimens.

Finally, regarding the numerical simulations, a composite panel stiffened with two T-stringers was simulated under compression using the LS-DYNA FE platform. The comparison concerning the maximum load for the contamination scenarios showed that all contamination scenarios had a negative influence on the load-bearing capacity of the stiffened panel. Also, as a result of the contamination, the debonding initiated earlier than in the reference case.

Based on the findings achieved here, in-process ENDT will be implemented to assess features characteristic either to the pre-bond adherend surfaces (see Chap. 3) or to the adhesive joints (see Chap. 4) that were manufactured following the described intentionally applied contamination scenarios.

References

1. Markatos DN, Tserpes KI, Rau E et al (2014) Degradation of mode-I fracture toughness of CFRP bonded joints due to release agent and moisture pre-bond contamination. J Adhes 90(2):156–173. https://doi.org/10.1080/00218464.2013.770720
2. da Silva LFM, Öchsner A, Adams RD (2011) Introduction to adhesive bonding technology. In: da Silva LFM, Öchsner A, Adams RD (eds) Handbook of adhesion technology, vol 2. Springer Berlin Heidelberg, Berlin, Heidelberg, pp 2–3

3. Charalambides MN, Hardouin R, Kinloch AJ et al (1998) Adhesively-bonded repairs to fibre-composite materials I. Experimental. Compos Part A: Appl Sci Manuf 29(11):1371–1381. https://doi.org/10.1016/s1359-835x(98)00060-8
4. Pantelakis S, Tserpes KI (2014) Adhesive bonding of composite aircraft structures: challenges and recent developments. Sci China Phys Mech Astron 57(1):2–11. https://doi.org/10.1007/s11433-013-5274-3
5. ComBoNDT "Quality assurance concepts for adhesive bonding of aircraft composite structures by advanced NDT" (2015–2018) Project funded from the European Union's Horizon 2020 research and innovation programme under grant agreement No 636494
6. Tornow C, Schlag M, Lima LCM et al (2015) Quality assurance concepts for adhesive bonding of composite aircraft structures—characterisation of adherent surfaces by extended NDT. J Adhes Sci Technol 29(21):2281–2294. https://doi.org/10.1080/01694243.2015.1055062
7. Markatos DN, Tserpes KI, Rau E et al (2013) The effects of manufacturing-induced and in-service related bonding quality reduction on the mode-I fracture toughness of composite bonded joints for aeronautical use. Compos B Eng 45(1):556–564. https://doi.org/10.1016/j.compositesb.2012.05.052
8. ENCOMB "Extended Non-Destructive Testing of Composite Bonds" (2010–2014) Project funded from the European Union's Seventh Framework Programme under grant agreement No 266226
9. AITM 1-0053—Airbus Industry Test Method (2006) Carbon fibre reinforced plastics, determination of fracture toughness energy of bonded joints, Mode I (AITM 1-0053)
10. Ebnesajjad S (2008) Adhesives technology handbook, 2nd edn. William Andrew Inc., Norwich, NY
11. Pearson RA, Blackman BRK, Campilho RDSG et al (2012) Quasi-static fracture tests. In: da Silva LFM, Dillard DA, Blackman B et al (eds) Testing adhesive joints: best practices, A221. Wiley-VCH Verlag GmbH & Co, KGaA, Weinheim, Germany, pp 163–191
12. ISO 9022-12 (2015) Optics and photonics—environmental test methods—Part 12: Contamination 37.020 (ISO 9022-12:2015)
13. Budhe S, Banea MD, Barros Sd et al (2017) An updated review of adhesively bonded joints in composite materials. Int J Adhes Adhes 72:30–42. https://doi.org/10.1016/j.ijadhadh.2016.10.010
14. Creemers F, Geurts KJ, Noeske M (2016) Influence of surface contaminations on the quality and bond strength of structural adhesive joints. In: European adhesion (EURADH) conference
15. Gause RL (1989) A noncontacting scanning photoelectron emission technique for bonding surface cleanliness inspection (NASA TM-100361 Technical Memorandum)
16. Moutsompegka E, Tserpes KI, Polydoropoulou P et al (2017) Experimental study of the effect of pre-bond contamination with de-icing fluid and ageing on the fracture toughness of composite bonded joints. Fatigue Fract Eng Mater Struct 40(10):1581–1591. https://doi.org/10.1111/ffe.12660
17. Tserpes KI, Markatos DN, Brune K et al (2014) A detailed experimental study of the effects of pre-bond contamination with a hydraulic fluid, thermal degradation, and poor curing on fracture toughness of composite-bonded joints. J Adhes Sci Technol 28(18):1865–1880. https://doi.org/10.1080/01694243.2014.925387
18. Hollander JM, Jolly WL (1970) X-ray photoelectron spectroscopy. Acc Chem Res 3(6):193–200. https://doi.org/10.1021/ar50030a003
19. ASTM International D5573-99 (2005) Standard practice for classifying failure modes in fiber-reinforced-plastic (FRP) Joints 83.120 (ASTM D5573-99). www.astm.org
20. AITM 1-0006—Airbus Industry Test Method (1994) Carbon fibre reinforced plastics, determination of interlaminar fracture toughness energy—Mode II (AITM 1-0006)
21. Hoffmann M, Tserpes K, Moutsompegka E et al (2018) Determination of adhesion strength of pre-bond contaminated composite-to-metal bonded joints by centrifuge tests. Compos B Eng 147:114–121. https://doi.org/10.1016/j.compositesb.2018.04.014
22. Rietz U, Lerche D, Hielscher S et al (2015) Centrifugal adhesion testing technology (CATT)—a valuable tool for strength determination. J Adhes Soc Jpn 51(s1):293–297. https://doi.org/10.11618/adhesion.51.293

23. LUM GmbH (2018) Technical specification od Adhesion Analyser LUMiFrac. https://www.lum-gmbh.com. Accessed 25 June 2018
24. Beck U, Reiners G, Lerche D et al (2011) Quantitative adhesion testing of optical coatings by means of centrifuge technology. Surf Coat Technol 205:S182–S186. https://doi.org/10.1016/j.surfcoat.2011.02.016
25. DIN EN 2823 European Association of Aerospace Industries (1998) Aerospace series—fibre reinforced plastics—determination of the effect of exposure to humid atmosphere on physical and mechanical characteristics (DIN EN 2823)
26. Choi DM, Park CK, Cho K et al (1997) Adhesion improvement of epoxy resin/polyethylene joints by plasma treatment of polyethylene. Polymer 38(25):6243–6249. https://doi.org/10.1016/S0032-3861(97)00175-4
27. Ochoa-Putman C, Vaidya UK (2011) Mechanisms of interfacial adhesion in metal–polymer composites—effect of chemical treatment. Compos A Appl Sci Manuf 42(8):906–915. https://doi.org/10.1016/j.compositesa.2011.03.019
28. Cysne Barbosa AP, Fulco PAP, Guerra ESS et al (2017) Accelerated aging effects on carbon fiber/epoxy composites. Compos B Eng 110:298–306. https://doi.org/10.1016/j.compositesb.2016.11.004
29. Collins DH, Freels JK, Huzurbazar AV et al (2013) Accelerated test methods for reliability prediction. J Qual Technol 45(3):244–259. https://doi.org/10.1080/00224065.2013.11917936
30. Ewert U, Jaenisch GJ, Osterloh K et al (2011) Performance control: nondestructive testing and reliability evaluation. In: Czichos H, Saito T, Smith L (eds) Springer handbook of metrology and testing. Springer, Berlin, Heidelberg
31. Johnson WS, Butkus LM (1998) Considering environmental conditions in the design of bonded structures: a fracture toughness mechanics approach. Fatigue Fract Eng Mater Struct 21(4):465–478. https://doi.org/10.1046/j.1460-2695.1998.00533.x
32. Liljedahl CDM, Crocombe AD, Wahab MA et al (2007) Modelling the environmental degradation of adhesively bonded aluminium and composite joints using a CZM approach. Int J Adhes Adhes 27(6):505–518. https://doi.org/10.1016/j.ijadhadh.2006.09.015
33. Pitt S, Jones R, Peng D (2012) Characterization of the durability of adhesive bonds. Fatigue Fract Eng Mater Struct 35(11):998–1006. https://doi.org/10.1111/j.1460-2695.2012.01688.x
34. Mubashar A, Ashcroft IA, Critchlow GW et al (2011) A Method of predicting the stresses in adhesive joints after cyclic moisture conditioning. J Adhes 87(9):1061–1089. https://doi.org/10.1080/00218464.2011.600675
35. Bowditch MR (1996) The durability of adhesive joints in the presence of water. Int J Adhes Adhes 16(2):73–79. https://doi.org/10.1016/0143-7496(96)00001-2
36. Moutsompegka E, Tserpes KI, Brune K et al (2017) The effect of pre-bond contamination with fingerprint and ageing on the fracture toughness of composite bonded joints. In: 7th EASN international conference on innovation in European aeronautics research, 26–29 September, Warsaw, Poland
37. Floros IS, Tserpes KI, Löbel T (2015) Mode-I, mode-II and mixed-mode I+II fracture behavior of composite bonded joints: experimental characterization and numerical simulation. Compos B Eng 78:459–468. https://doi.org/10.1016/j.compositesb.2015.04.006
38. Tserpes KI, Peikert G, Floros IS (2016) Crack stopping in composite adhesively bonded joints through corrugation. Theoret Appl Fract Mech 83:152–157. https://doi.org/10.1016/j.tafmec.2015.10.003

Open Access This chapter is licensed under the terms of the Creative Commons Attribution 4.0 International License (http://creativecommons.org/licenses/by/4.0/), which permits use, sharing, adaptation, distribution and reproduction in any medium or format, as long as you give appropriate credit to the original author(s) and the source, provide a link to the Creative Commons license and indicate if changes were made.

The images or other third party material in this chapter are included in the chapter's Creative Commons license, unless indicated otherwise in a credit line to the material. If material is not included in the chapter's Creative Commons license and your intended use is not permitted by statutory regulation or exceeds the permitted use, you will need to obtain permission directly from the copyright holder.

Chapter 3
Extended Non-destructive Testing for Surface Quality Assessment

Mareike Schlag, Kai Brune, Hauke Brüning, Michael Noeske, Célian Cherrier, Tobias Hanning, Julius Drosten, Saverio De Vito, Maria Lucia Miglietta, Fabrizio Formisano, Maria Salvato, Ettore Massera, Girolamo Di Francia, Elena Esposito, Andreas Helwig, Rainer Stössel, Mirosław Sawczak, Paweł H. Malinowski, Wiesław M. Ostachowicz, and Maciej Radzieński

Abstract This chapter introduces various extended non-destructive testing (ENDT) techniques for surface quality assessment, which are first characterized, then enhanced, and finally applied to assess the level of pre-bond contaminations intentionally applied to carbon fiber reinforced plastic (CFRP) adherends following the procedures described in the previous chapter. Based on two user cases comprising different scenarios that are characteristic of either aeronautical production or repair, the detailed tests conducted on two types of sample geometry, namely flat coupons and scarfed pilot samples with a more complex shape, form the basis for applying the advanced ENDT procedures for the monitoring of realistic and real aircraft parts, as will be described in Chap. 5. Specifically, the reported investigations were performed to assess the surface quality of first ground and then intentionally contaminated CFRP surfaces using the following ENDT tools: the aerosol wetting test (AWT), optically stimulated electron emission (OSEE), two differently implemented approaches based on electronic noses, laser-induced breakdown spectroscopy (LIBS), Fourier-transform infrared (FTIR) spectroscopy, laser-induced fluorescence (LIF), and laser vibrometry.

M. Schlag (✉) · K. Brune · H. Brüning · M. Noeske
Fraunhofer Institute for Manufacturing Technology and Advanced Materials IFAM, Wiener Str. 12, 28359 Bremen, Germany
e-mail: mareike.schlag@ifam.fraunhofer.de

C. Cherrier · T. Hanning · J. Drosten
Automation W+R GmbH, Messerschmittstraße 7, 80922 Munich, Germany

S. De Vito · M. L. Miglietta · F. Formisano · M. Salvato · E. Massera · G. Di Francia · E. Esposito
ENEA – National Agency for New Technologies, Energy and Sustainable Economic Development, TERIN-FSD, Portici Research Center, P.le E. Fermi 1, 80055 Portici, Italy

A. Helwig · R. Stössel
Airbus Defence and Space GMBH, Willy-Messerschmitt-Straße 1, 82024 Taufkirchen, Germany

M. Sawczak · P. H. Malinowski · W. M. Ostachowicz · M. Radzieński
Institute of Fluid–Flow Machinery, Polish Academy of Sciences, Fiszera 14, 80-231 Gdańsk, Poland

© The Author(s) 2021

W. Leite Cavalcanti et al. (eds.), *Adhesive Bonding of Aircraft Composite Structures*,
https://doi.org/10.1007/978-3-319-92810-4_3

Keywords ENDT for surface quality assessment · Aerosol wetting test · Optically stimulated electron emission · Electronic noses · Laser-induced breakdown spectroscopy · Fourier-transform infrared · Laser-induced fluorescence · Laser vibrometry

3.1 Introduction

In the previous chapters, we detailed that one of the reasons inhibiting the certification of adhesive bonding for primary aircraft structures is the sensitivity of the bondline integrity to the presence of defects that can affect the strength of the joints. These defects are not accessible to visual monitoring during the bonding process. Furthermore, the most critical defects arising during the manufacture of adhesive joints are those that are not detectable by currently available NDT methods. This has led us to develop extended NDT (ENDT) methods capable of detecting such effects on CFRP adherends, whereby we evaluate their efficiency and assess their applicability benefits based on the analysis of specimens with increasingly complex sample geometries, starting from flat coupon samples that exhibit distinct levels of intentionally applied contaminations [1] and moving toward CFRP panels with more complex/curved geometries that might even exhibit multiple contaminations. The present chapter describes the respective contributions of the individual partners of the ComBoNDT consortium [2], thereby detailing the different specialist approaches within a jointly developed concept for quality assurance.

The subsequently detailed ENDT procedures for surface quality assessment constitute an essential input into the framework for the overall concept for the quality assessment of adhesively bonded joints described in this book. The results presented in this chapter were achieved in the research conducted into the applied ENDT methods. Looking ahead, we would like to highlight here that in certain contamination scenarios of the aircraft production and repair user cases, these pre-bond in-process methods were sensitive to impacts that were shown to affect a strength reduction of successively manufactured adhesive bonds and, therefore, could potentially be utilized to identify not-in-order (NIO) adherends during a surface quality assessment procedure.

3.2 Aerosol Wetting Test (AWT)

In this section, we introduce the aerosol wetting test (AWT) as a tool for surface quality assessment and detail how its performance was enhanced in the ComBoNDT project for the in-process monitoring of CFRP adherends.

3.2.1 Principle and Instrumentation

AWT allows the inline monitoring of the surface state, specifically through an inspection of its wettability.

Throughout the last decade, various aspects of this technology have been enhanced, whereby the most recent advances were achieved in the ComBoNDT project. Hereby, both the hardware and software were adapted in order to achieve more relevant and more reliable results in terms of measurement, data evaluation, and post-processing.

3.2.1.1 Measurement Principle

AWT allows the monitoring of a surface state by analyzing its wetting properties. In its most common implementation, an aerosol of ultra-clean water is sprayed onto the surface using an ultrasonic spray nozzle. Depending on the wetting behavior and wettability of the surface, the droplet pattern, diameter, and distribution vary, as exemplified in Fig. 3.1. The wetting behavior is then automatically analyzed based on the images recorded by a camera system and image processing algorithms.

This surface inspection method has various advantages, which are briefly:

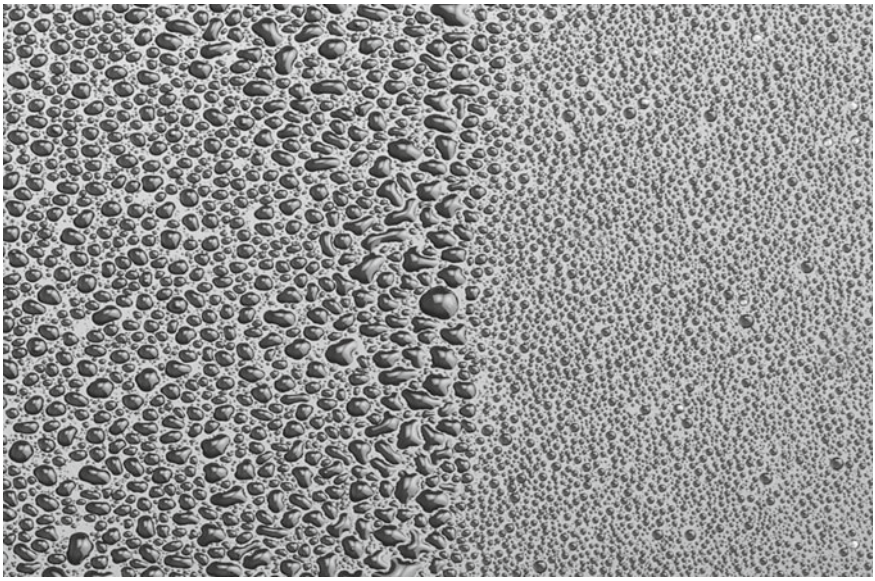

Fig. 3.1 Aerosol wetting test (AWT) droplet pattern influenced by the local wettability of the substrate surface: a more wettable surface region (left) with less and larger droplets compared to a less wettable surface region (right) exposed to the same amount of droplets from a water aerosol generated by an ultrasonic nozzle

- The inspection speed and the size of the inspected surface.

AWT is particularly adapted to the measurement of the properties of the droplet pattern at the edge of a part. The inspection is conducted on a 30 mm wide area at a speed of 6 m per minute; therefore, it is especially suitable for inspecting specific, narrow bonding areas. In practice, each image is separated from the previous one and then the evaluation is performed. The values in this book are given based on calibrated image dimensions, such as the base area (30 × 30 mm).

- Its low impact on the surface.

This method is non-destructive and has a minimal influence on the investigated part. Approximately 0.2 μL of ultra-clean water is deposited by the spray per square centimeter. After drying (which takes less than a minute for most substrate materials), the surface typically does not show any residue since the water used is ultra-clean.

- Its simplicity of use and implementation.

The system enables the inspection of various parts with only a few limitations. The measurement can take place in various environments (for example, on a production line), on various materials, and it only needs a standard energy supply.

- The simplicity of achieving the results.

Once the images are captured, various image processing algorithms and decision-making processes run simultaneously. If the calibration of the system has been flawlessly achieved, the result can be integrated into a simple IO/NIO signal for the inspector, saving the more complex data for later analysis.

3.2.1.2 Software Enhancement

During the ComBoNDT project, various software modifications were made to the existing system, most significantly to the image processing algorithms. Once the images of the droplet patterns have been generated by the camera, the main task, which is also the hardest, is detecting the droplets (and their lateral boundaries) and separating them on the image from the background formed by the material texture.

At the beginning of the project, this was accomplished by a very straightforward image processing step (thresholding followed by morphological operations); however, it emerged that this approach is extremely unstable if there are variations of the surface properties (texture, structure…).

In a first step, this rather simple image processing method was replaced with a more complex one that can nevertheless be considered standard image processing. This enhancement primarily facilitates the detection of droplets on surfaces with slight variations in color or also light intensity. This first step was fully integrated into the research system and already is implemented on the system for inline detection.

However, for some complex surfaces or distinct contamination scenarios resulting in more varied and unpredictable droplet appearances and patterns, even this enhanced image processing was not sufficiently effective. Hence, further improvements were made, with the detection and evaluation of the droplet pattern being done by a convolutional neural network (CNN). We trained the network on various datasets generated by the AWT system (various materials, various contaminations, and/or activation of the surface). With a wide set of samples, the network was trained to separate the image pixels belonging to a droplet from the pixels belonging to the background.

We visualize the various stages of the up-to-date image processing in the table displayed in Fig. 3.2.

Following this use of a CNN to detect the droplets, further classical image processing approaches were integrated for an easier decision-making process. Consequently, a sequence of various filters was applied to the image, and local values for the standard parameters (e.g., wetted area percentage, deposited water droplet diameter, drop count to evaluate the droplet number density) were calculated and graphically displayed, as shown in Fig. 3.3.

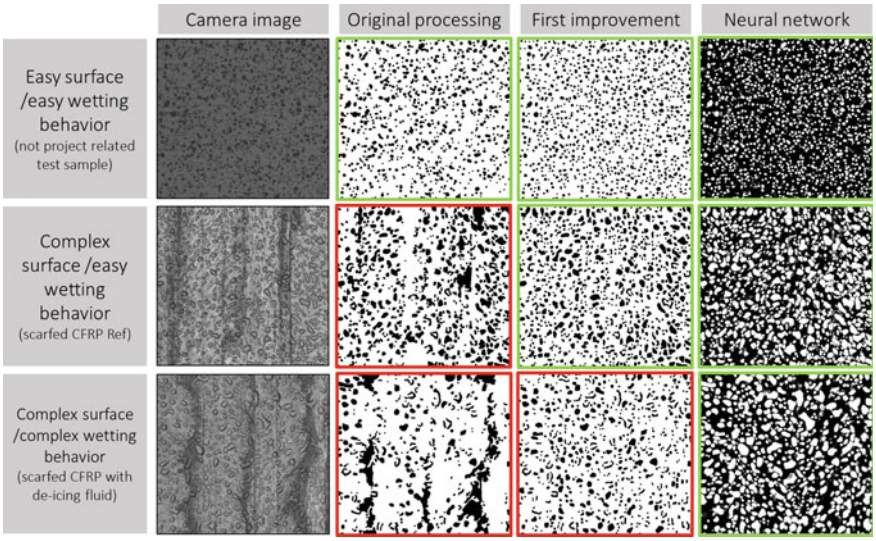

Fig. 3.2 Various AWT image processing generations on various surfaces with distinct complexities. Droplet images with green frames highlight a successful droplet detection; some droplet detections (marked by a red frame) were not successful enough for a meaningful analysis

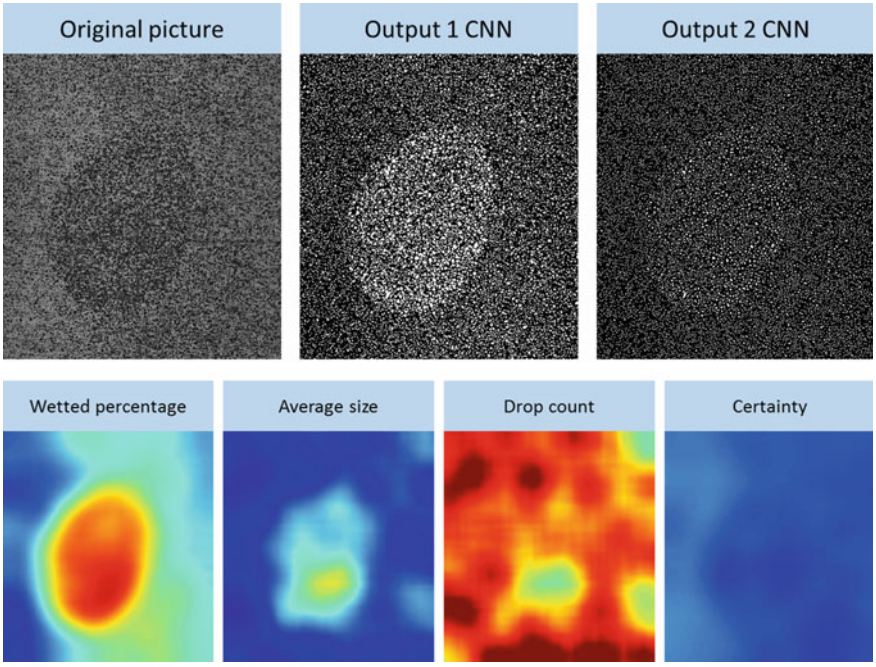

Fig. 3.3 Example output of the so-called heatmap after convolutional neural network (CNN) processing. The displayed example was obtained within a fingerprint contamination scenario

3.2.1.3 Hardware Enhancement

Some improvements were also made to the hardware, mainly concerning the AWT measurement head, which was fully redesigned. This was motivated by various considerations:

- Improving the optical system properties.
- Facilitating the use of a robot to perform the measurements on parts with complex geometries, which are presented in Chap. 5.

Specific hardware with high computing power was used in order to integrate the CNN image processing.

3.2.1.4 Up-to-Date Measurement Apparatus

By the end of the project, the updated AWT system consisted of three main components, namely the measurement head, the electrical cabinet, and the processing computer system, as presented in Fig. 3.4.

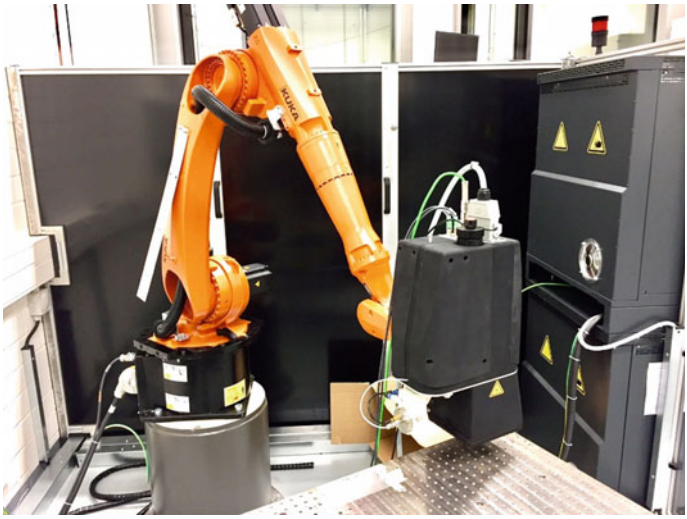

Fig. 3.4 Updated robot-aided bonNDTinspect AWT measurement head imaged during the full-scale demonstration (detailed in Chap. 5) conducted at Fraunhofer IFAM in Bremen

3.2.2 AWT Results

Here, we present our findings achieved by applying AWT to assess distinct contamination scenarios for CFRP adherends with different shapes.

3.2.2.1 AWT Results for the Coupon Level Samples

In the following investigations, the various test results for each of the distinct contamination scenarios and three different contamination levels are compared to the results for the clean ground reference samples, which differ depending on the respective production or repair user case.

The results shown here are always presented for those two droplet pattern features out of the four subsequently listed ones that showed the best differentiating correlation with the respectively applied contamination levels. The four evaluated features are as follows:

- Average droplet diameter.
- Wetted percentage, i.e., the percentage of the surface covered by water.
- Number of droplets per surface area, i.e., the droplet density.
- Average droplet compactness, whereby the compactness of each droplet is calculated by determining the area to perimeter ratio.

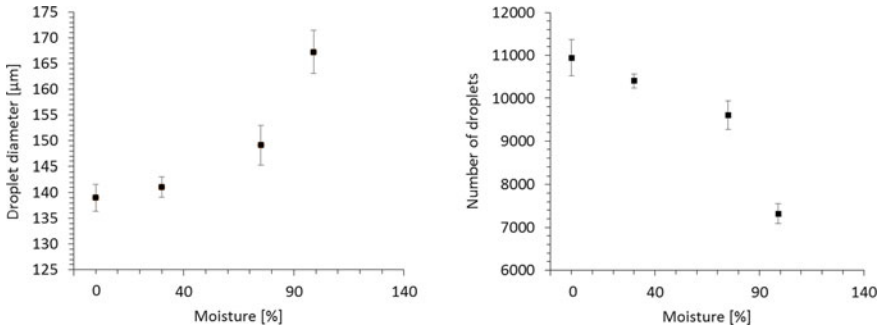

Fig. 3.5 Evaluation results for the AWT features of droplet diameter and number of droplets as obtained for the CFRP samples from the MO scenario

3.2.2.2 Detection of the Moisture of CFRP Substrates (P-MO)

The moisture contamination of CFRP parts from the production user case was successfully revealed and distinguished for the three different contamination levels achieved by material exposure to environments with distinct relative humidities, as shown in Fig. 3.5.

3.2.2.3 Detection of Release Agent (P-RA)

Release agent contamination was successfully revealed and distinguished for the three different contamination levels achieved by depositing distinct amounts of a silicon-containing release agent onto the surface, as shown in Fig. 3.6.

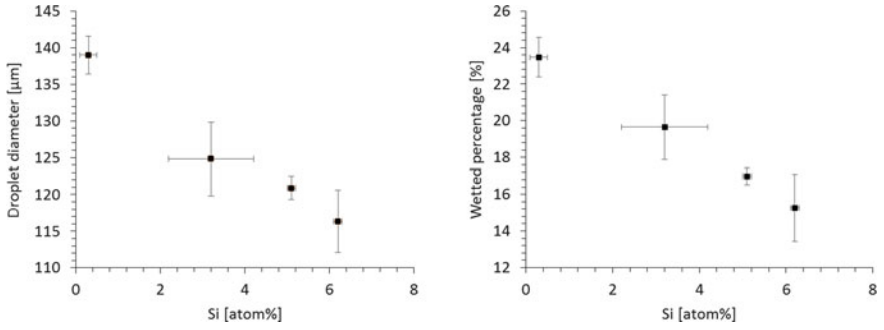

Fig. 3.6 Evaluation results for the AWT features of droplet diameter and wetted percentage as obtained for the CFRP samples from the scenario involving a silicon-containing release agent deposited at atomic concentrations, characterized by XPS investigations

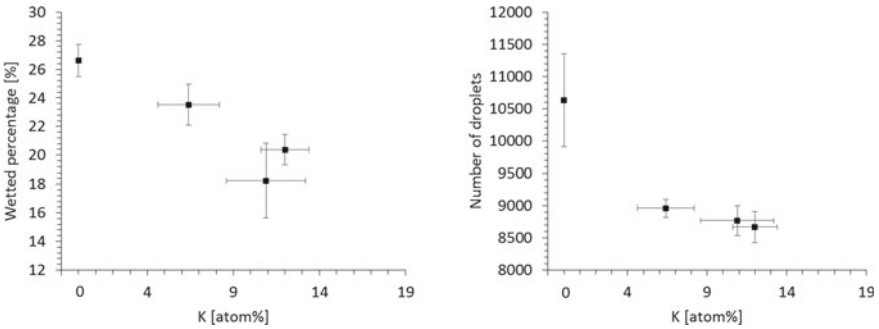

Fig. 3.7 Evaluation results for the AWT features of wetted percentage and number of droplets as obtained for the CFRP samples from the de-icing fluid scenario involving a potassium-containing de-icing fluid deposited at atomic concentrations, characterized by XPS investigations

3.2.2.4 Detection of Fingerprints on Production Samples (P-FP)

The fingerprint contamination within the production user case was contrasted and detected using AWT, although discrimination between the different contamination levels could not be achieved. For locally deposited contaminations, such as the fingerprints used here, the detection was also successfully achieved with local image processing algorithms, which allowed the characterization of the size and position of the contamination.

3.2.2.5 Detection of De-icing Fluid (DI)

The de-icing fluid contaminations were clearly revealed by AWT when comparing the droplet patterns obtained on intentionally contaminated CFRP specimens with those of clean reference samples. However, the different contaminations levels could barely be differentiated from each other, see Fig. 3.7.

3.2.2.6 Detection of Fingerprints on Repair Samples (R-FP)

Contaminations applied to CFRP surfaces for the fingerprint scenario within the repair user case were barely detected with AWT, and the distinct contamination levels were not differentiated.

3.2.2.7 Detection of Thermal Degradation (R-FP)

The effects of the thermal impact on CFRP coupon specimens were clearly detected by AWT. However, the different contamination levels were only barely differentiated.

		No detection	Partial detection	Clear detection	Partial discrimination of contamination level	Discrimination of contamination level
Production	Moisture (MO)					X
	Release agents (RA)					X
	Fingerprint (FP)			X		
	RA + FP				X	
Repair	De-icer (DI)				X	
	Fingerprint (FP)		X			
	Thermal degradation (TD)				X	
	TD + DI				X	

Fig. 3.8 Summary of the detection capacity (marked X) observed for the flat CFRP coupon samples for the production or repair user cases (first column) within the respective contamination scenarios (second column)

3.2.2.8 Summary of the Performance of AWT for Contaminated CFRP Coupon Samples

The summary presented in Fig. 3.8 shows the detection capacity of AWT for various contamination scenarios. The samples considered here are the flat CFRP coupon samples, which may not be directly relevant for the evaluation of the performance of the AWT method in terms of real parts.

3.2.3 AWT Results for the Pilot Level Samples

The AWT results obtained for the scarfed CFRP pilot samples are presented in the following. They cannot be directly compared with the results for the coupon samples or those of the realistic parts. Indeed, the variations between part type, geometry, and surface have a significant influence on the AWT measurement and evaluation results.

Therefore, we perform comparisons only among similar parts of the same type. The analytical process was set up following the objective of detecting surface contamination on the respective part.

3.2.3.1 Pilot Samples for the Production User Case with Combined Release Agent and Fingerprint Contamination

Regarding the surface constitution/texture, the pilot samples of the production user case showed a strongly structured surface and were slightly curved. The AWT droplet detection was partially successful with the first image processing improvement, and it was successful in all cases using neural network processing, see Fig. 3.9.

In this case, the geometrically strongly structured background as well as the combination of two contamination processes involving two types of deposited contaminants led to a more difficult differentiation of the various contamination levels, see Fig. 3.10.

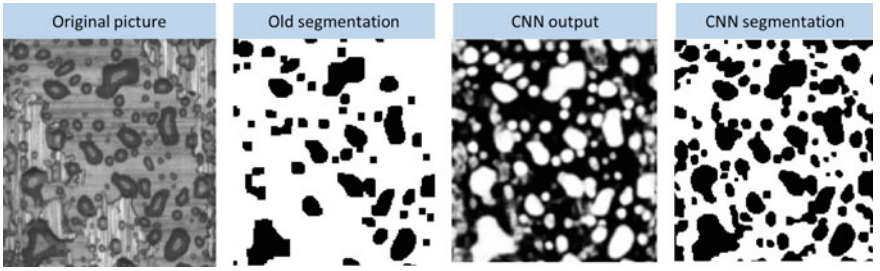

Fig. 3.9 Overview of the findings from different AWT droplet image evaluation and processing procedures for the production pilot samples, starting from an original image (left), after performing the droplet segmentation with standard image processing (labeled "old segmentation"), and after training a CNN

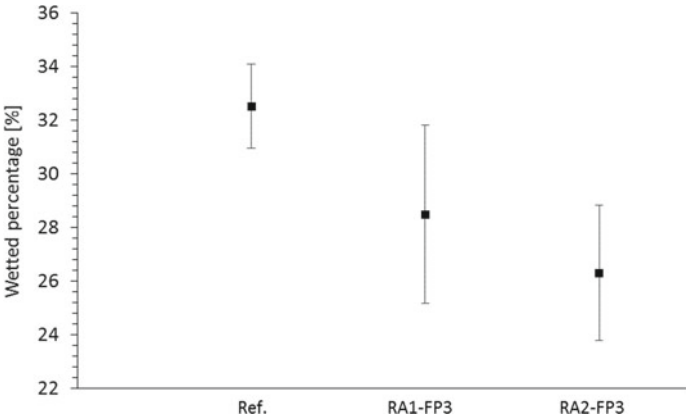

Fig. 3.10 AWT findings when evaluating the feature of wetted percentage for distinct levels of the intentionally deposited combined "release agent (RA)+fingerprint (FP)" contamination within the production user case with pilot CFRP samples

3.2.3.2 Repair Scenario Pilot Samples with Combined "Thermal Impact+De-icing Fluid" Contamination

We would like to reiterate here that in contrast to the smooth CFRP specimens of the respective production user case, the pilot samples within the repair user case were shafted CFRP samples. In the following, we focus on the contamination scenario that is based on distinct levels of combined thermal degradation and subsequent de-icing fluid contamination.

Similar to the production pilot samples, the detection of the applied water droplets following the AWT procedure was challenging, even though the surface did not show a very strong texture/structure. However, the deposited waterborne de-icing fluid contamination (as similarly observed on coupon samples) leads to a very good

spreading of the droplets. Therefore, identifying individual droplets during the detection step of the AWT data evaluation process was harder since the droplets appeared to be "open" on the captured images instead of being assigned a roundish and "closed" contour. This type of droplet is not detectable using standard image processing. Once again, for such a scenario, the processing of the images with the CNN proved to be quite efficient, see Fig. 3.11.

Both the detection of contamination and the differentiation from the reference CFRP surface state were easily achieved through the observation of the AWT "droplet diameter" feature. The differentiation of various contamination levels was also possible here, see Fig. 3.12.

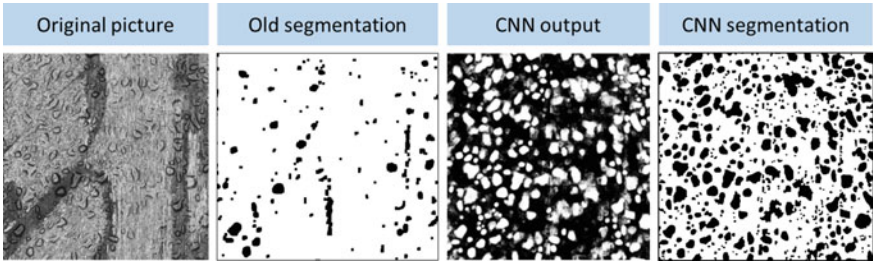

Fig. 3.11 Starting from the captured original AWT image, this sequence was obtained from distinct droplet segmentation approaches using standard image processing ("old segmentation", left) and convolutional neural network ("CNN segmentation", right) when applying AWT to intentionally contaminated CFRP pilot samples within the repair user case

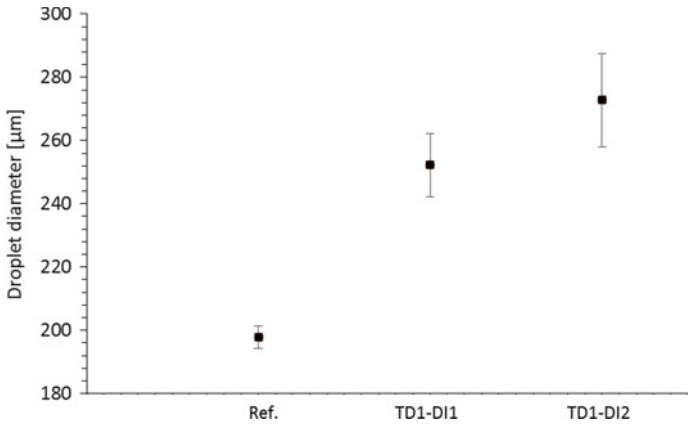

Fig. 3.12 AWT findings when evaluating the "droplet diameter" feature obtained for the CFRP pilot samples prepared within the combined "thermal impact+de-icer" contamination scenario

3.2.4 AWT Performance in Inline Surface Quality Assessment

In order to establish and enhance the performance of AWT when inspecting the surface states of CFRP parts relevant for specific aeronautical user cases, we iteratively determined and advanced the abilities of the system on flat coupon samples, pilot samples, and realistic parts and then conducted an assessment of the potential inline application of the technology. As explained, this technology relies on a comparative assessment of the surface state. Hereby, the very powerful systematic AWT inspection procedure, based on a convolutional neural network (CNN), must be taught to differentiate contaminations. Once the system had been trained to correctly detect the droplets and to differentiate the contaminations, its use in inline applications was straightforward.

The inline application allows fast and non-destructive monitoring and classification of the surface states and clearly exceeds the performance of the NDT approaches used so far (e.g., the water break test). Most contaminations investigated during the ComBoNDT research project in distinct scenarios with various degrees of contamination were successfully detected, and even the relevant contamination levels investigated here could be differentiated.

In conclusion, we developed sensitive and productive AWT procedures that not only facilitated the differentiation between the surface states of clean and intentionally contaminated parts but also permitted discrimination between distinct levels of contamination for several contamination scenarios. As the significance of AWT investigations and the thus obtained findings are based on contrasts in the wetting behavior of the inspected surfaces, our investigations plausibly indicate that AWT is a very surface-sensitive technique that enables a significant differentiation between clean surfaces and surfaces with sub-monolayer and monolayer contamination. However, AWT does not allow discrimination between surface states composed of a few or several molecular layers of contaminants. Finally, the integration of the technology in inline applications without major constraints was achieved.

3.3 Optically Stimulated Electron Emission (OSEE)

In this section, we introduce optically stimulated electron emission (OSEE) as a tool for surface quality assessment and detail how its performance was enhanced in the ComBoNDT research project for the in-process monitoring of CFRP adherends. Using OSEE for the surface inspection of carbon/epoxy composite and CFRP substrates has been described in several works over the last decades [3, 4], and the method is presently gaining visibility in surface quality assessment prior to bonding [1, 5, 6].

3.3.1 Principle and Instrumentation

OSEE is a surface analytical technique that relies on recording the photocurrent emitted from a sample surface region illuminated with UV light, typically under environmental conditions that prevail in cleaning or adhesive bonding processes. There are two modes of operation. During "microscopic" OSEE mapping, the sample is scanned using an electron collector, typically by applying lateral movements with a speed ranging from 1 mm to 1 cm per second. Meanwhile, during "spectroscopic" local measurements, the photocurrent is measured at fixed positions upon varying and recording the hold-up time. We performed our OSEE experiments under ambient conditions using an SQM300 surface quality monitor (purchased from Photo Emission Tech., Inc. (PET), USA).

Regarding the principle of an OSEE measurement in more detail, during the local inspection, regions of the sample surface are exposed to UV light from a mercury vapor lamp with prominent emission maxima at 4.9 and 6.7 eV. As the work function of the respective substrate surface amounts to approximately 5 eV, the emission maximum at the higher energy of 6.7 eV essentially contributes to the photoelectrons emitted by the sample surface, and the emitted electrons exhibit kinetic energies of less than approximately 2 eV. A sub-micrometer information depth of this method is observed when investigating the surface of a solid sample covered with a film exhibiting a thickness of some nanometers. This allows for the sensitive detection of thin films on substrates that do not significantly trap electric charges upon photoelectron emission. The interaction of the emitted photoelectrons with the ambient atmosphere is dominated by an electric field effective at the collector of the sensor to an extent that permits sensor-surface distances in the millimeter range during OSEE measurements. Carefully controlling the distance between the sensor and the surface is a prerequisite for effectively applying the setup presented in Fig. 3.26, see Fig. 3.13.

To mount the substrates for analysis, we equipped a commercial OSEE device with an electrically conductive and earthed moving table upon which we positioned the analyte sample using movements in two perpendicular horizontal directions (x and y) under the sensor. The vertical distance between the sample surface and the sensor (z) was set using a micrometer screw attached to the holder of the sensor. The enhanced OSEE setup developed during the ComBoNDT research project permitted vertical sensor movements with the aid of an electric motor, and the most advanced OSEE procedure was achieved with robot-aided three-dimensional sensor positioning. In OSEE implementations depending on a moving table for positioning the CFRP specimens, a surface scan was performed, with the table programmed to move according to a certain step size and number of steps in both horizontal directions, defined by the user through the machine-associated software. As the scan advanced, a photocurrent was obtained for each part of the scanned surface, and an apparently dimensionless value (which actually indicates a current converted into a voltage [7], given in centivolts), henceforth denoted as the OSEE signal, was indicated on a display and digitally recorded. Finally, a digital worksheet with the emission values for the entire

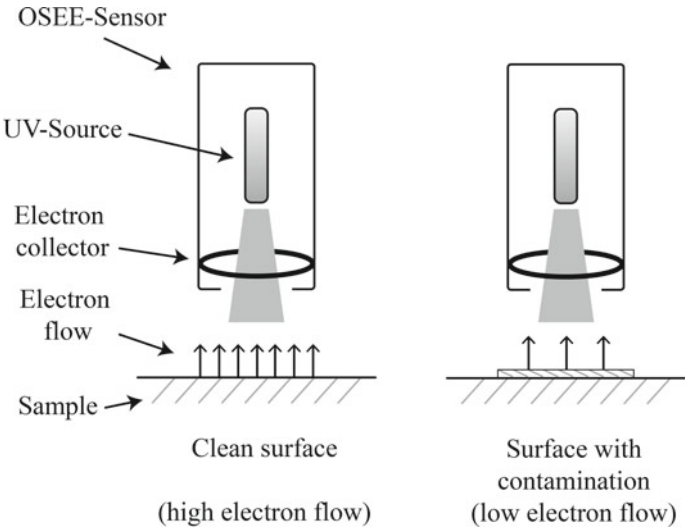

Fig. 3.13 Diagram showing the components and the principle of optically stimulated electron emission (OSEE) for measuring a photocurrent to reveal the surface state of a substrate

analyzed sample, i.e., an OSEE map, was obtained as a result of the test. For further evaluation of these maps especially for non-localized contaminations, the mean value of all the data points in the map together with its standard deviation was calculated.

3.3.2 OSEE Results

In the following, we report the OSEE enhancements and findings obtained in the ComBoNDT research project, in which the consortium partners at Fraunhofer IFAM performed the in-process monitoring of CFRP adherends with different shapes that are relevant for distinct technologically relevant user cases and which had undergone an intentional application of various contamination scenarios.

3.3.2.1 OSEE Results Obtained on CFRP Coupon Level Samples

First, we detail the advancements of the OSEE technique. Then, we report the respective OSEE results for the production user cases, characterized by a grayish abrasive dust obtained during the grinding of the CFRP surface, and the repair user cases, characterized by black abrasive dust obtained during the grinding of the CFRP surface. When assessing the surface quality of the coupon level CFRP specimens, we used OSEE to investigate a set of three 10 cm wide square samples to examine the surface state. For each sample, a surface scan was performed using a 6 mm wide aperture

at a constant sensor-surface distance, with the table being programmed to move according to 15 steps with a width of 5 or 6 mm (in both horizontal directions), as defined by the user through the machine-associated software.

In going beyond the commercially available state of the art, and thereby increasing the technology readiness level of the OSEE technique, three principal advances were performed within the ComBoNDT project. First, we aimed at improving the reliability of the technique by considering the influence of topography, especially the sample-sensor distance, on the sensor signal and by controlling or also avoiding electrostatic charging effects. Second, we sought an adaption of the device setup and control systems to the automated scanning of CFRP surfaces used in real manufacturing processes within the production or repair user cases. Third, we manufactured the electronic parts for the OSEE adaptation (e.g., serial interface, power supply, and relay board) as defined by Fraunhofer IFAM within the project. The achieved advancements are presented in Fig. 3.14.

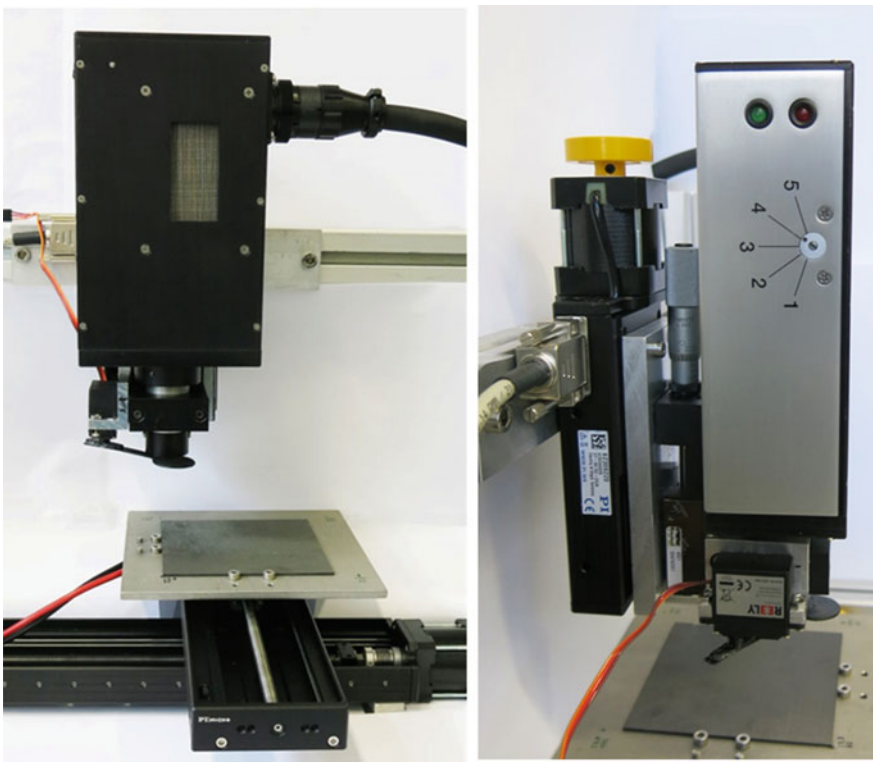

Fig. 3.14 Images showing the technological advancements achieved for optically stimulated electron emission (OSEE) in the ComBoNDT research project: The developed motor-driven shutter for the UV light source (left; below the electron collector) and the drive for the sensor holder, permitting a variation of the distance between the sensor and the substrate surface (right)

In terms of the abovementioned "microscopic" and "spectroscopic" operation modes of OSEE, a hybrid operation mode was developed and implemented. Based on rapidly opening a shutter in the light path of the UV source after having reached a measurement position (by laterally moving the newly developed x, y scanning table), an instant time-dependent ("in-time") sample mapping was facilitated that allowed combining the x, y mapping option while recording the local charging behavior or also recording the local height (i.e., sensor-surface distance) dependence of the OSEE signal. Specifically, by introducing an automatized variation of the sample-sensor distance based on a third precision drive (for the vertical z-direction), the variation of the OSEE signal upon changing the sensor-surface distance became possible. This also enables an assessment of surface topographies that are more complex than flat surfaces.

Production user case based on CFRP coupons

For the production user case based on CFRP coupon specimens, we investigated three different contamination scenarios, and the respectively obtained OSEE results were compared to the reference surface state of the production samples (P-RE):

- First, different levels of surface contaminations with a silicone-based release agent (P-RA) were prepared, as described in Chap. 2, and the degree of contamination was quantified by XPS analysis.
- Second, for the production fingerprint scenario (P-FP), samples were contaminated by different amounts of a synthetic sweat formulation according to DIN ISO 9022-12, as also detailed by Moutsompegka et al. [8].
- Third, a moisture scenario during production (P-MO) was considered.

Figure 3.15 presents the respectively obtained OSEE maps for the three samples prepared following the clean reference (P-RE) scenario. With the instrumental settings applied, an average OSEE intensity of 754 ± 152 a.u. (arbitrary units) was obtained.

In the following, we present plots showing the average OSEE intensity for the three contamination scenarios P-RA, P-FP, and P-MO in comparison to that obtained for P-RE.

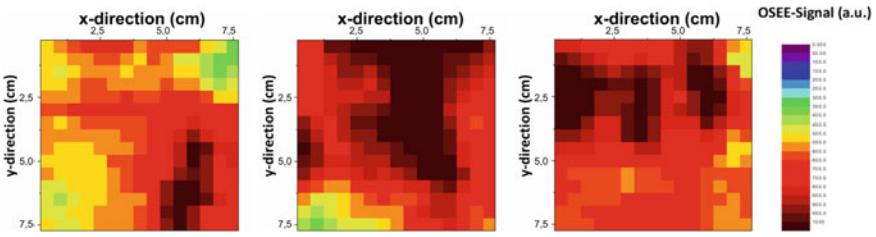

Fig. 3.15 Optically stimulated electron emission (OSEE) maps (15 × 15 pixels) for the three samples prepared following the clean reference scenario of the production user case (P-RE), based on CFRP coupon specimens resulting from a grinding process that was characterized by producing a grayish abrasive dust